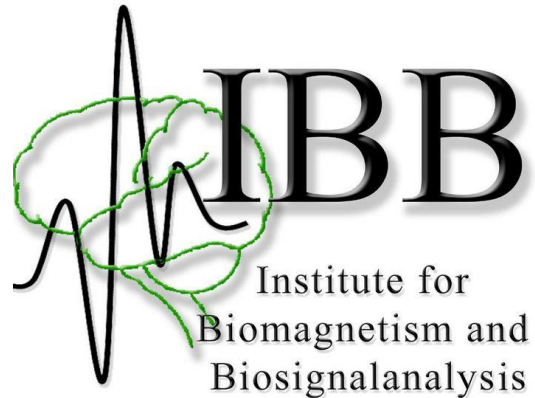


Fachhochschule
Münster University of
Applied Sciences



UNIVERSITY OF APPLIED SCIENCES MÜNSTER

DEPARTMENT OF ENGINEERING PHYSICS

PROF. DR. ULRICH STÖBER

MEDICAL IMAGING AND PROCESSING

UNIVERSITY HOSPITAL MÜNSTER

INSTITUTE FOR BIOMAGNETISM AND BIOSIG-
NALANALYSIS

PROF. DR. RER. NAT. CARSTEN WOLTERS
STIMULATION, IMAGING AND MODELING OF
NEURONAL NETWORKS IN THE HUMAN BRAIN
RESEARCH GROUP

COLLABORATION

Optimization of transcranial electrical stimulation montages to reduce seizure frequency and severity in patients with refractory focal epilepsy

Master's Thesis

Fabian Kaiser

Biomedical Engineering Master

Contents

NOMENCLATURE

INTRODUCTION I-2

FUNDAMENTALS II-3

THE HUMAN BRAIN.....II-3

Basic functional System.....II-3

Gross Anatomy.....II-5

Pathology of the Human Brain.....II-7

EPILEPSY.....II-8

Definition and Epidemiology.....II-8

Etiology.....II-8

Classification.....II-9

Diagnostics.....II-11

Diagnosing Seizures by their Semiology.....II-11

Establishing Etiology and Co-morbidities.....II-12

Presurgical Examination.....II-12

Therapy.....II-14

Therapeutic Walkthrough.....II-14

Surgical Approach.....II-15

Dietary Approach.....II-16

Neurostimulation Approach.....II-16

Transcranial Direct Current Stimulation (tDCS).....II-18

METHODS III-19

ETHICS STATEMENT AND PATIENT.....III-19

STUDY DESIGN.....III-19

TDCS HARDWARE.....III-20

TDCS MONTAGES.....III-20

dCMI optimized.....III-21

ActiSham.....III-21

EEG DATA ACQUISITION.....III-21

IED DETECTION	III-22
SOURCE ESTIMATION	III-22
STATISTICAL ANALYSIS	III-22
QUESTIONNAIRES	III-23
FIGURES AND VISUALIZATIONS	III-23
RESULTS	IV-24
IED FREQUENCY	IV-24
<i>Statistical Analysis</i>	IV-24
Mixed ANOVA Assumptions	IV-24
Mixed ANOVA Results	IV-25
Post-Hoc Multiple Comparisons	IV-26
<i>Relative Frequency of IEDs – Comparison between Factors</i>	IV-27
<i>Absolute Frequency of IEDs in Detail</i>	IV-29
<i>IED Frequency Evolution over Time</i>	IV-31
SOURCE ESTIMATION	IV-33
<i>Epileptologist 1</i>	IV-33
Global Average Moving Dipole	IV-33
PreStim Average Moving Dipole	IV-35
PostStim Average Moving Dipole	IV-37
PreSham Average Moving Dipole	IV-39
PostSham Average Moving Dipole	IV-41
Stim Week Baseline Average Moving Dipole	IV-43
Sham Week Baseline Average Moving Dipole	IV-45
<i>Epileptologist 3</i>	IV-47
Global Average Moving Dipole	IV-47
PreStim Average Moving Dipole	IV-49
PostStim Average Moving Dipole	IV-51
PreSham Average Moving Dipole	IV-53
PostSham Average Moving Dipole	IV-55
Stim Week Baseline Average Moving Dipole	IV-57
Sham Week Baseline Average Moving Dipole	IV-59
IMPROVED SEGMENTATION	IV-61
<i>Skull leakages</i>	IV-61
TOLERABILITY AND SYMPTOMS	IV-61
DISCUSSION	V-62

EFFECT OF PERSONALIZED AND dCMI OPTIMIZED TDCS ON IED FREQUENCY	V-62
EFFECT OF PERSONALIZED AND dCMI OPTIMIZED TDCS ON SEIZURE SEVERITY	V-63
EFFECT OF PERSONALIZED AND dCMI OPTIMIZED TDCS ON IED SOURCE LOCATION AND ORIENTATION	V-63
EFFECT OF PERSONALIZED AND dCMI OPTIMIZED TDCS ON IED SOURCE DIPOLE CURRENT DENSITY	V-67
<i>Short-term</i>	V-67
<i>Long-term</i>	V-67
EFFECT OF INCREASED QUALITY IN SEGMENTATION ON dCMI MONTAGE	V-68
TDCS AS AN EPILEPSY THERAPY	V-68
PHYSIOLOGICAL EXPLANATION	V-69
CONCLUSION	VI-70
ACKNOWLEDGEMENTS	VII-71
LIST OF FIGURES	VIII-72
LIST OF TABLES	IX-80
REFERENCES	X-83
EIDESSTATTLICHE ERKLÄRUNG	XI-96

Nomenclature

AED	Antiepileptic drug
VNS	Vagus nerve stimulation
DBS	Deep brain stimulation
FCD	Focal cortical dysplasia
tDCS	Transcranial direct current stimulation
SF	Seizure frequency
dCMI	Distributed constrained maximum intensity
ActiSham	Active sham
IED	Interictal epileptiform discharge
CSF	Cerebrospinal fluid
TBI	Traumatic brain injury
BT	Brain tumor
ILAE	International league against epilepsy
CNS	Central nervous system
EEG	Electroencephalography
MRI	Magnetic resonance imaging
CT	Computed tomography
ECG	Electrocardiogram
FDG-PET	Fluorodeoxyglucose-positron emission tomography
SPECT	Single-photon emission computerized tomography
fMRI	Functional MRI
iEEG	Intracranial EEG
MEEG	Combined Magneto-/Electroencephalography
DRE	Drug resistant epilepsy
AE	Adverse events
TMS	Transcranial magnetic stimulation
RNS	Responsive neurostimulation
DTI	Diffusion tensor imaging
SEP/SEF	Somatosensory evoked potential or field
ANOVA	Analysis of variance
Tukey-HSD	Tukey's honestly significant difference test

Introduction

About 50 million people suffer from epilepsy and about 30% of those cases are resistant to anti-epileptic drugs (AEDs) (Kalilani et al., 2018; Picot et al., 2008). Surgical resection of the epileptogenic zone has the greatest chance of producing remission, while other treatments like diet therapies and electrical nerve stimulation (for example vagus nerve stimulation (VNS) and deep brain stimulation (DBS)) are often considered to be just palliative (Dalic & Cook, 2016). Furthermore, neurostimulation therapies are mainly effective over years, are invasive, meaning that they are often not reversible, can cause serious adverse effects, and are expensive (Kaufmann et al., 2021). Unfortunately, when a focal cortical dysplasia (FCD) is located close to eloquent cortex, resection of the assumed epileptogenic zone is often not advised due to severe consequences which include loss of sensory processing, linguistic ability and paralysis (Choi & Kim, 2019).

Hope was renewed when it was shown that transcranial Direct Current Stimulation (tDCS) can significantly reduce seizure frequency (SF) in refractory focal epilepsy (Kaufmann et al., 2021; Yang et al., 2020). To further explore and enhance the power of tDCS to treat epilepsy, our work group developed the optimization algorithm distributed Constrained Maximum Intensity (dCMI) for tDCS montages that offers excellent directionality as well as an improved trade-off between focality and intensity of the electrical current at the target brain region compared to previous optimization approaches (Khan et al., 2022, 2019). In this thesis, a double-blind sham-controlled pilot/feasibility clinical trial was performed: a patient with refractory focal epilepsy has been treated with personalized and dCMI optimized tDCS as well as with active sham (ActiSham) and effects of the proposed treatment controlled by ActiSham on interictal epileptiform discharges (IEDs) were examined.

To produce the optimized tDCS montage, a multimodal source and conductivity analysis pipeline is essential. For this study the pipeline originally proposed by Dr. Antonakakis was used (Marios Antonakakis, 2021). Additionally, the impact of improved quality of segmentation as well as the increase in amount of tissue compartments from an originally six- to a now seven compartment model on the optimized montage was examined.

Fundamentals

The Human Brain

The human brain is a mass of nerve tissue in the anterior/superior part of the human organism that is protected by multiple tissue layers which include skin, muscles, fat, skull, dura mater, and cerebrospinal fluid (CSF). It is a highly complex primary organ. Central to the nervous system, it is connected to the entire body through the spinal cord and regulates most of the body's activities, being supplied with information by the sense organs, while also constantly processing information to generate consciousness, emotion, thought, memory, and sensation (Agur & Dalley, 2018).

Basic functional System

Two types of cells mainly constitute the nervous system: neurons (nerve cells) and supportive glial cells.

Glial Cells

The three main types of glial cells found in the brain are: 1) Astrocytes which regulate blood flow, maintain the homeostasis, and regulate data transmission at the synapse; 2) microglia which remove dead cell and debris and 3) oligodendrocytes which produce myelin (Rasband, 2016).

Neurons

Neurons consists of 4 parts (**Figure 1**): 1) The dendrites which receive and process incoming information (Johnston et al., 1996) and are connected to 2) the soma (cell body). 3) Axons carry information via electrical impulses and are coated with an insulating layer called 4) myelin or the myelin sheath which increases data transmission speed (**Figure 3**) (SCHMITT & BEAR, 1939).

The synapses connect the axons and dendrites of different neurons and are gaps before which the electrical signal is converted into a chemical signal, travels the synapse, and is converted back into an electrical signal in the postsynaptic neuron (Ginsborg, 1964).

Signals can be excitatory or inhibitory; the sum of all the signals, that enter a neuron, shift its membrane potential from its resting potential and if it gets depolarized enough past the threshold potential, an action potential is fired (depolarization) across the axon. Lastly, the membrane potential is rebuilt (re- and hyperpolarization) (**Figure 2**) (Barnett & Larkman, 2007).

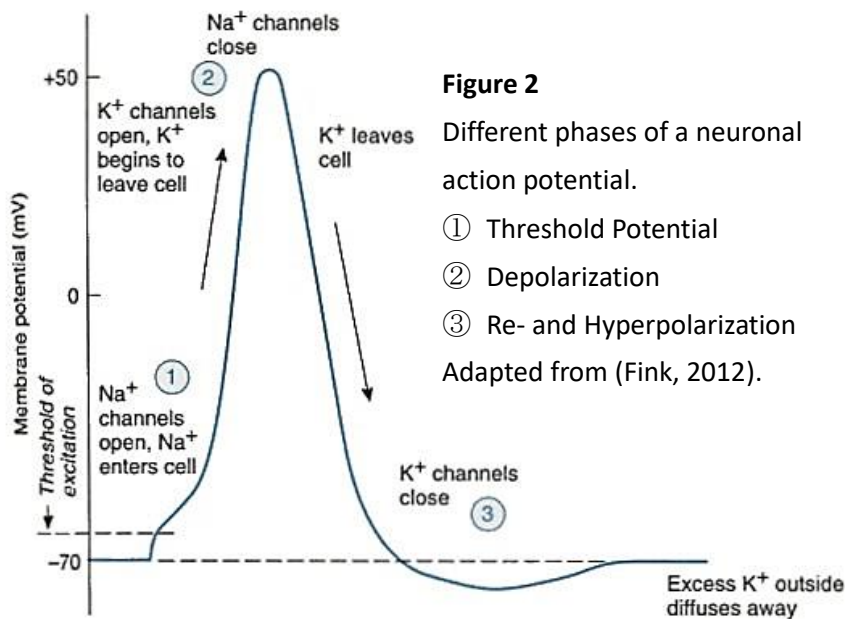
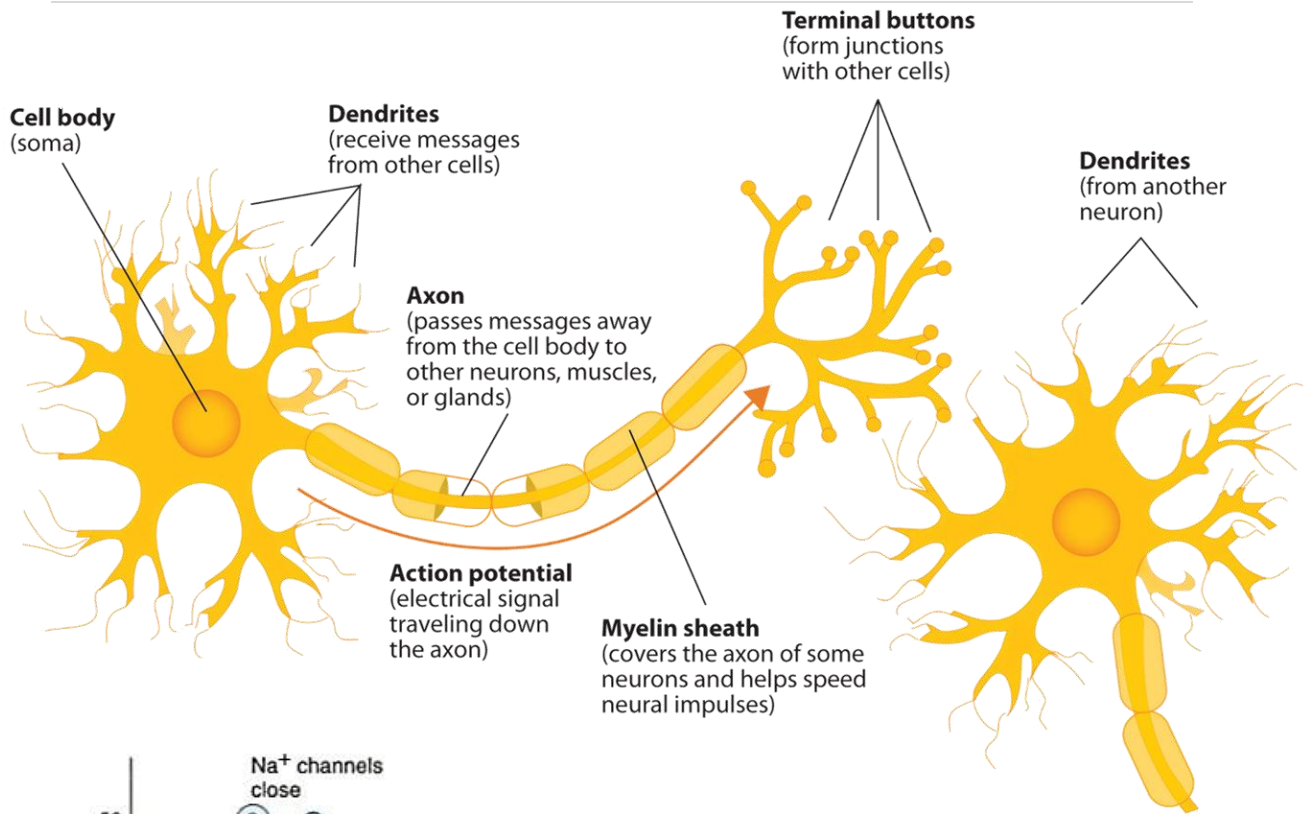
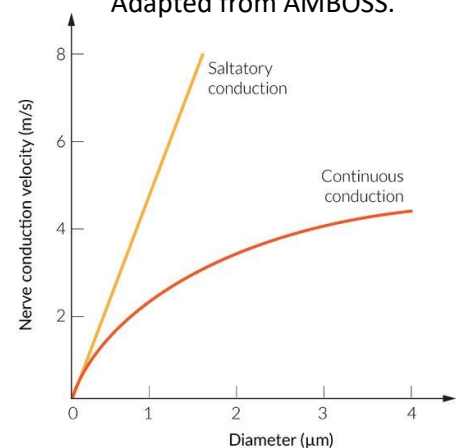
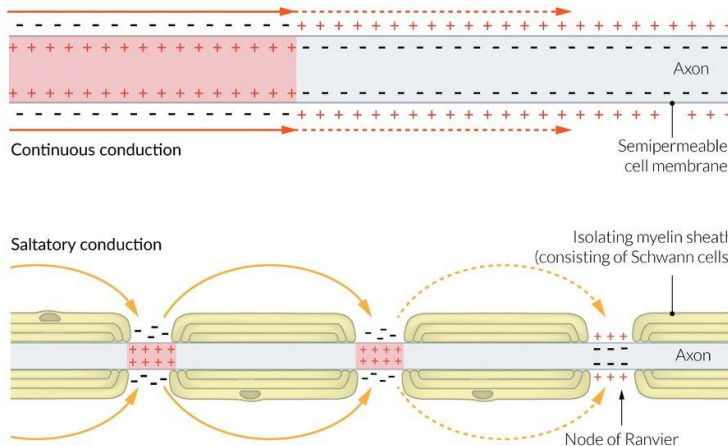


Figure 1

The structure of a neuron. Adapted from Introduction to Psychology - 1st Canadian Edition by Jennifer Walunga.

Figure 3

Shows that the myelin sheath increases nerve conduction velocity of an axon by saltatory conduction. Adapted from AMBOSS.



Another important ability of neurons is neuroplasticity. Important for the theoretical effectiveness of tDCS is the consideration of activity-dependent plasticity which allows neurons to change their excitability long term with use (Patten et al., 2016).

Gross Anatomy

At the highest level, the brain consists of the cerebrum, the cerebellum, the brain stem, and the limbic System.

Cerebrum

This is the largest and uppermost part of the brain. It is split by the longitudinal fissure into two hemispheres which are connected by the corpus callosum and is further divided by deep sulci into the four main lobes. Gray matter contains a higher concentration of neuron somas, while white matter contains more axons. The gray matter of the cerebrum is called the cerebral cortex and is positioned on top of the brain's white matter. There are subcortical structures like the basal ganglia or the hippocampus deeper inside the brain (Agur & Dalley, 2018). The four main lobes and their functions are (Jawabri & Sharma, 2019):

1. The **Frontal Lobe** is the largest lobe and as its name suggests the most anterior positioned lobe. Its functions include prospective memory, speech, language, personality, executive function, emotional regulation, and movement control.
2. The **Parietal Lobe** is located posterior to the frontal lobe and superior to the temporal lobe. Its functions include interpreting of somatosensory signals (touch, position, vibration, pressure, pain, temperature), motor planning action, sensorimotor planning, learning, language, spatial recognition, stereognosis (differentiation between objects by using tactile information like texture, size, shape, weight, and temperature).
3. The **Temporal Lobe** is located in the middle cranial fossa, posterior to the frontal lobe, and inferior to the parietal lobe. Its functions include translating and processing all auditory phenomena, consciousness, semantic memory (common knowledge), assigning meaning to words, decoding gaze directions, visual and facial perception (interpreting content of vision), declarative memory (long term memory; concepts, ideas and events learned throughout life).
4. The **Occipital Lobe** is the smallest lobe. It is located as its name suggests in the most posterior region of the brain. Its functions include visual processing and interpretation.

Cerebellum

The cerebellum is located inferior to the tentorium cerebella or tentorial membrane in the posterior cranial fossa. It approximately makes up 10% of the brain's size but contains more than 50% of the total number of neurons which are found in the brain. It regulates motor movement and controls balance. Specifically, it coordinates gait, maintains posture, controls muscle tone and voluntary muscle activity but cannot initiate muscle contraction (Jimshelishvili & Dididze, 2019).

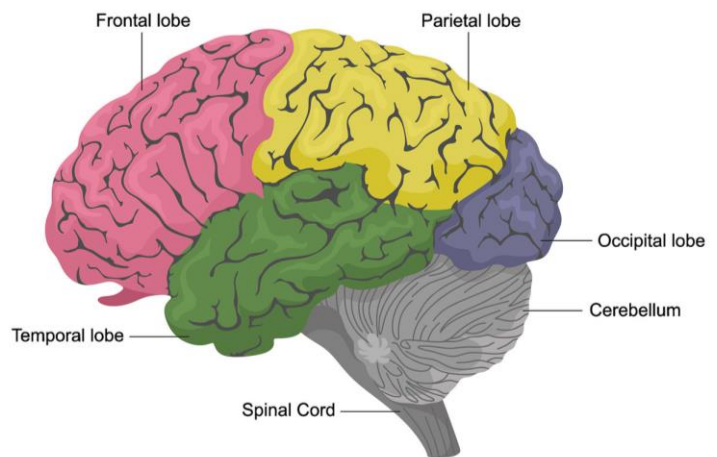


Figure 4

Gross anatomy of the brain. Cerebral lobes in color; cerebellum and spinal cord in gray. Adapted from John Hopkins University.

Brainstem

The brainstem is the most inferior located part of the brain but still superior to the spinal cord. It forms a connection between the cerebrum, cerebellum, and spinal cord. Its functions include breathing, blood pressure, heart rate, sleep, body temperature, hunger, and thirst (Snell, 2016).

Limbic System

The limbic system is consisting of multiple structures and can be broadly found spiraling the inside of the brain covering the thalamus and corpus callosum, but it escapes a definition of strict anatomic boundaries. Important structures include the amygdala, the hippocampus, and the cingulate gyrus. Understanding of the functions of the limbic system remains limited but it has been associated with emotional behavior (Jones, 2011; Snell, 2016).

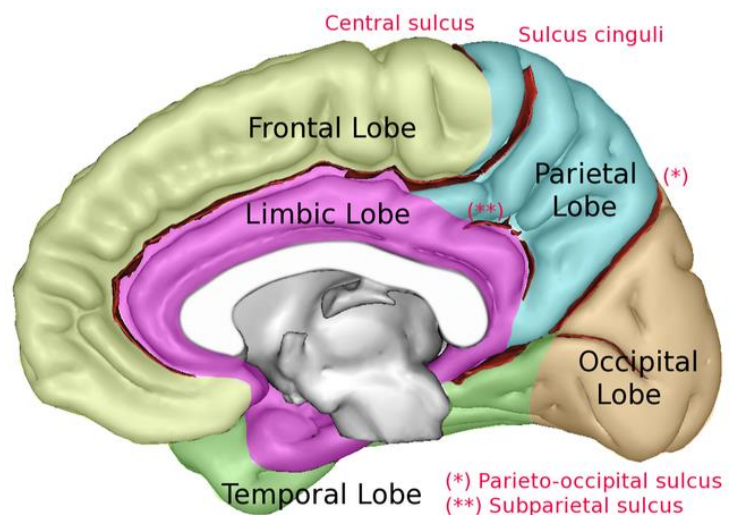


Figure 5

Shows the location of the limbic lobe in relation to cerebral lobes. Adapted from wikicommons.

Pathology of the Human Brain

Pathology can befall the human brain in numerous ways. To give an overview, let's divide disorders by cause with some that fall under multiple categories and would require differential diagnosis but for this simple list, such cases are treated as if they fall under only one category:

1. **Traumatic brain injuries** (TBI) are injuries resulting from external mechanical forces on the brain or head which temporarily or permanently impair brain function and cause structural damage (Parikh et al., 2007). Around 69 million people are estimated to sustain a TBI each year (Dewan et al., 2019).
2. The category "**neurodegenerative diseases**" is named after the progressive loss of structure or function of neurons which may lead to cell death. But still, individual neurodegenerative disorders are heterogeneous in their clinical presentations and underlying physiology even though they often share overlapping features. These include Alzheimer's disease, frontotemporal dementia, supranuclear palsy, corticobasal degeneration, Parkinson's disease, dementia with Lewy bodies, multiple system atrophy, and Huntington's disease (Erkkinen et al., 2018).
3. **Infections** caused by viruses, bacteria, and fungi. Can cause inflammation of the meninges (meningitis) and the brain matter (encephalitis). Additionally, intracerebral abscesses can be formed. In developed countries, brain infections are rare (Sarrazin et al., 2012). Proteinaceous infectious particle (prion) diseases are neurodegenerative diseases caused by transmissible particles that contain a pathogenic isoform of the prion protein (Johnson, 2005). The most common prion disease in humans is Creutzfeldt-Jakob disease and it has a global incidence of 0.5 to 1.5 million per year (Johnson & Gibbs, 1998).
4. **Brain tumors** (BTs) can be primary or metastatic, benign, or malignant, though most malignant brain tumors are metastatic. Primary malignant BTs have a global annual incidence of 3.7 per 100 thousand for men and 2.6 per 100 thousand for women (Bondy et al., 2008).
5. **Mental disorders** which still defy widely accepted definitions (Telles-Correia et al., 2018).
6. **Epilepsy** which is gonna be discussed in more detail in the next part of the thesis.
7. **Congenital brain disorders** which are a result of genetic and chromosomal mutations. These include Tay-Sachs disease (Fernandes Filho & Shapiro, 2004) and lissencephaly, which is characterized as a "smooth brain" or impaired cortical folding (Fry et al., 2014).

8. **Stroke** or apoplexy is an acute neurologic condition resulting from a disruption of blood circulation in the brain. It is either ischemic (insufficient cerebral blood flow) or hemorrhagic (bleeding within the brain parenchyma) (Sacco et al., 2013). In 2017, 11.9 million incidences of strokes were reported worldwide (Krishnamurthi et al., 2020).

Epilepsy

Definition and Epidemiology

The current official conceptual definition of the International League Against Epilepsy (ILAE) was first published by (R. S. Fisher et al., 2005):

*“An **epileptic seizure** is a transient occurrence of signs and/or symptoms due to abnormal excessive or synchronous neuronal activity in the brain.*

***Epilepsy** is a disorder of the brain characterized by an enduring predisposition to generate epileptic seizures and by the neurobiologic, cognitive, psychological, and social consequences of this condition. The definition of epilepsy requires the occurrence of at least one epileptic seizure.”*

This was accompanied in 2014 by practical definitions and diagnostic criteria (R. S. Fisher et al., 2014), reached consensus in the ILAE in 2017 (J. J. Falco-Walter et al., 2018; R. S. Fisher et al., 2017; Scheffer et al., 2017) and the most recent addition for classifications for seizures in neonates was published in 2020 by the ILAE (Pressler et al., 2021). This forms the basis of the current understanding and classification of epilepsy.

Knowledge and understanding of the epidemiology of epilepsy are constantly progressing and changing, but it is estimated that 10% of the global population has experienced seizures, while between 1 and 2% of all people are afflicted by epilepsy (J. Falco-Walter, 2020).

Etiology

Before we discuss the etiology of epilepsy and epileptic seizures, we have to be differentially aware, that some seizures are not associated with epilepsy including most febrile seizures and those that present themselves along a specific cause (seizure-related disorders), such as TBI, stroke and anoxic encephalopathy (Beghi et al., 2010; Neligan et al., 2012; Thurman et al., 2011). Additionally, events may present themselves as epileptic seizures, but miss the abnormal excessive or synchronous neuronal activity; these are known as psychogenic non-epileptic

seizures (PNES) (Devinsky et al., 2011).

The causes for epilepsy can be divided into 6 groups (Maschio, 2012; Scheffer et al., 2017):

1. **Genetic etiologies** include genetic mutations of ion channels or transmitter receptors, chromosomal aberrations, genetic metabolic disorders, and mitochondrial diseases.
2. **Structural etiologies** include chronic cerebral lesions or abnormalities, TBI, cancer, perinatal injury, hippocampal sclerosis, tuberous sclerosis, congenital cerebral or arteriovenous malformations, microcephaly, megalencephaly, cortical dysplasia, and cranial radiation therapy.
3. **Metabolic etiologies** include inborn errors of metabolism and porphyria.
4. **Immune etiologies** result directly from immune disorders such as autoimmune encephalitis.
5. **Infectious etiologies** are the most common type of etiologies. Here the epilepsy is evoked by chronic or acute infections of the central nervous system (CNS).

Classification

The classification of epilepsies according to (R. S. Fisher et al., 2017; Scheffer et al., 2017) is carried out on three levels (**Figure 6**). On each of the levels comorbidities and etiologies should be assessed: At the first level, seizures are identified according to the conceptual definition (found under *Epilepsy, Definition and Epidemiology*, page 8) and the seizure type is determined by consideration of the location of the onset of abnormal neuronal activity, level of awareness of the patient during the seizure, symptoms, aura, and other factors. The three main types of seizures are “Focal”, “Generalized” and “Unknown”. An overview for the basic classification of seizures can be seen in **Table 1**.

	Focal Seizures	Generalized Seizures	Unknown Seizures
Abnormal EEG Onset	<i>From within a single hemisphere</i>	<i>From both hemispheres</i>	<i>Unclear whether focal or generalized</i>
Awareness during seizure	<i>Aware and impaired awareness</i>	<i>N/a</i>	<i>N/a</i>
Symptoms	<i>Motor and nonmotor onset</i>	<i>Motor (such as tonic-clonic) and nonmotor (absence)</i>	<i>Motor (such as tonic-clonic) and nonmotor</i>
Other	<i>Focal to bilateral tonic-clonic</i>	<i>N/a</i>	<i>Unclassified</i>

Table 1
Basic ILAE 2017 operational classification of seizure types.

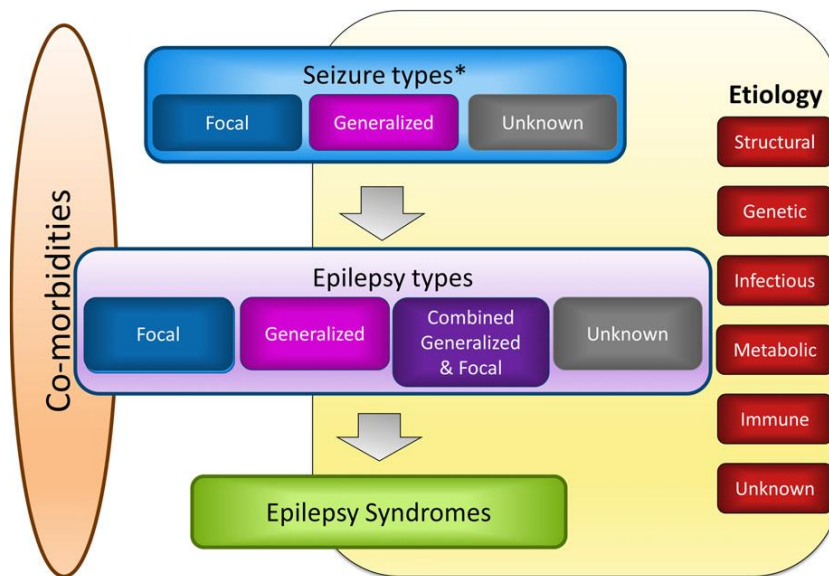


Figure 6
 Framework for classification of the epilepsies. Adapted from (Scheffer et al., 2017).

Further on we enter the second level which concerns the classification of the 4 epilepsy types.

1. **Focal Epilepsy** which requires the identification of the lobe from which seizures arise. They include unifocal and multifocal disorders, as well as seizures involving one hemisphere. Possible seizure types include focal aware seizures, focal impaired awareness seizures, focal motor seizures, focal non-motor seizures, and focal to bilateral tonic-clonic seizures. Typical interictal Electroencephalography (EEG) shows focal epileptiform discharges and support the ictal and clinical findings.
2. **Generalized Epilepsy** which usually shows generalized spike-wave activity on the EEG of the patient. Possible seizure types include absence, myoclonic, atonic, tonic and tonic-clonic. Typical interictal EEG discharges support the ictal and clinical findings.
3. **Combined Generalized and Focal Epilepsies** are afflicting patients with both generalized and focal seizures.
4. **Unknown Epilepsies** apply when it is clear that the patient has epilepsy but the necessary information to determine the other types is either missing or discordant.

The third level concerns the classification of the epilepsy syndromes which are a cluster of features, such as seizure types, EEG, and imaging features that usually come about together. Etiology, prognosis, and treatments are not however firmly tied to epilepsy syndromes though. Specific syndromes will not be discussed in this thesis, as there is no formal classification by the ILAE to this date (Berg et al., 2010), and this lack of information on syndromes won't be affecting the understanding of the content this thesis puts forward.

Diagnostics

The exact nature of epilepsy hasn't been understood as of yet, so as we have seen earlier (*Etiology*, pages 8-9; *Classification*, pages 9-10), correlating etiologies, comorbidities, and seizure types are used to diagnose epilepsy, but the underlying mechanics are not yet understood enough to construct a classification on a scientifically rigorous basis (Berg et al., 2010). Additionally, the initial diagnosis of a seizure or epilepsy is prone to errors (Scheepers et al., 1998; Stroink et al., 2003). Even the method hailed as the "gold standard in epilepsy diagnosis" EEG can be noninformative, have information that is exceedingly difficult to interpret or be discordant to other finds. It has been stated that the degree of experience of the treating physician is critical (Chadwick & Smith, 2002; Leach et al., 2005). If you additionally consider that an uncorrected diagnosis of epilepsy can be life-threatening in some cases (Zaidi et al., 2000), it follows that diagnosis is often made on a conglomerate of supporting evidence of as many modalities as is feasible. Since the stakes are highest in presurgical examination, here is where we find the most complete consideration of modalities. It is generally advised to combine different methods before clinical decision making, especially when it comes to estimating the epileptogenic zone (Brodbeck et al., 2010; Chassoux et al., 2010; Duez et al., 2019). Modern bleeding edge presurgical epilepsy diagnosis includes the use of teleconference systems where international experts of every part of the diagnostic process can review and discuss evidence together to achieve the highest degree of experience possible (Kakisaka et al., 2018). To summarize, ictal symptoms need to be considered together with the electrophysiological and neuroimaging findings to correctly diagnose the epileptic syndrome (Lüders et al., 1998; S. Noachtar et al., 1998).

Diagnosing Seizures by their Semiology

The first group of modalities to consider are used to investigate the seizure semiology:

- **Medical history** is taken in regards of the history of present illness (for aware seizures: descriptions by patient and/or witnesses; for impaired awareness seizure: description of witnesses), potential triggers (e.g., sleep deprivation), ictal and postictal symptoms and past medical history (history of epilepsy and of potential underlying conditions, such as head trauma, stroke, tumor, and CNS infection) (Wolf et al., 2020).

- **Physical examination** includes visual inspections (e.g., bruises from falls) and evaluation for cardiovascular disorders (Nowacki & Jirsch, 2017).
- **Long-term video EEG** allows for visual observation of the patient during seizures and synchronized EEG readings to examine ictal, as well as post- and interictal activity. Characteristic post- and interictal EEG patterns include epileptiform activity bursts, such as spikes and sharp waves, while ictal patterns include epileptiform discharges, such as spikes, sharp waves, spike waves and complete discharge patterns for specific epilepsy syndromes, such as hypersarrhythmia in West syndrome (Soheyl Noachtar & Rémi, 2009).

Establishing Etiology and Co-morbidities

The second group of modalities investigate the etiologies and co-morbidities:

- **Magnetic Resonance Imaging (MRI)** which is lauded to be the modality of choice for structural etiologies. It has a higher resolution than computed tomography (CT) and is more sensitive for identifying soft-tissue lesions. Clinical findings include tumors, malformations of cortical development, vascular malformations, mesial temporal sclerosis, and neocortical gliosis (Bernasconi et al., 2019).
- **Electrocardiogram (ECG)** is used to discover cardiogenic causes, such as cardiac arrhythmias and vasovagal syncope (Wong et al., 2008).
- **Genetic Testing** includes epilepsy gene panels, chromosome microarrays, whole exome sequencing and targeted single gene tests (Ritter & Holland, 2020).
- **Laboratory screening** is used to investigate metabolic disorders and infectious diseases. Possible tests include blood tests (glucose, electrolytes, toxicology screening), urine analysis, and CSF examination (Beghi et al., 2006).
- **Angiography** is used to discover potential vascular aberrations (Shorvon, 2009).

Presurgical Examination

Zones in Epilepsy

Of highest importance for the presurgical examination for epilepsy surgery is the localization of the epileptogenic zone. This zone is only one of 6 zones which we need to consider, so definitions of every zone, the modalities used to localize them and how they relate to each other follow (Carreño & Lüders, 2013):

1. The **epileptogenic zone** is the cortical area capable of generating seizures, and whose removal or disconnection will result in seizure freedom.
 - *Modalities:* No direct localization of this zone is possible with any modality.
2. The **symptomatogenic zone** is the cortical area that, after being stimulated by the epileptic discharge, produces the patient's typical ictal symptoms. Important for estimating the location of the epileptogenic zone is the symptomatogenic zone that produces the initial ictal symptoms. These two zones do not usually overlap, but the estimation of the symptomatogenic zone allows hints as to whether the findings for the other zones are sensible.
 - *Modalities:* Medical history, physical examination, and long-term video EEG.
3. The **lesional zone** or epileptogenic lesion is a structural lesion visible by neuroimaging techniques that is capable of generating seizures. The connection between the lesional zone and the epileptogenic zone may be complex. Not all lesions are responsible for the patient's seizures; in the case of multiple lesions, one or any number of them might be responsible. Complete resection of this zone also doesn't always guarantee seizure freedom, but even incomplete resection might grant it.
 - *Modalities:* MRI with support from the modalities of other zones to figure out which lesions may be epileptogenic.
4. The **functional deficit zone** is the cortical area that shows abnormal functioning in the interictal period. The size of this zone often varies depending on the modality. It can be more extensive than the epileptogenic zone, can include lesions not related to seizure generation, or areas of significant distance to the seizure focus.
 - *Modalities:* Detailed neurological examination, detailed neuropsychological evaluation, intracarotid amobarbital procedure (Wada test), interictal 2-[¹⁸F]-fluoro-2-deoxyglucose (FDG) positron emission tomography (PET), interictal single-photon emission computerized tomography (SPECT), and functional MRI (fMRI).
5. **The ictal onset zone** is the cortical area from which it can be objectively demonstrated that seizures arise from. This zone and the epileptogenic zone don't necessarily share the same space, it has been shown that partial resection of this zone freed a patient of seizures, but other patients couldn't attain seizure freedom even after complete resection of this zone.
 - *Modalities:* Long-term EEG, intracranial EEG (iEEG), fMRI (Eyndhoven et al., 2019) and ictal SPECT.

6. The **irritative zone** is the area of cortex capable of generating interictal spikes on the EEG. Unfortunately, this zone is not a fixed and static region, and its boundaries can change over time. The irritative and epileptogenic zones don't have to overlap, and one can be bigger or smaller than the other.
 - *Modalities*: MEEG (combined Magneto-/Electroencephalography) spike source estimation which can additionally be used to identify subtle MRI lesions, even if the initial MRI examination found no abnormalities (Itabashi et al., 2014), and iEEG to support the findings (Almubarak et al., 2014).

So, we can see that the modalities are actually always estimating one of the 5 zones that are not the epileptogenic zone, but through the combination of the estimates of these zones, the most informed guess about the epileptogenic zone can be reached.

Therapy

Therapeutic Walkthrough

1. The first line of treatments against epilepsy constitutes **pharmacological therapy with AEDs**: It is generally advised that a newly diagnosed patient undergoes monotherapy first (Kwan & Brodie, 2000), potentially branching out into polytherapy if at least two monotherapies have failed (Brodie, 2005; Shih et al., 2017; St. Louis, 2009).
2. A patient who is unresponsive even to the second AED trial is considered to have **drug-resistant epilepsy** (DRE) according to the ILAE (Kwan et al., 2010) and should be re-assessed in a dedicated epilepsy center to either exclude the causes of pseudo-pharmacoresistance or diagnose the correct epilepsy type (Fattorusso et al., 2021).
3. When DRE is established, it is advantageous to consider **surgery** right away because the likelihood of seizure remission is elevated in patients who are directly referred to specialized centers for epilepsy surgery compared to those that continue with subsequent drug trials (Fattorusso et al., 2021).
4. If clinicians decide against surgery, **trials of duo or even triple therapy** may have to follow, though they only offer a lower percentage of remission (Lee et al., 2019; Park et al., 2019). Selecting the appropriate drugs for polytherapy requires considerations of the difficult and complex pharmacodynamic interactions between drugs to maximize efficacy and minimize adverse events (AEs) (Deckers et al., 2001). Quadruple therapy should be avoided, if possible,

since the likelihood of AEs is heightened with only a small improvement of seizure control compared to triple therapy (López González et al., 2015).

5. After 5 drug trials (duo, triple, or quadruple therapy) have failed, **alternative therapies** such as neurostimulation or diet approaches should be considered (Fattorusso et al., 2021).

Before we discuss the alternatives to the pharmacological therapies, I would like to point out in summation that the approach to treating epilepsy is dominated by the use of AEDs. Even in the case of DRE, pharmacological treatments are still pursued. Only surgery has established itself as a main line treatment option besides medication even to the point of being preferred over medication in treating DRE when applicable. Discussing the alternatives, I hope each of their significance and place in the list of treatments for epilepsy becomes clear as well as the need for another non-invasive therapy option like personalized and optimized tDCS that has the potential to establish itself next to medication and surgery at the top of that list; filling the huge blind spot that currently occupies its space.

Surgical Approach

Epilepsy surgery includes resection of brain matter or disconnection of neuronal circuits:

- **Resection** of possibly epileptogenic lesions (lesionectomy) or larger parts of the brain that are assumed to contain the epileptogenic zone (Moore et al., 1993), either by removing a part or the whole of a cerebral lobe (lobectomy), or in severe cases removing an entire hemisphere (hemispherectomy) (Lettori et al., 2008).
- **Disconnection of neuronal circuits** to inhibit the spread of ictal activity and its associated damage to the brain by either cutting through the corpus callosum (Callosotomy) (Asadi-Pooya et al., 2008) or surgically disconnecting the cortex of one hemisphere entirely from the ipsilateral subcortical structures and the cortex of the other hemisphere without removal of the affected hemisphere (de Ribaupierre & Delalande, 2008).

Resective surgery is by far the best therapeutic option in treating DRE when patients are carefully selected and the absolute risk reduction for seizure reoccurrence compared to treatment with AEDs is very high (Wiebe & Jetté, 2012). Unfortunately, when the location estimate of the epileptogenic zone is located close to eloquent cortex or even overlaps with it, resection of the assumed epileptogenic zone is often not advised due to severe consequences which include loss of sensory processing, linguistic ability and paralysis (Choi & Kim, 2019). These cases, as well as

those in which the epileptogenic zone can't be identified , add up to a significant number of patients that are not advised to undergo resective surgery and are often treated with neurostimulation (Lattanzi et al., 2018).

Dietary Approach

The ketogenic diet is used as a treatment for a specific group of children with DRE consisting of a strict dietary regimen characterized by high fat and low carbohydrate intake but isn't used long-term due to concerns about growth and overall health (Operto et al., 2020; Verrotti et al., 2020). More high-quality data is needed to show its effectiveness as well as demonstrating the use for treating adults with DRE (Martin-McGill et al., 2020).

Neurostimulation Approach

Following neurostimulation modalities are used to treat DRE; some of them need to be implanted, others are non-invasive; some of them provide continuous stimulation (open-loop), while others stimulate as a response to detected brain activity (closed-loop) (Boon et al., 2018; Starnes et al., 2019):

- The most studied and established modality **vagus nerve stimulation** (VNS) is achieved through a programmable pulse generator, that is implanted subcutaneously under the left clavicle and delivers periodic electrical stimulation directly to the vagus nerve distal through a lead wire that is wrapped around it (Pérez-Carbonell et al., 2020). Nowadays, adults and children suffering from focal or generalized seizures are treated with VNS (Morris et al., 2013). The underlying mechanism of the effect of VNS on seizure control is not completely understood, though one may assume that the modulation of noradrenergic and serotonergic projections based on the increased levels of serotonin measured in patients treated with VNS which is concordant with the findings of increased levels of the inhibitory neurotransmitter GABA and decreased levels of excitatory amino acid aspartate (Ben-Menachem et al., 1995). Adverse effects include voice alteration and hoarseness, cough, dyspnea, pain, paresthesia, nausea, and headaches (Panebianco et al., 2015). Generally, results of major randomized controlled trials are in agreement that 26% to 40% of DRE patients treated with VNS showed at least a 50% reduction in seizure frequency) (Chambers & Bowen, 2013).
- **Deep brain stimulation** (DBS) is achieved through implanted electrodes connected to a

pulse generator stimulating deep brain structures such as the anterior nucleus of the thalamus, hippocampus, the centromedian nucleus of the thalamus, cerebellum and globus pallidus (Fattorusso et al., 2021). Again, the underlying mechanism of the effect of DBS on reducing interictal discharges is not completely understood but it is thought that it disrupts networks involved in seizure propagation (Chiken & Nambu, 2016). According to the SANTE (Stimulation of the Anterior Nucleus of the Thalamus for Epilepsy) trial, the most frequent adverse effects were implant site pain or paresthesia (in 23%), implant site infection (in 12.7%) and lead misplacement (in 8.2%) (Salanova et al., 2015; Starnes et al., 2019). It was shown that DBS may cause depression and memory impairment (Sprengers et al., 2017; Starnes et al., 2019). In terms of efficacy, the SANTE trial shows a median seizure rate reduction of 69% percent after 5 years of follow up (R. Fisher et al., 2010; Salanova et al., 2015). Other DBS targets might see different results, so these results may not be indicative of the efficacy with other stimulation targets.

- **Responsive neurostimulation (RNS)** is achieved through a closed-loop device that detects epileptogenic activity and focally stimulates to inhibit seizure activity. It consists of a pulse generator implanted under the scalp with a lead placed in the ictal onset zone, and an external computer with which the personal therapeutic parameters can be set (Matias et al., 2019). RNS delivers seizure frequency reduction, as well as long-term iEEG (Matias et al., 2019; Starnes et al., 2019). Reported adverse effects were typical for neurostimulation devices but were never severe (Nair et al., 2020). In terms of efficacy, a randomized controlled trial showed median seizure reduction of 53% 2 years after implantation (Bergey et al., 2015) and long-term improved quality of life and cognitive domains were reported (Nair et al., 2020). Not available in Germany due to data protection laws.
- **Honorable mentions** include chronic subthreshold cortical stimulation, transcranial magnetic stimulation (TMS), transcutaneous vagus nerve stimulation, and trigeminal nerve stimulation (Boon et al., 2018; Starnes et al., 2019). We won't be discussion these in detail, as there isn't any good clinical data available as of yet, they remain something to keep an eye on for the future (Fattorusso et al., 2021).

Transcranial Direct Current Stimulation (tDCS)

Transcranial Direct Current Stimulation (tDCS) introduces a constant, low direct current into the brain using electrodes which are attached to the scalp. It can either raise or lower focal brain excitability (Nitsche & Paulus, 2000). It has been investigated to improve memory and reduce anxiety, stress, and depression in patients with epilepsy (Gouveia et al., 2021; Meisenhelter & Jobst, 2018). Interesting in regard to this study though is the efficacy, safety, and tolerability of tDCS as a treatment for DRE: Side effects were consistently reported as mild and transient (Vanhaerents et al., 2020), while seizures were not induced as previously feared (Sudbrack-Oliveira et al., 2021). Clinical trials of tDCS epilepsy therapy have shown efficacy in terms of significant decreases of IEDs and seizure frequency, however they still differ too largely regarding samples and methodology (Sudbrack-Oliveira et al., 2021) and weren't always conclusive in regard to efficacy (San-Juan et al., 2017). Even a single tDCS session could invoke an antiepileptic effect (Auvichayapat et al., 2013; Fregni et al., 2006) but persistency and strength were further improved by repeated treatments (San-Juan et al., 2017; Yang et al., 2020), a "refresh" intervention within the after-effect of the first intervention (Monte-Silva et al., 2010; Yang et al., 2020), as well as enhanced stimulation durations (Shekhawat et al., 2016). The clinical trial discussed in this thesis is, to my knowledge, the first that doesn't use a 2-Patch montage. The 2-Patch montage tDCS might produce inconsistent results due to broadly distributed electric fields in the brain, as well as intra- and inter-subject variability (Khan et al., 2022). The personalized and dCMI optimized multi-channel montage used for this trial delivers excellent intensity, focality, and directionality with an optimized trade-off between these attributes (Khan et al., 2022; Marios Antonakakis, 2021). This approach requires personalized head volume conductor forward modeling which is laborious compared to the "plug and treat" nature of 2-Patch tDCS but fortunately, diligent presurgical examination in epilepsy already includes most of this extra work.

Methods

Ethics Statement and Patient

The study protocol was approved by the local ethics committee and the patient provided written informed consent prior to the beginning of the study. The patient is 23 years old and possesses a normal intellectual state without focal neurological deficits. Epilepsy was first diagnosed at the age of 14, with seizure semiology mainly being distributed thinking and an inability to speak or follow a conversation. They did not experience any motor symptoms or impairment of awareness. The seizure frequency was four times per day. The patient did not achieve freedom from seizures despite treatment with multiple AEDs, so their diagnosis was further specified as DRE. Even though semiology is and was rather mild, the patient was highly disturbed by the seizures. Presurgical evaluation was performed. Non-invasive video-EEG monitoring showed seizure onset in the left frontal area. FDG-PET showed hypometabolism in the left superior frontal gyrus suggesting a functional deficit zone. Based on the evidence derived from non-invasive video-EEG, MRI, and FDG-PET, iEEG was performed but the actual epileptogenic zone was unfortunately missed. An FCD type IIb was only found in T1w-MRI after consideration of MEEG source estimation of IEDs. The FCD is located in very close proximity to Broca's area (which could explain seizure semiology) which is eloquent cortex, so resection would have been associated with high risk of aphasia. No resection was recommended, several unsuccessful AED polytherapies followed. In 2019, another MEEG recording was performed, finding 1050 IEDs while AED therapy was put on hold, so that source estimation could happen. The patient has kept a seizure diary.

Study Design

The goal of this double-blind sham-controlled clinical trial is to investigate the effect of personalized and dCMI-optimized tDCS on IED frequency. Therefore, we stimulated the patient twice in one block (1st 20 mins stimulation, 2nd 20 mins break, 3rd 20 mins stimulation: total one-hour block) every day for 5 days in a single week. For control, we developed an ActiSham stimulation montage, in which we stimulate the patient with adjacent cathodes and anodes (in the same positions as the dCMI-optimized montage) to minimize stimulating the brain but maximize the sensation of stimulation in the scalp. Since we assumed the patient to be accustomed to pain because of a life with refractory epilepsy and their desire to receive a treatment that feels real,

we decided to forgo anesthetizing the scalp with a local anesthetic like Lidocaine. The side effects of tDCS have historically been very mild and don't compare in magnitude with the suffering that epilepsy can bring. The ActiSham was also applied 5 times in a single week just after the patient had 5 weeks of rest to recuperate from the effects of the stimulation, so that we had as close circumstances for the control to the initial stimulation as possible. One-hour blocks of EEG were taken directly before and after the stimulation block every day and the first day of the Stimulation-, as well as the first day of the ActiSham week, saw a two-hour block of EEG before the first Stim/ActiSham block to form a baseline. In the analysis, data of interest from this two-hour block is averaged into a one-hour block, unless otherwise stated.

Since the amount of IEDs can vary even from hour to hour due to circadian rhythms (Langdon-Down & Russell Brain, 1929), it was important for this study to always measure IED amount at the same times of day. Additionally, ActiSham was also used to control for unknown underlying ultradian rhythms becoming out of sync between days (Spencer et al., 2016).

Lastly, it is important to mention, that EEG measurements and stimulation blocks were conducted under medical supervision in the University Clinic Münster by medical staff that was blinded to the design of the study. The management and control software for tDCS was set up by me beforehand and stimulation parameters were hidden to those actually performing tDCS.

tDCS Hardware

A StarStim® device developed by Neuroelectronics Barcelona SL (Neuroelectronics, 2015) was used for tDCS together with the NE019 Neoprene Headcap from the same company with 39 predefined positions based on a subset of the 10-10 EEG system. Automatic impedance checking was applied before every stimulation. Ramp in and ramp out time was 60 seconds each.

tDCS Montages

Current Density in A/m ²	dCMI $\lambda = 80$	ActiSham
In Target Area	0.2986	0.0405
In Non-Target Area	0.0874	0.0121
Directionality	0.2124	0.0318

Table 2

Shows Current Density in A/m² for the dCMI montage with a λ of 80 and the ActiSham montage. The values for ActiSham are very small which implies near zero efficacy.

dCMI optimized

The dCMI montage for the main treatment was created by Dr. Antonakakis using his pipeline, for detailed information, please refer to his dissertation (Marios Antonakakis, 2021). It combines automatic segmentation of 6 head tissue types from T1- and T2w-MRI with manual segmentation of burr holes (from iEEG) from CT, accounting for white matter and gray matter tissue conductivity anisotropy with DTI (diffusion tensor imaging), calibration of skull conductivity with SEP/SEF (somatosensory evoked potential or field) source estimation as ground truth, and finally, calculation of tDCS montage with optimization using dCMI (Khan et al., 2022, 2019).

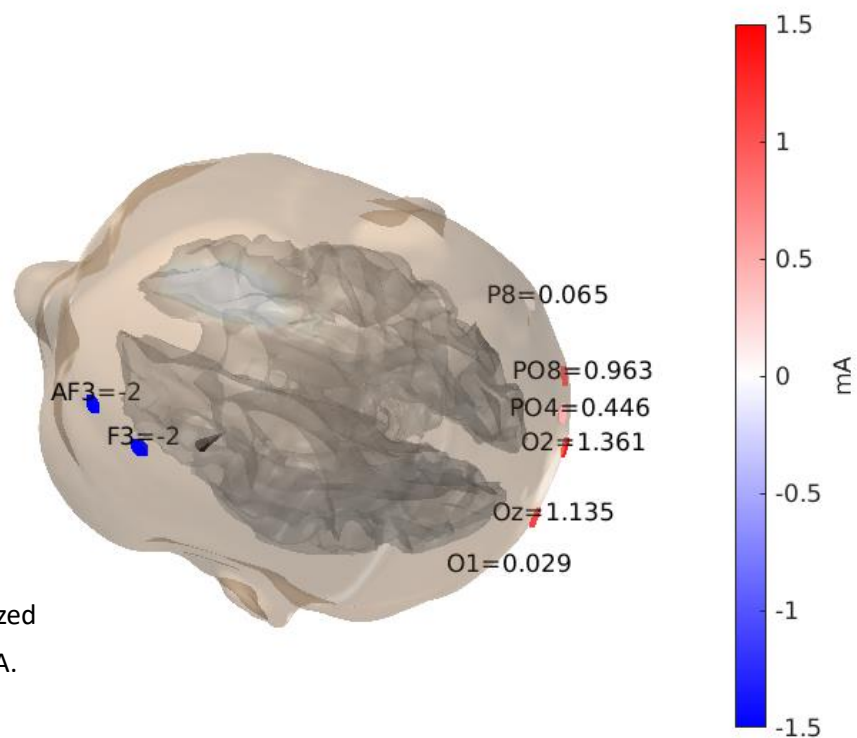


Figure 7

Shows the dCMI optimized montage with current in A.

ActiSham

The ActiSham montage is the same as the dCMI optimized montage when it comes to electrode positions. The difference lies in the applied current: AF3: -2 mA, F3: 2 mA, O2: 2 mA, Oz: -2 mA and the rest: 0 mA.

EEG Data Acquisition

EEG measurements in this study were acquired by an EEG Machine (Nihon Kohden, Tokyo, Japan) with a sampling frequency of 200 Hz with 19 electrodes placed in the tDCS headcap as a subset of the 10-10 system.

IED Detection

IED markings were performed by three experienced epileptologists. The EEG data files were cut into 1-hour segments, completely anonymized, and labeled with code names, so that the epileptologists had no information about time or order, they were completely blinded. The data was securely exchanged through password protected zipped packages over Sciebo (Vogl et al., 2015) according to ERA PerMed approved PerEpi data management plan (ERA PerMed, n.d.) and IEDs were marked by eye using the software BESA (Scherg et al., 2018).

Source Estimation

Source estimation was performed with CURRY 8 (Compumedics Neuroscan, 2022) on IED averages. To obtain these averages, the EEG data was first rereferenced to the common average and epoched from 50 ms before IED peak to 100 ms after. The epochs were temporally peak corrected with a custom MATLAB tool (Aydin et al., 2014), which was only possible for markings from epileptologists 1 and 3, since the second epileptologist didn't consistently mark spikes at even roughly the same propagation phase of the epileptic activity.

Irritatingly, all current densities calculated with CURRY 8 are in μAmm^{-2} but the output shows μAmm .

Statistical Analysis

It was shown that IEDs follow a multidienn rhythm in most subjects, which most of the time possesses an even greater magnitude than circadian modulations (Baud et al., 2018). This means that even though we have only investigated one subject so far and are not considering a group of people, the IED frequency on any given day can be vastly different than on the next even in that same patient. As we will see in the data, that assumption seemed to hold true. I decided, that to control for this effect, measurements of IED frequency before and after any given Stim/ActiSham block should be paired (or dependent) while data measured on different days should be considered independent. So statistically speaking, "PrePost" treatment is a within-subjects factor, while the "subjects" are the days of treatment. Statistics really can be confusing, can't it? Our first between-subject factor is "TypeOfTreatment" and the second is "Epileptologists" because experience and personality decide how many IEDs each epileptologist considers to be true and not some unrelated activity or noise.

To test for group effects, a mixed ANOVA was applied to the data. Assumptions of normality were tested with Shapiro-Wilk while homoscedasticity was investigated with Levene's Test. Sphericity on the other hand is given, since the within-subject factor "PrePost" only has two steps. Post-hoc multiple comparisons were elucidated by Tukey's HSD (honestly significant difference) test.

Questionnaires

We used standard questionnaires from the latest reviews for tDCS (Antal et al., 2017) and specialized questionnaires adapted to the patient's specific form of focal epilepsy to assess tolerability and symptoms during and after tDCS as well as relevant patient information. For example, in the specialized questionnaires we asked for problems regarding speech-production during stimulation. Sensations during the stimulations were assessed on a 5-point numerical rating scale (1 = no sensation, 5 = extreme sensation). Results were reported in mean, standard deviation, and ranges for quantitative data. Comparisons in intensity of sensations between personalized and dCMI optimized tDCS and ActiSham were made using Lilliefors test to assess normality, two-sample F-test of equality of variance to identify homo- or heteroscedasticity, two sample t-test for normal data and Wilcoxon rank-sum test for not normally distributed data. Every day the patient was asked about whether they thought they received a "real" stimulation or placebo.

Figures and Visualizations

Segmentation results were shown with FSLeaves (McCarthy, 2021). Average moving dipole locations and topographies of scalp potentials were visualized with CURRY 8 (Compumedics Neuroscan, 2022). Other results were visualized with custom MATLAB code, as well as the Statistics and Machine Learning Toolbox (MathWorks, 2021b) from MATLAB (MathWorks, 2021a). Tables were created with Microsoft Excel (Microsoft Corporation, 2022). Thesis was written in Microsoft Word (Microsoft Corporation, 2022) and exported to PDF.

Results

IED Frequency

Statistical Analysis

Mixed ANOVA Assumptions

Test for Normality	Shapiro-Wilk p
Stim/Epileptologist 1	0.3328
ActiSham/Epileptologist 1	0.5809
Stim/Epileptologist 2	0.0185
ActiSham/Epileptologist 2	0.5415
Stim/Epileptologist 1	0.3328
ActiSham/Epileptologist 2	0.3531

Table 3

Tests for Normality with Shapiro-Wilk. Normality is only rejected for the “Stim/Epileptologist 2” data group.

The only group of data that saw its assumption of normality being rejected was “Stim/Epileptologist 2” ($p < 0.05$) (**Table 3**). We will see that this is explained by the outlier found in the “Stim/Epileptologist 2” group in **Figure 10**. Mixed ANOVA is quite robust in terms of a rejected normality assumption (Glass et al., 1972; Harwell et al., 1992), especially for only a small part of the overall data. The risk in this case is generally that the result won’t be significant. I decided not to correct for it. Levene’s test confirmed homoscedasticity between groups for every step of our within-subject factor (**Table 4**).

Group Summary Table			
Group	Count	Mean	Std Dev
Pre	30	456.117	519.515
Post	30	267.033	294.641
Pooled	60	361.575	422.32
Levene's statistic (quadratic)	2.26385		
Degrees of freedom	1, 58		
p-value	0.13785		

Table 4

Homoscedasticity between groups established using Levene’s test ($p > 0.05$).

Mixed ANOVA Results

Mixed ANOVA Results	SumSq	DF	MeanSq	F	pValue	pValueGG	pValueHF	pValueLB
(Intercept):PrePost	536287.6	1	536287.6	18.176224	0.0002346	0.0002346	0.0002346	0.0002346
Epileptologists:PrePost	407203.51	2	203601.75	6.900609	0.0039446	0.0039446	0.0039446	0.0039446
TypeOfTreatment:PrePost	232939.7	1	232939.7	7.8949507	0.0092908	0.0092908	0.0092908	0.0092908
Error(PrePost)	767127.31	26	29504.896	1	0.5	0.5	0.5	0.5

Table 5

Shows the mixed ANOVA results of effects of within-subject factor “PrePost” and its interactions with between-subject factors “Epileptologists” and “TypeOfTreatment” on the dependent variable “IED Frequency”.

There was a statistically significant main effect of “PrePost” on “IED Frequency”, $F(1,26)=18.18$, $p<0.001$, a statistically significant interaction between “PrePost” and “Epileptologists”, $F(2,26)=6.9$, $p<0.01$ and a statistically significant interaction between “PrePost” and “TypeOfTreatment”, $F(1,26)=7.89$, $p<0.01$ (**Table 5**).

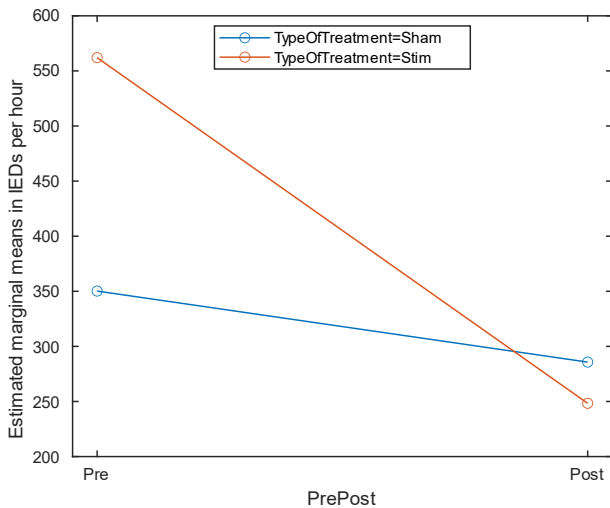


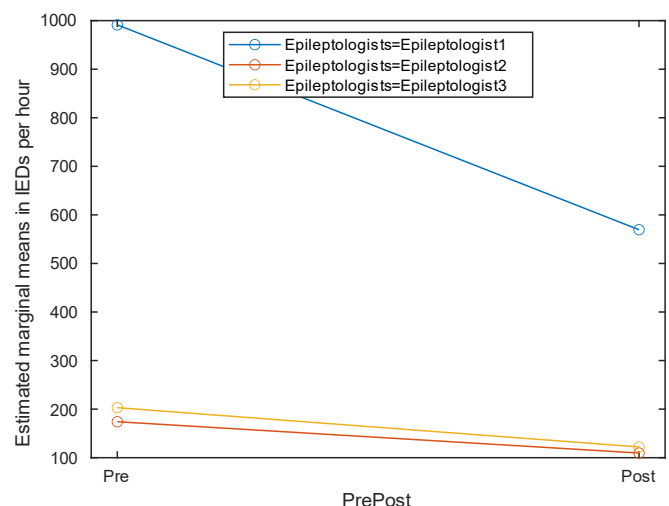
Figure 8

Shows interaction effect of “PrePost” and “TypeOfTreatment” on IED Frequency.

Because interaction “TypeOfTreatment*PrePost” is disordinal (the orange and blue lines cross, **Figure 8**), the main effect of “PrePost” on IED Frequency cannot be sensibly interpreted (Pedhazur & Schmelkin, 1991). At the same time, we can see, that no matter which type of treatment was applied or which epileptologist marked IEDs, IED frequency is reduced after treatment as compared to before (**Figures 8, 9**).

Figure 9

Shows interaction effect of “PrePost” and “Epileptologists” on IED Frequency.



Post-Hoc Multiple Comparisons

TypeOfTreatment	PrePost	PrePost	Difference	StdErr	pValue	Lower (5% CI)	Upper (95% CI)
Stim	Post	Pre	-313.7	62.721497	3.34744E-05	-442.62588	-184.7741
Sham	Post	Pre	-64.466667	62.721497	0.313500262	-193.39255	64.459217

Table 6

Shows the Tukey-HSD results of effects of stages of between-subject factor “TypeOfTreatment” on the difference in IED Frequency between levels of within-subject factor “PrePost”.

According to the Tukey-HSD, IED frequency after treatment (“Post”) differed significantly from IED frequency before treatment (“Pre”) when applying personalized and dCMI-optimized tDCS (“Stim”) as treatment (-313.7, $p < 0.00001$) but didn’t differ significantly when applying ActiSham (“Sham”) as treatment (-64.47, $p > 0.05$) (**Table 6**).

Epileptologists	PrePost	PrePost	Difference	StdErr	pValue	Lower (5% CI)	Upper (95% CI)
Epileptologist1	Post	Pre	-421.9	76.817832	9.21286E-06	-579.80131	-263.9987
Epileptologist2	Post	Pre	-64.45	76.817832	0.4091185	-222.35131	93.451314
Epileptologist3	Post	Pre	-80.9	76.817832	0.301965858	-238.80131	77.001314

Table 7

Shows the Tukey-HSD results of effects of stages of between-subject factor “Epileptologists” on the difference in IED Frequency between levels of within-subject factor “PrePost”.

According to the Tukey-HSD, IED frequency after treatment (“Post”) differed significantly from IED frequency before treatment (“Pre”) when Epileptologist 1 marked IEDs (-421.9, $p < 0.000001$) but didn’t differ significantly when Epileptologist 2 (-64.45, $p > 0.05$) or Epileptologist 3 (-80.9, $p > 0.05$) marked IEDs (**Table 7**). The mean difference is obviously higher for Epileptologist 1 due to Epileptologist 1 marking 17012 spikes for the whole study as compared to only 3049 and 3657 spikes marked by Epileptologists 2 and 3, respectively.

Relative Frequency of IEDs – Comparison between Factors

The relative frequency of IEDs left after treatment is the amount of IEDs per hour EEG after treatment divided by the amount of IEDs per hour EEG before treatment. The data is visualized in a box chart in **Figure 10**.

1. For “Epileptologist1” and
 - i. “Stim” the median is 34.08%, the quartiles are 31.14% and 57.14%, and the nonoutlier minimum and maximum are 23.56% and 68.76%, respectively.
 - ii. “Sham” the median is 74.67%, the quartiles are 64.61% and 93.03%, and the nonoutlier minimum and maximum are 59.83% and 120.7%, respectively.
2. For “Epileptologist2” and
 - i. “Stim” the median is 25.59%, the quartiles are 13.81% and 65.82%, and the nonoutlier minimum and maximum are 7.87% and 65.82%, respectively.
 - ii. “Stim” there is an outlier at 162.4% (Day 1).
 - iii. “Sham” the median is 106.6%, the quartiles are 46.19% and 360.4%, and the nonoutlier minimum and maximum are 14.29% and 820.7%, respectively.
3. For “Epileptologist3” and
 - i. “Stim” the median is 41.55%, the quartiles are 28.87% and 66.87%, and the nonoutlier minimum and maximum are 4.07% and 75%, respectively.
 - ii. “Sham” the median is 85.13%, the quartiles are 47.52% and 113.6%, and the nonoutlier minimum and maximum are 47.42% and 150.8%, respectively.

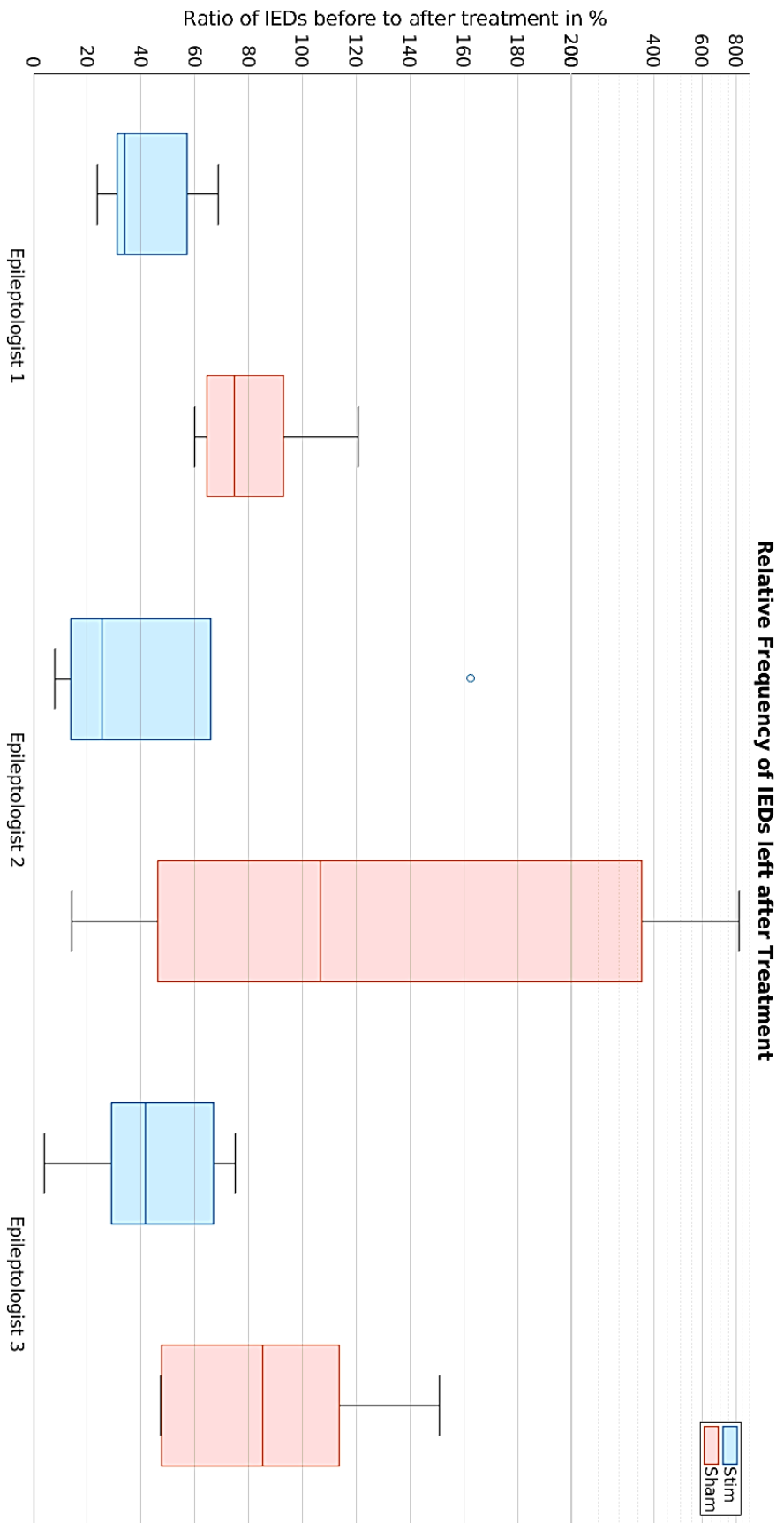


Figure 10

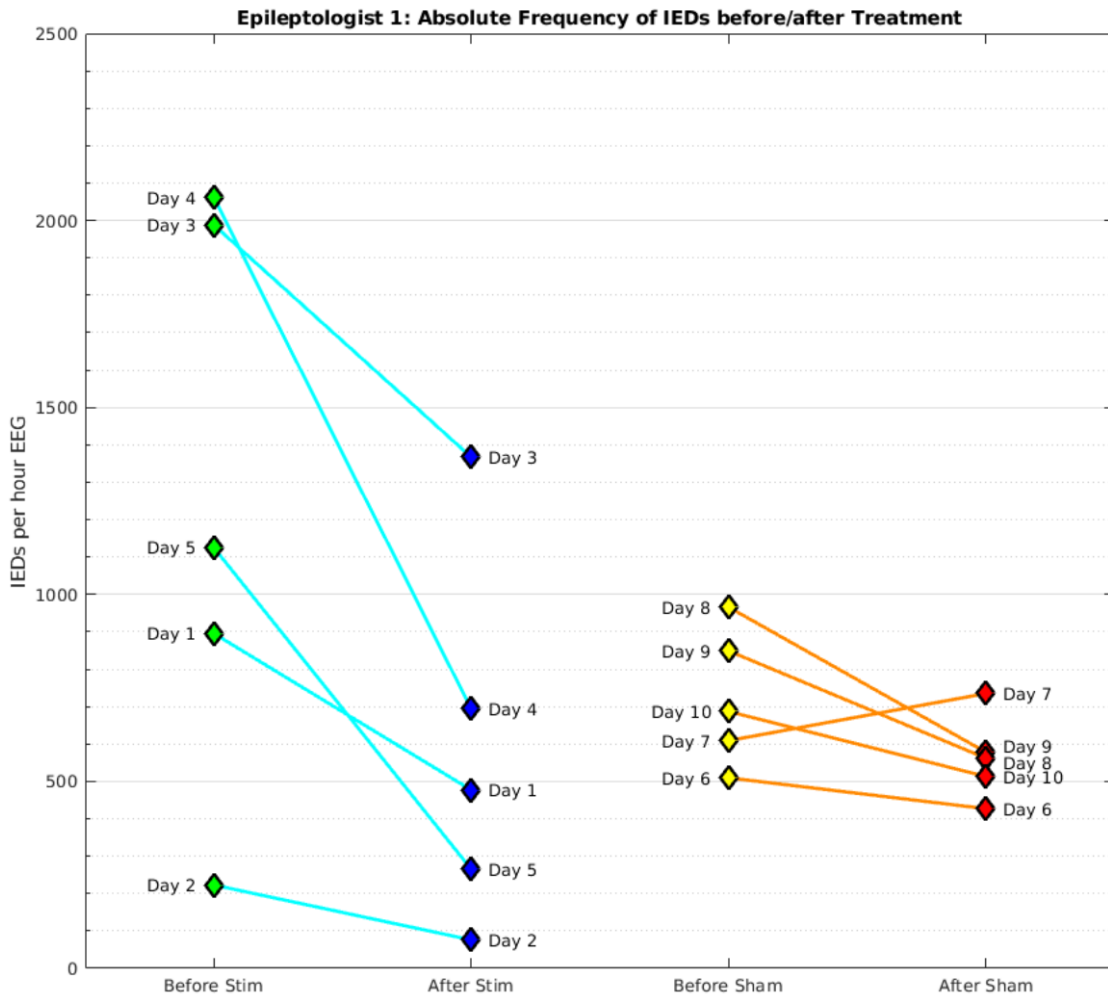
Shows box plot for relative frequency of IEDs after treatment to before treatment for every "Epileptologists" "TypeOfTreatment" combination. There is an outlier in the "Stim/Epileptologist2" data group.

Absolute Frequency of IEDs in Detail

Frequency of IEDs is always higher before “Stim” than after “Stim” for all Epileptologists except for Epileptologist 2 (**Figure 12**). This increase is the outlier in **Figure 10** and the reason for the violation of normality for its data group (**Table 3**). Epileptologist 2 reported that they had difficulty with a persistent strong artifact in one of the EEG files on the first day of “Stim” and couldn’t mark as many IEDs as they otherwise could have. Only after the blind status of the epileptologists had been lifted did Epileptologist 2 manage to subdue said artifact. But then it was too late to include new data into the analysis without possibly introducing bias. Comparing the frequency of IEDs before and after “Sham” reveals that it can show an increase or decrease, as well as stay the same (**Figures 11,12 and 13**). The different frequency scales (y scales) in these figures are explained by the difference in total and average spikes found by each epileptologist.

Figure 11

Shows frequency of IEDs before and after treatment (“PrePost”) for every day and “TypeOfTreatment” with data marked by Epileptologist 1.



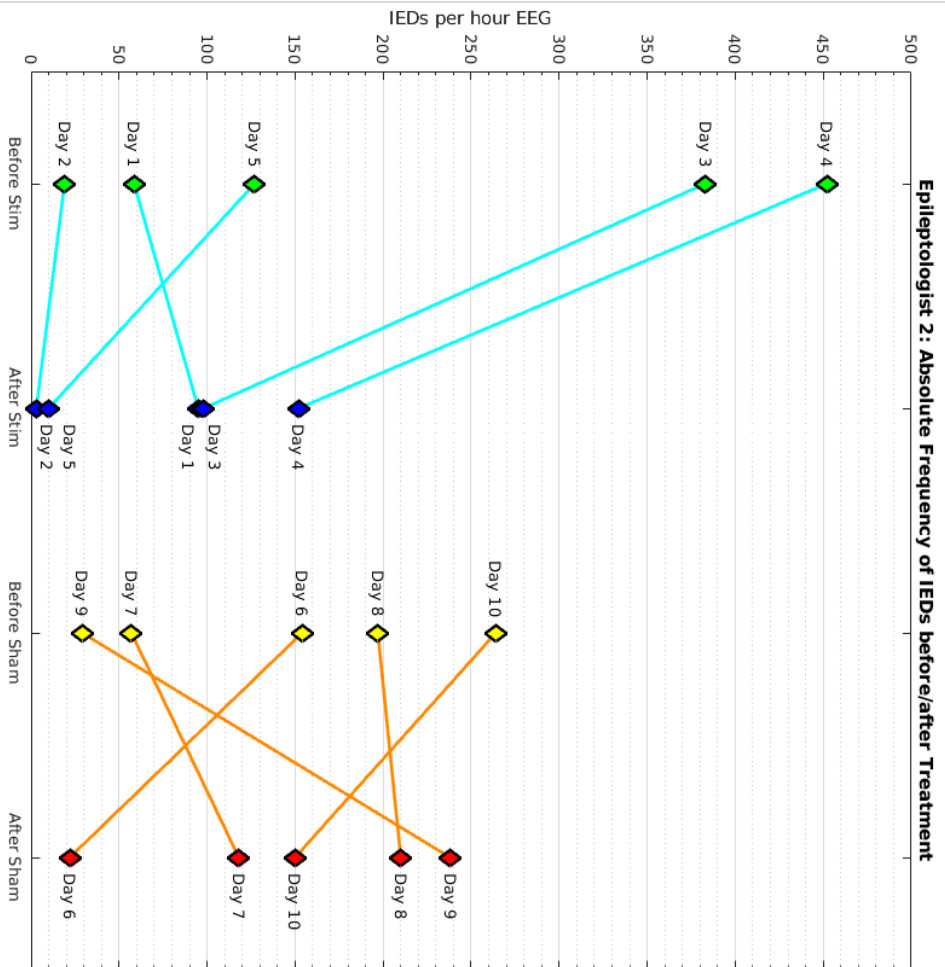


Figure 12

Shows frequency of IEDs before and after treatment (“PrePost”) for every day and “TypeOfTreatment” with data marked by Epileptologist 2.

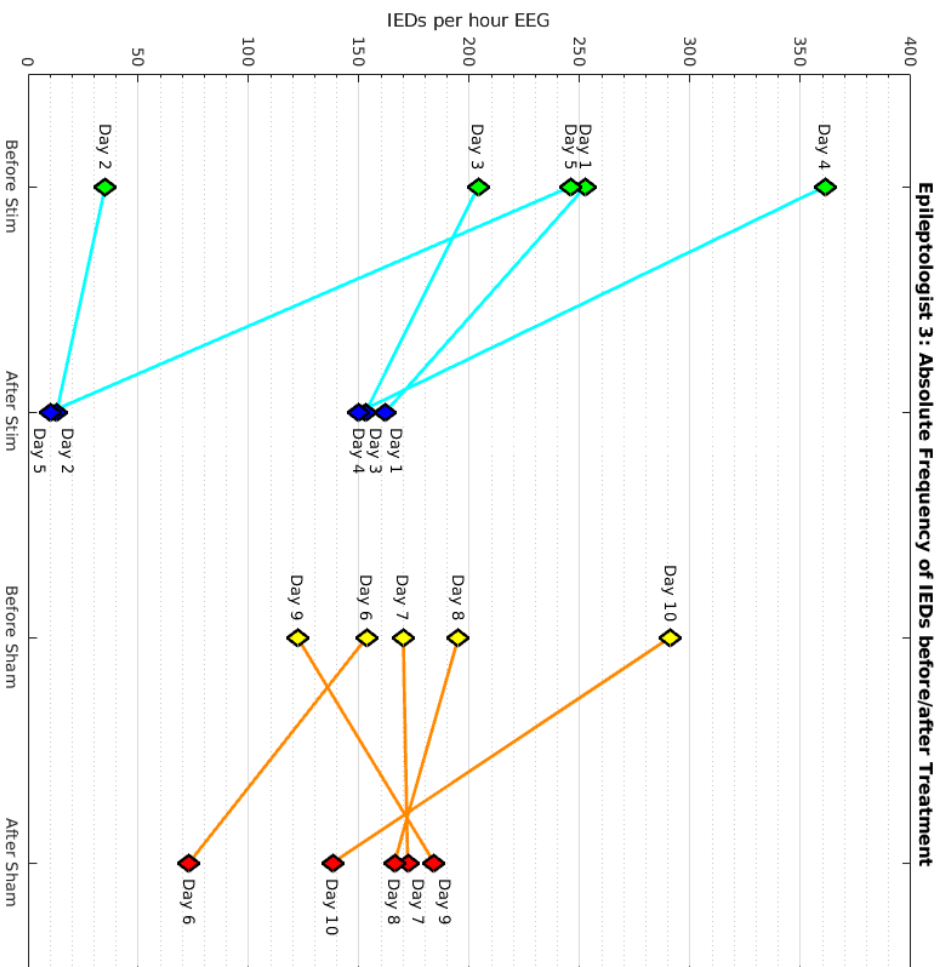


Figure 13

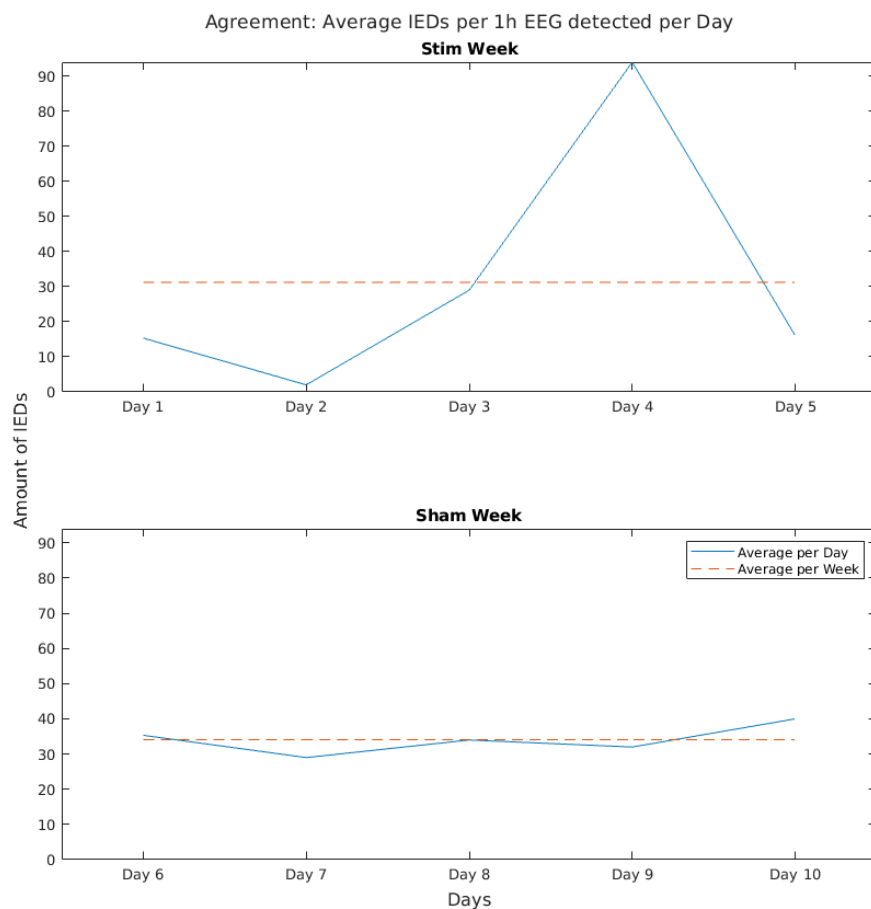
Shows frequency of IEDs before and after treatment (“PrePost”) for every day and “TypeOfTreatment” with data marked by Epileptologist 3.

IED Frequency Evolution over Time

In the “Stim” week, the patient reported a seizure which was uncharacteristically muted in terms of usual symptoms: they were having a conversation with a significant other when a seizure hit. Usually, the patient would forget the conversation and be retold after the seizure ends. This time, they weren’t able to speak during the seizure but were able to continue the conversation right after it ended. Unfortunately, at the time of the release of this thesis, I don’t have access to the patient’s seizure diary, so I cannot say whether it was on day 2, 3 or 4. This will be remedied in time for the publication of this study. Additionally, the patient reported slowed speech on day 2 and 4 when discussing more complex topics, while having trouble finding the right words to say on all 3 days (day 2, 3 and 4). Furthermore, they reported to experience heightened difficulty understanding language in general on day 3.

According to the literature (Baud et al., 2018), seizures preferentially occur during the rising phase of multidien IED cycles, which correlates to the rising flank in IED frequency over these 3 days (**Figure 14**), the reportedly increased symptoms and the actual seizure with peculiarly muted semiology.

Figure 14 Shows averaged daily frequency of IEDs over the “Stim” and “Sham” weeks. The IEDs considered for this figure are the ones that every epileptologist could agree on, hence the comparably low values. The average frequency of IEDs is 31.27 IEDs per hour for the “Stim” week and 34.07 IEDs per hour for the “Sham” week.



Source Estimation

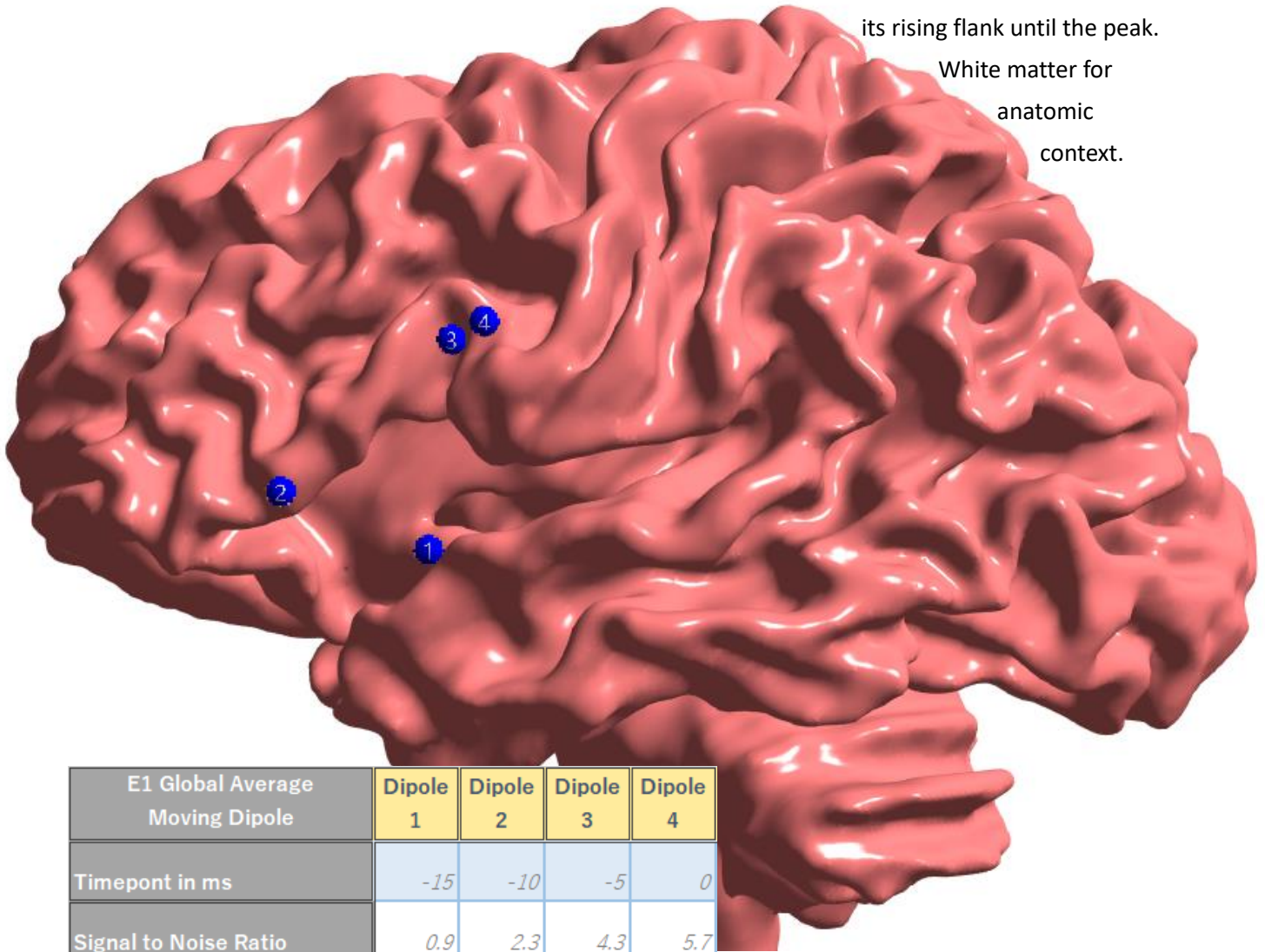
This part will be only a conglomeration of results. For convenience of the reader, any and all interpretations, as well as comparisons of particular interest, will be made in *Discussion*.

Epileptologist 1

Global Average Moving Dipole

Figure 15

Shows location of the Global Average Moving Dipole (of IEDs marked by Epileptologist 1) at different times during its rising flank until the peak. White matter for anatomic context.



E1 Global Average Moving Dipole	Dipole 1	Dipole 2	Dipole 3	Dipole 4
Timepont in ms	-15	-10	-5	0
Signal to Noise Ratio	0.9	2.3	4.3	5.7
Explained Signal	79%	84%	90%	83%
Current Density in μ Amm	27.1	38.3	75.7	134
Maximum Amplitude at 0 ms in μ V			Max at: F3	-9.37

Table 8

Epileptologist 1 Global Average Moving Dipole of IEDs. Summarizes information about dipoles of the rising flank of the average IED marked by Epileptologist 1.

0s

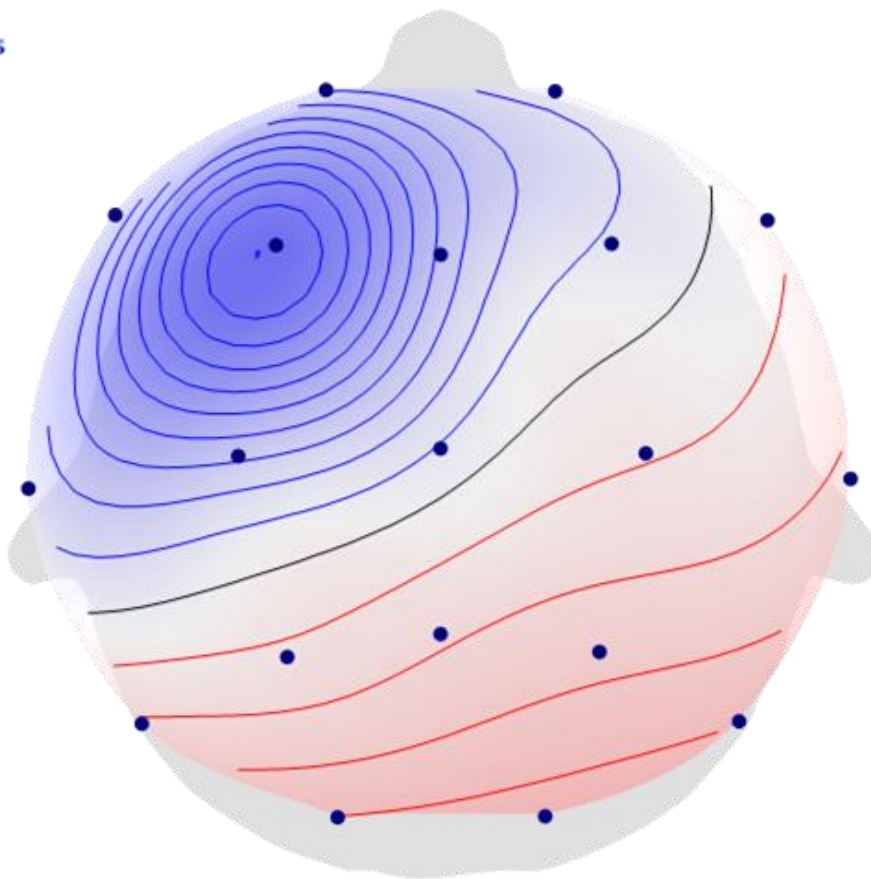
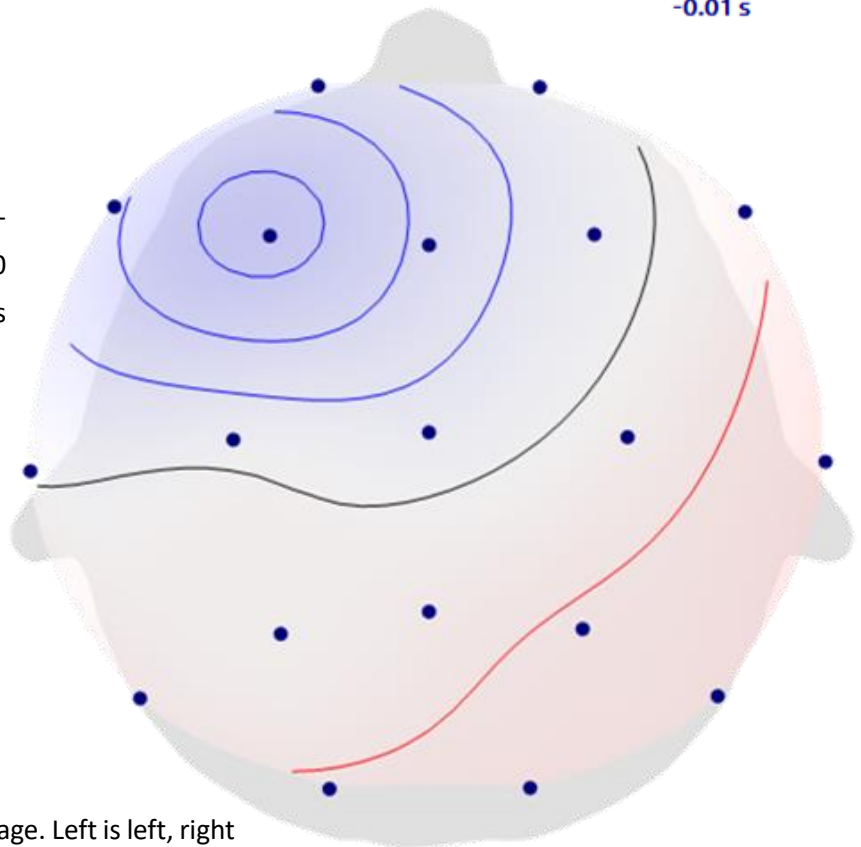
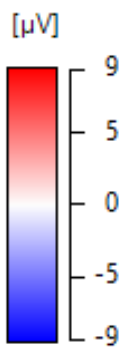


Figure 16
Shows topography of scalp potentials at the peak (0 ms) of the global average of IEDs marked by Epileptologist 1.

-0.01 s

Figure 17
Shows topography of scalp potentials at the rising flank (-10 ms) of the global average of IEDs marked by Epileptologist 1.

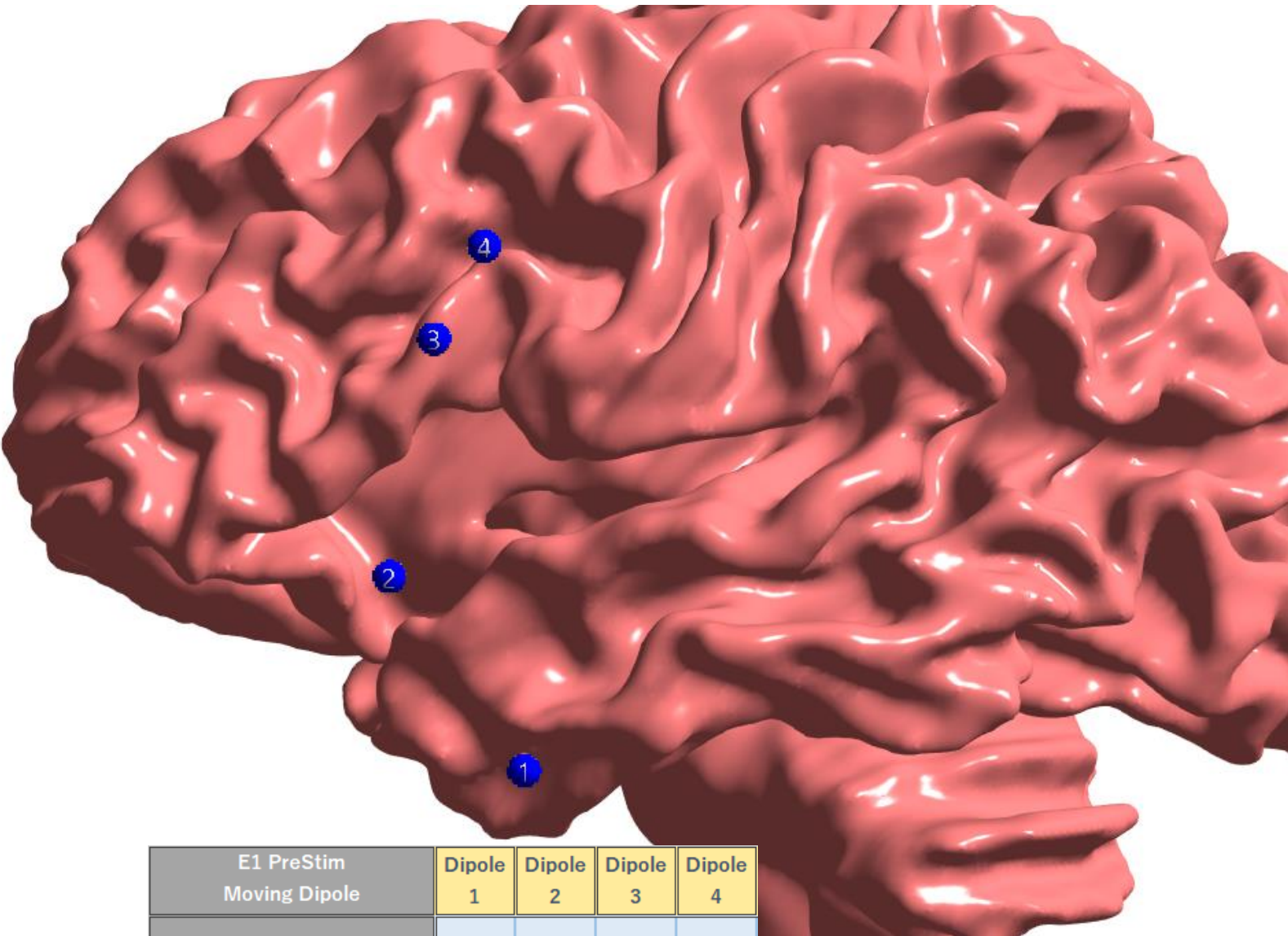


Scale for all Topologies on this page. Left is left, right is right, up is anterior and down is posterior.

PreStim Average Moving Dipole

Figure 18

Shows location of the PreStim Average Moving Dipole (of IEDs marked by Epileptologist 1) at different times during its rising flank until the peak. White matter for anatomic context.



E1 PreStim Moving Dipole	Dipole 1	Dipole 2	Dipole 3	Dipole 4
Timepont in ms	-15	-10	-5	0
Signal to Noise Ratio	0.9	2.3	4	5.1
Explained Signal	68%	81%	86%	83%
Current Density in μ Amm	37.4	65.3	105	136
Maximum Amplitude at 0 ms in μ V			Max at: F3	-9.55

Table 9

Epileptologist 1 PreStim Average Moving Dipole of IEDs. Summarizes information about dipoles of the rising flank of the average IED in the hour before “Stim” marked by Epileptologist 1.

0 s

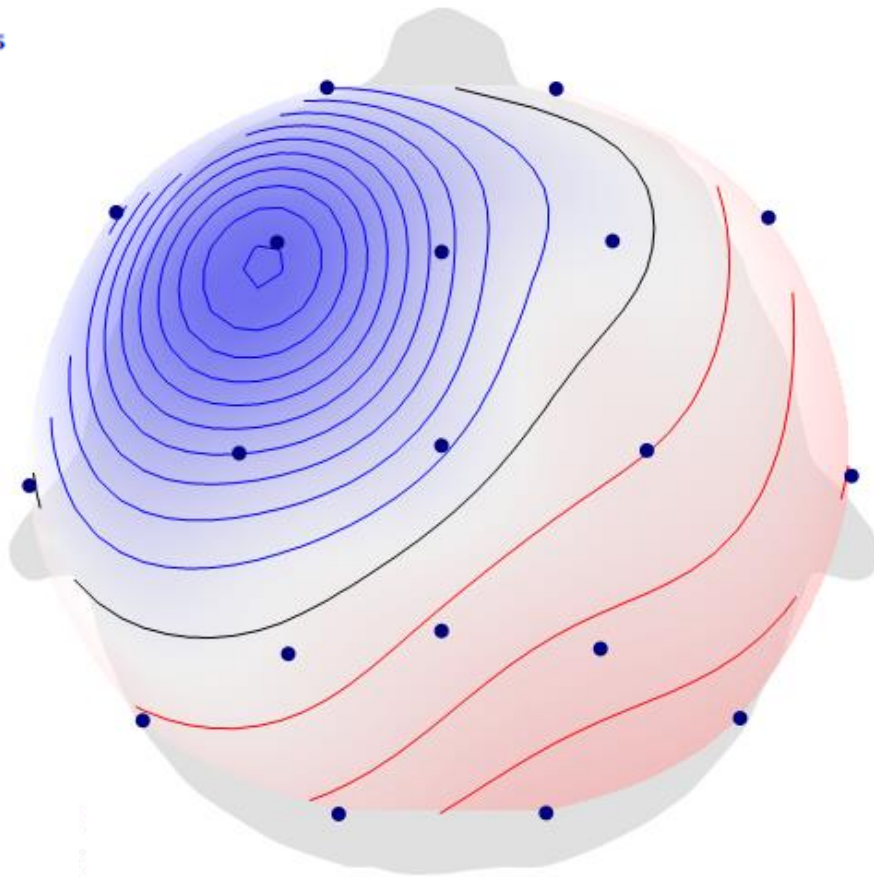
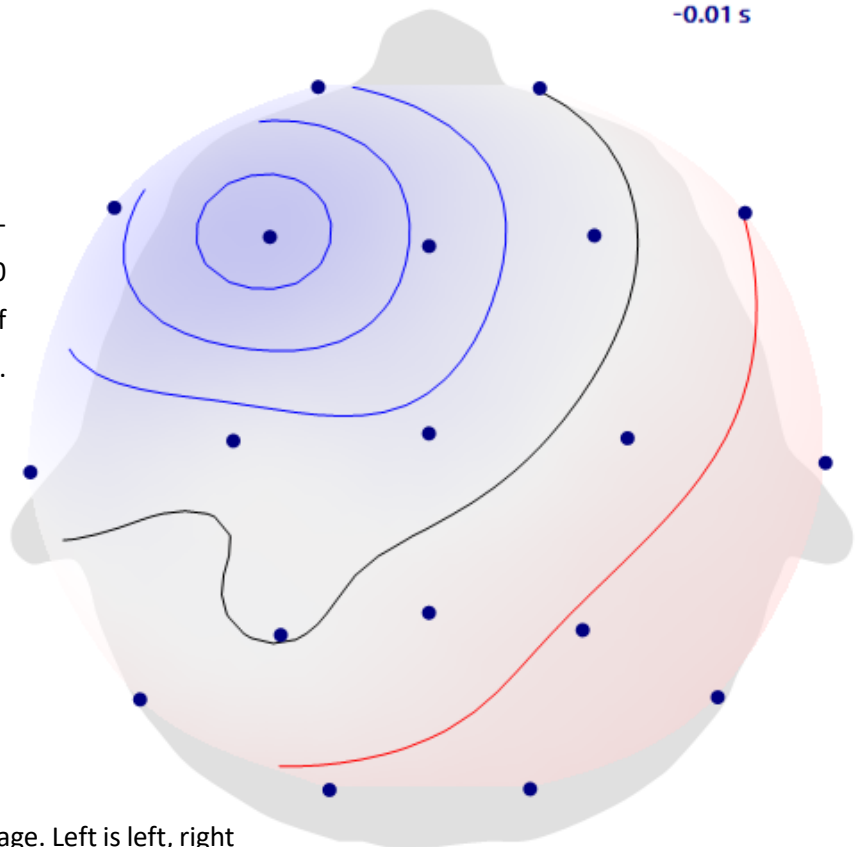
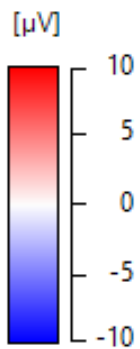


Figure 19
Shows topography of scalp potentials at the peak (0 ms) of the PreStim average of IEDs marked by Epileptologist 1.

-0.01 s

Figure 20

Shows topography of scalp potentials at the rising flank (-10 ms) of the PreStim average of IEDs marked by Epileptologist 1.

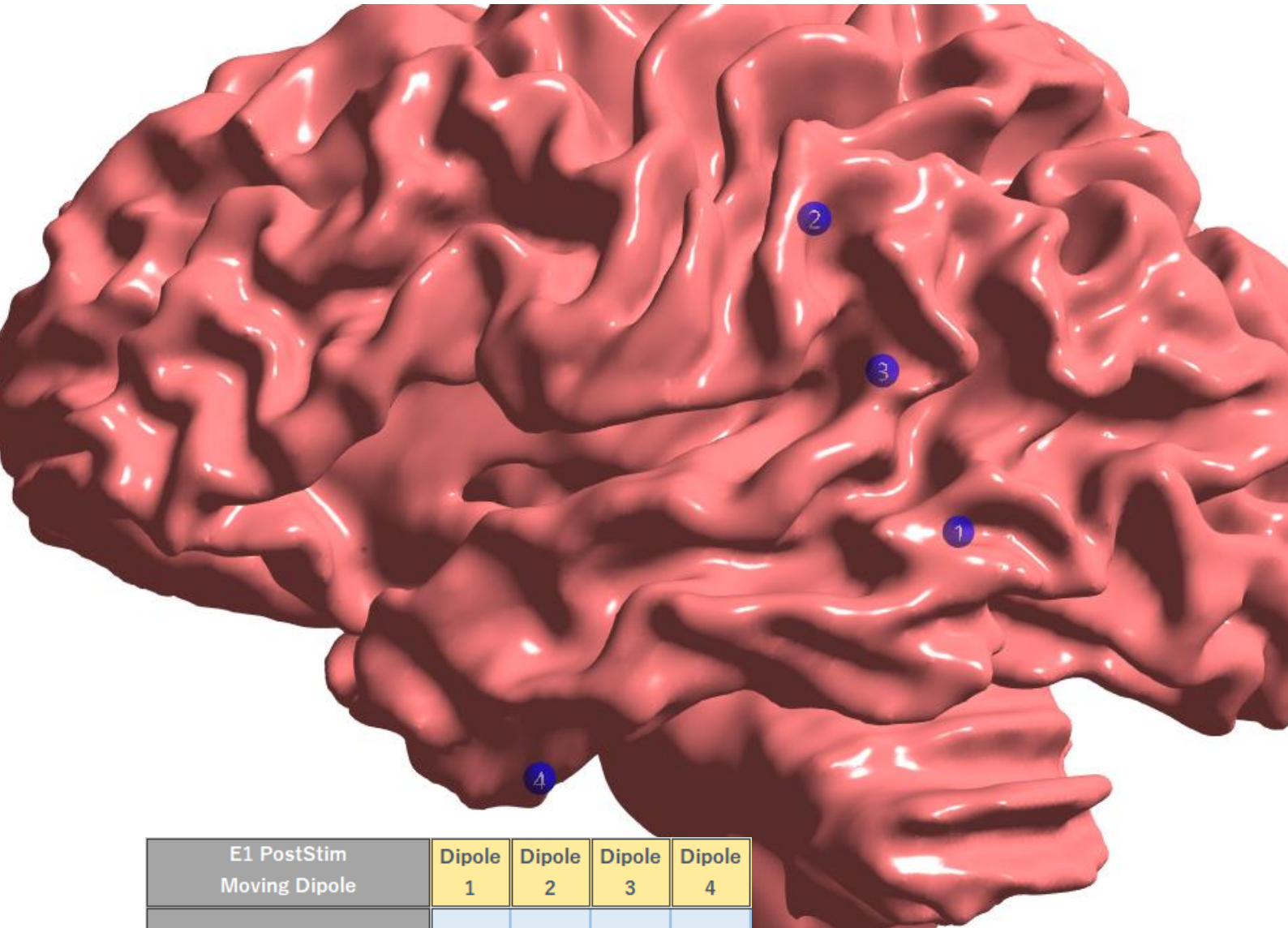


Scale for all Topologies on this page. Left is left, right is right, up is anterior and down is posterior.

PostStim Average Moving Dipole

Figure 21

Shows location of the PostStim Average Moving Dipole (of IEDs marked by Epileptologist 1) at different times during its rising flank until the peak. White matter for anatomic context.



E1 PostStim Moving Dipole	Dipole 1	Dipole 2	Dipole 3	Dipole 4
Timepont in ms	-15	-10	-5	0
Signal to Noise Ratio	0.8	1.1	2.8	5
Explained Signal	82%	81%	76%	71%
Current Density in μ Amm	11.6	10.2	36.9	155
Minimum and Maximum Amplitude at 0 ms in μ V	Min at: T3	-2.94	Max at: O1	3.105
Amplitude at F3 in μ V			F3	-2.44

Table 10

Epileptologist 1 PostStim Average Moving Dipole of IEDs. Summarizes information about dipoles of the rising flank of the average IED in the hour after “Stim” marked by Epileptologist 1.

0s

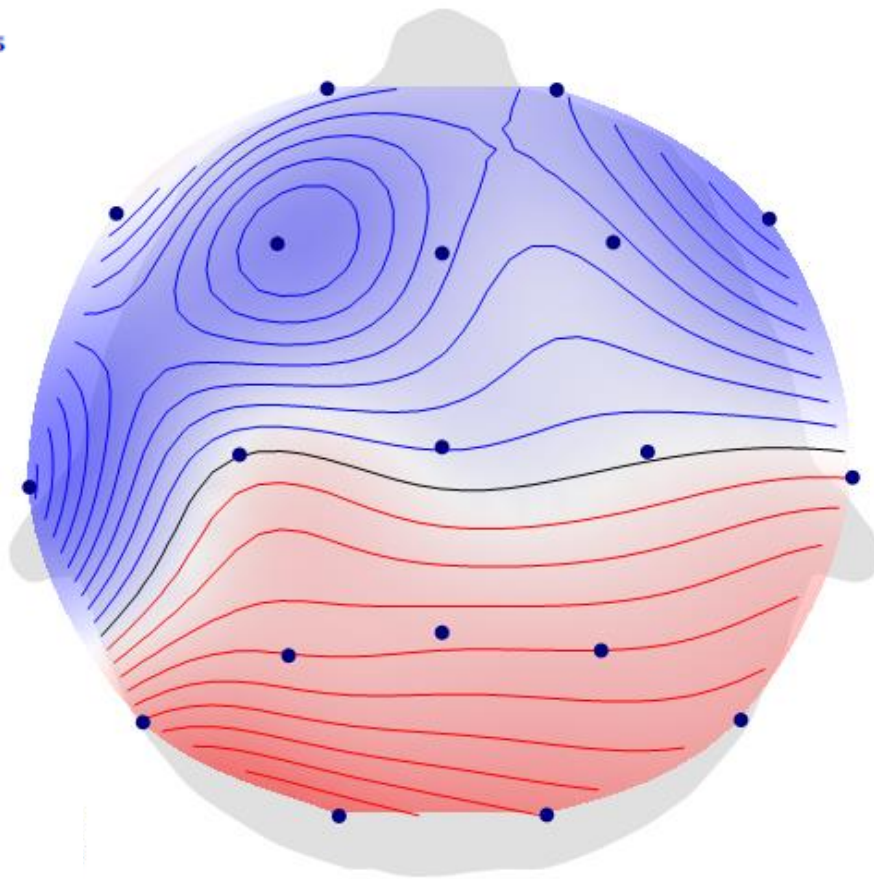
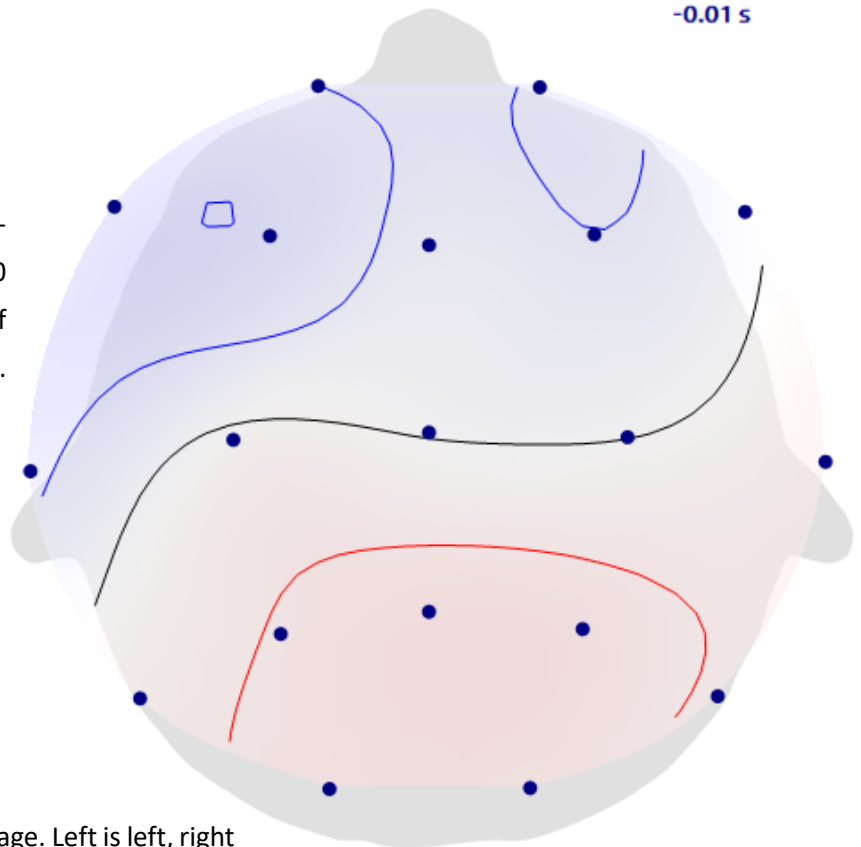
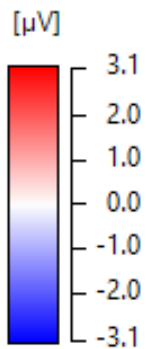


Figure 22
Shows topography of scalp potentials at the peak (0 ms) of the PostStim average of IEDs marked by Epileptologist 1.

Figure 23
Shows topography of scalp potentials at the rising flank (-10 ms) of the PostStim average of IEDs marked by Epileptologist 1.

-0.01 s

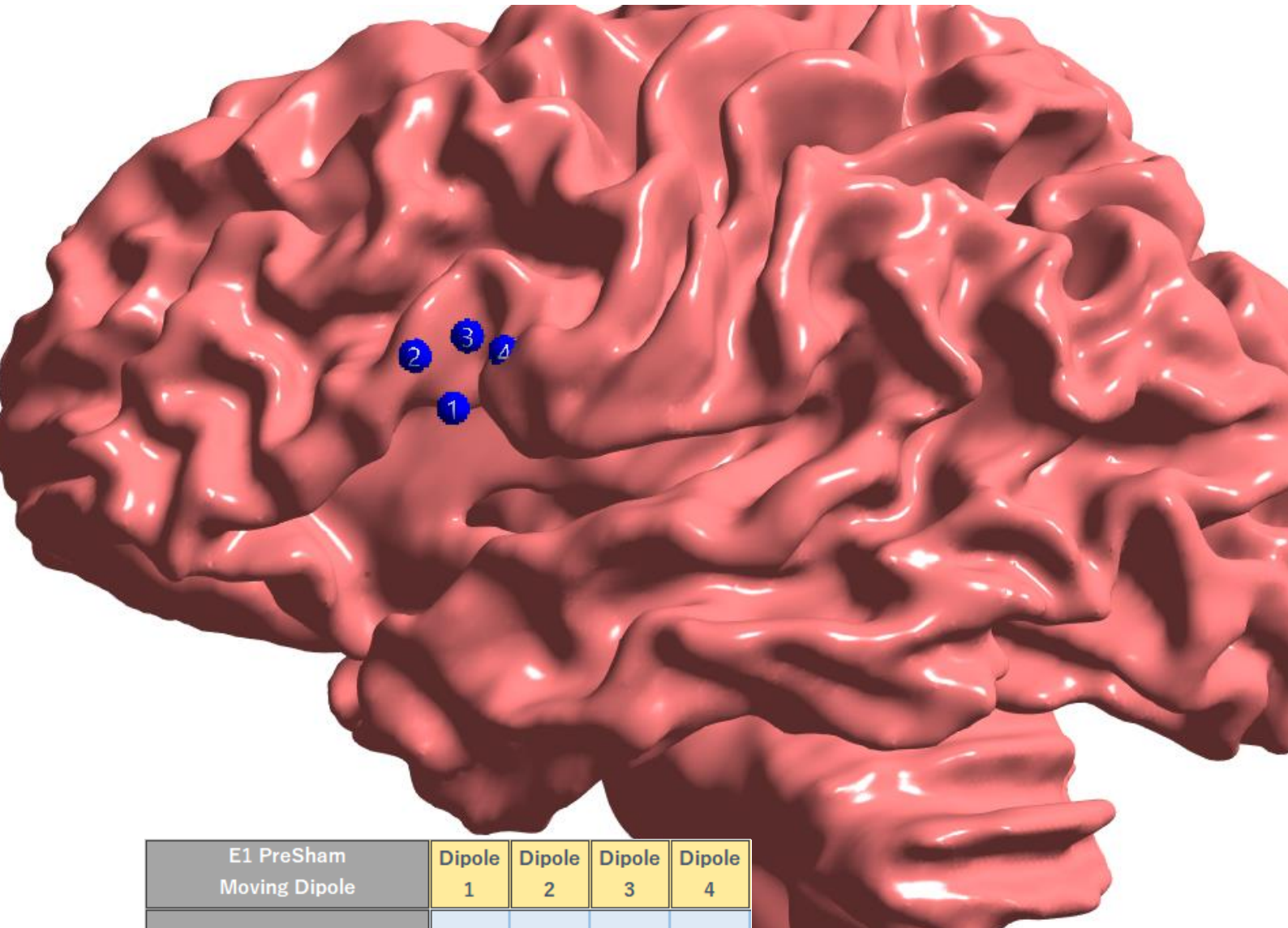


Scale for all Topologies on this page. Left is left, right is right, up is anterior and down is posterior.

PreSham Average Moving Dipole

Figure 24

Shows location of the PreSham Average Moving Dipole (of IEDs marked by Epileptologist 1) at different times during its rising flank until the peak. White matter for anatomic context.



E1 PreSham Moving Dipole	Dipole 1	Dipole 2	Dipole 3	Dipole 4
Timepont in ms	-15	-10	-5	0
Signal to Noise Ratio	1.3	3.5	6.7	9.1
Explained Signal	75%	89%	93%	84%
Current Density in μ Amm	31.8	74.4	110	182
Maximum Amplitude at 0 ms in μ V			Max at: F3	-13.4

Table 11

Epileptologist 1 PreSham Average Moving Dipole of IEDs. Summarizes information about dipoles of the rising flank of the average IED in the hour before "Sham" marked by Epileptologist 1.

0 s

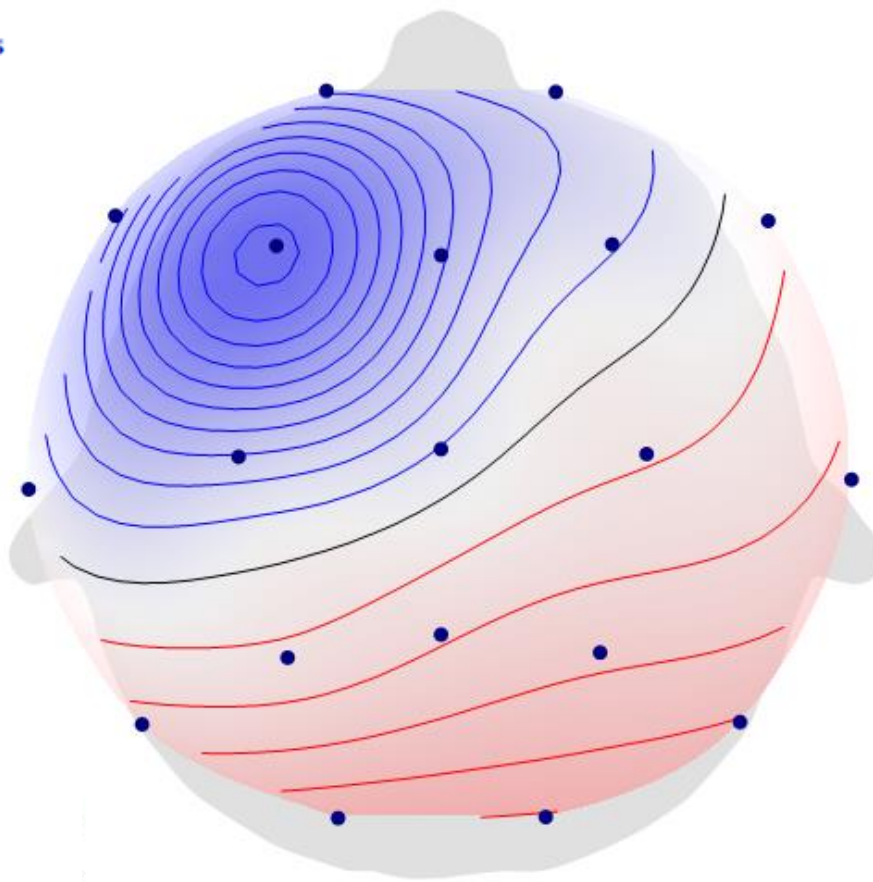
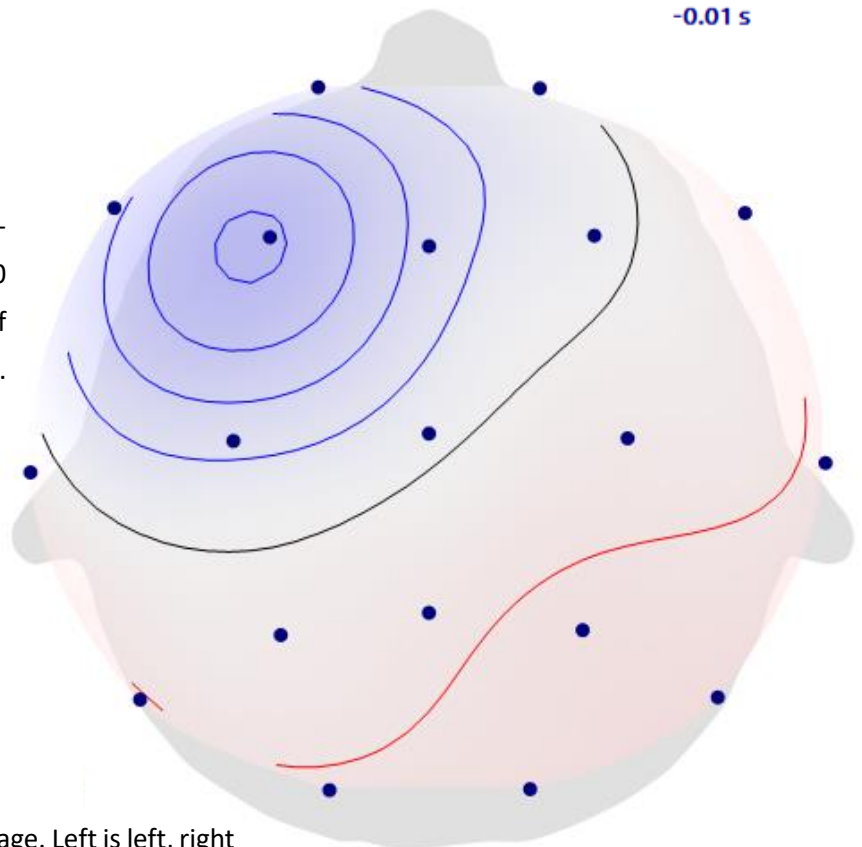
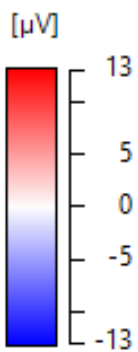


Figure 25
Shows topography of scalp potentials at the peak (0 ms) of the PreSham average of IEDs marked by Epileptologist 1.

-0.01 s

Figure 26

Shows topography of scalp potentials at the rising flank (-10 ms) of the PreSham average of IEDs marked by Epileptologist 1.

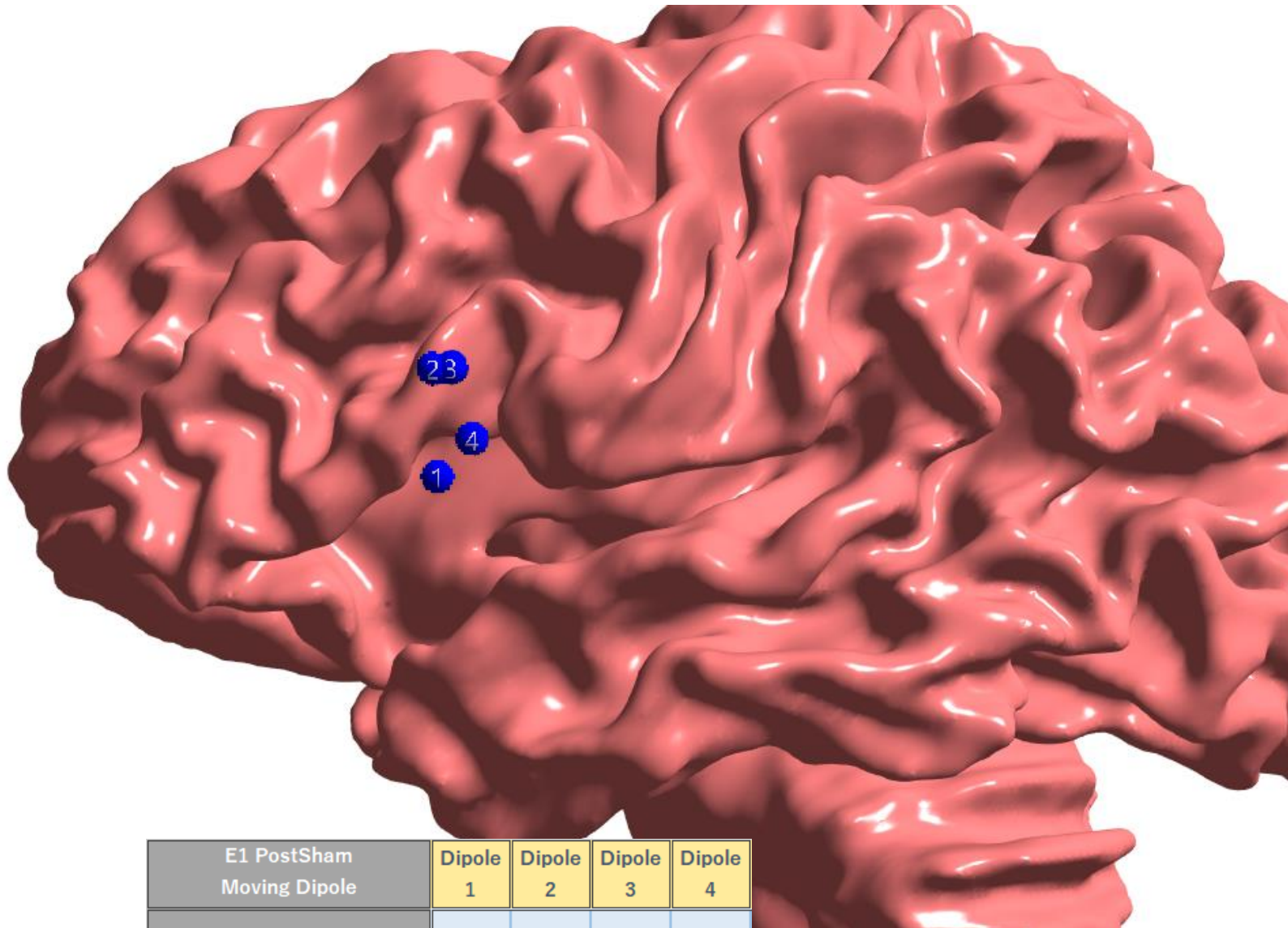


Scale for all Topologies on this page. Left is left, right is right, up is anterior and down is posterior.

PostSham Average Moving Dipole

Figure 27

Shows location of the PostSham Average Moving Dipole (of IEDs marked by Epileptologist 1) at different times during its rising flank until the peak. White matter for anatomic context.



E1 PostSham Moving Dipole	Dipole 1	Dipole 2	Dipole 3	Dipole 4
Timepont in ms	-15	-10	-5	0
Signal to Noise Ratio	1	2.3	4.2	5.5
Explained Signal	87%	89%	91%	85%
Current Density in μ Amm	24.6	53.6	81.1	86.4
Maximum Amplitude at 0 ms in μ V			Max at: F3	-7.88

Table 12

Epileptologist 1 PostSham Average Moving Dipole of IEDs. Summarizes information about dipoles of the rising flank of the average IED in the hour after "Sham" marked by Epileptologist 1.

0s

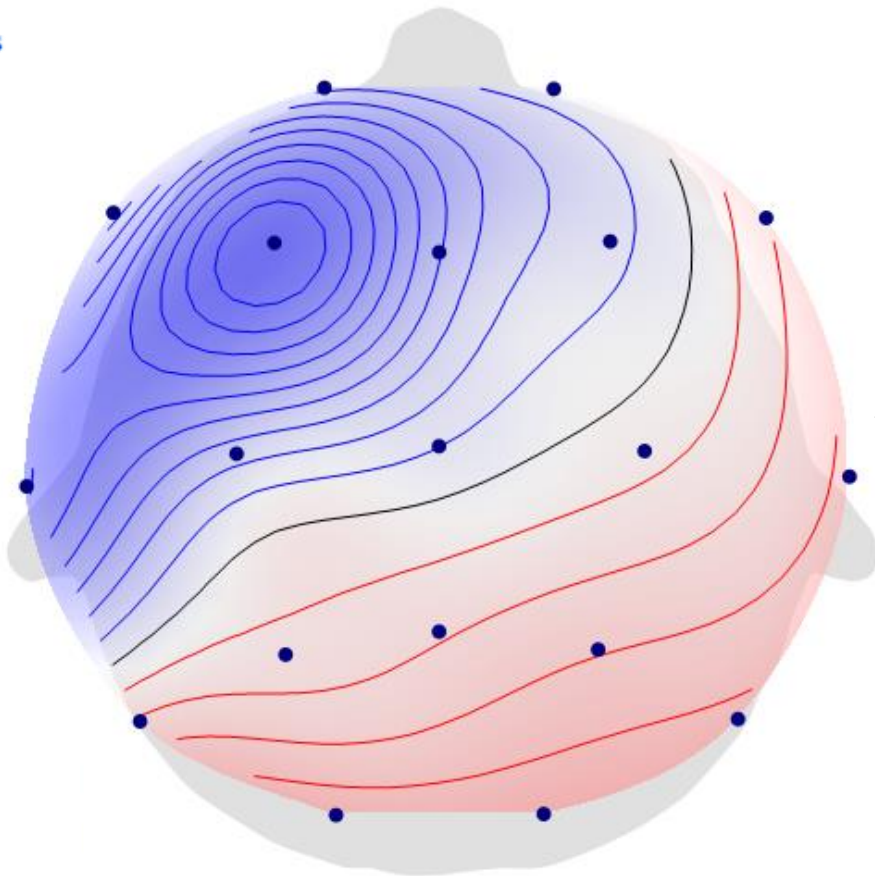
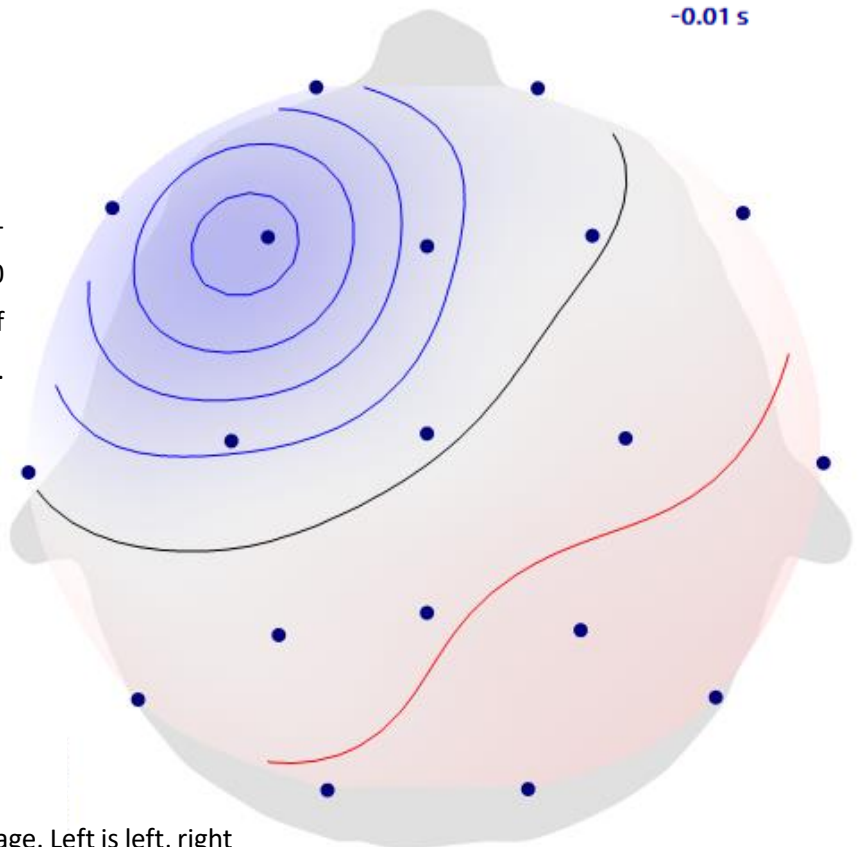
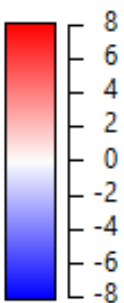


Figure 28
Shows topography of scalp potentials at the peak (0 ms) of the PostSham average of IEDs marked by Epileptologist 1.

-0.01 s

Figure 29
Shows topography of scalp potentials at the rising flank (-10 ms) of the PostSham average of IEDs marked by Epileptologist 1.

[μ V]

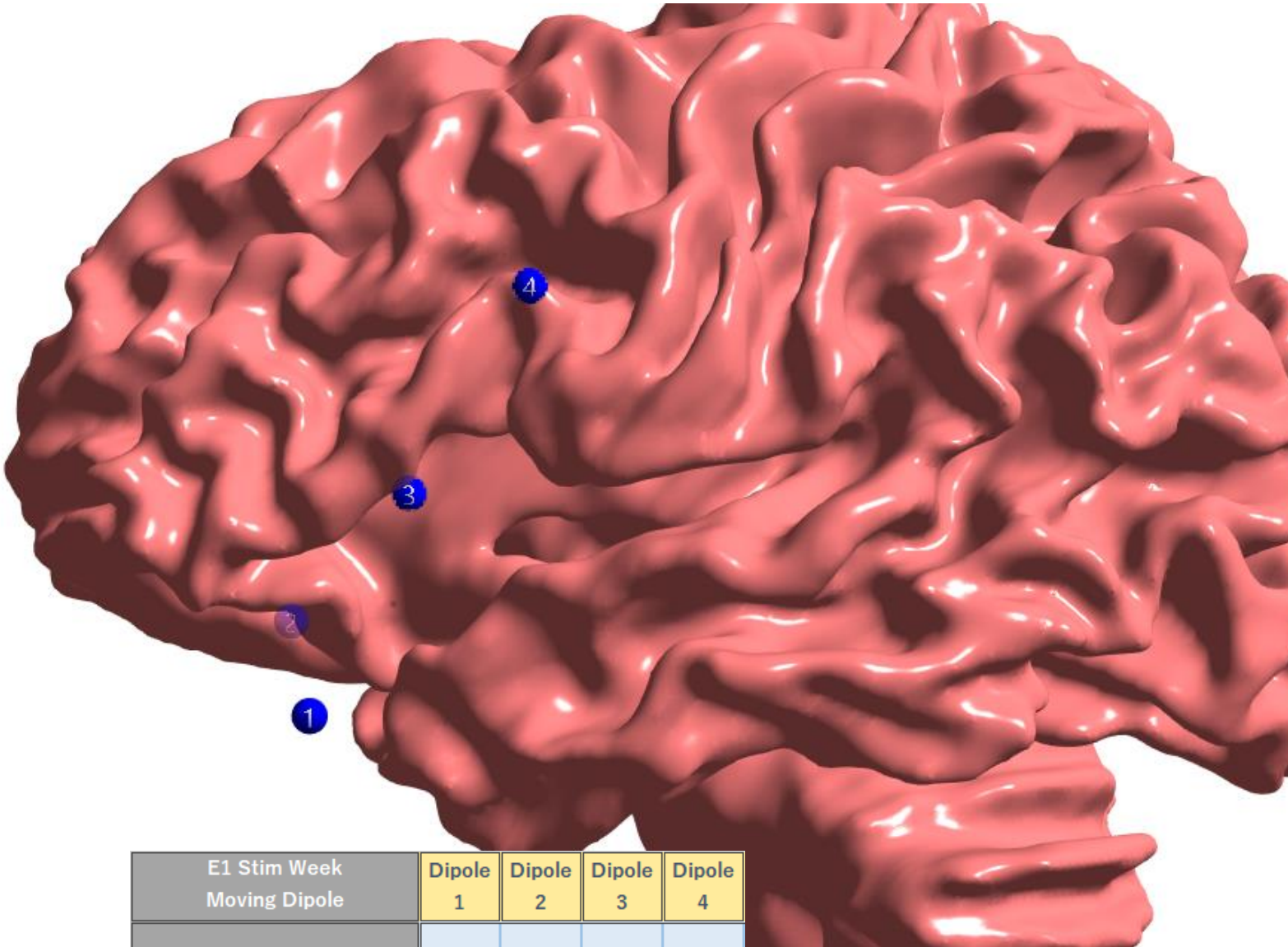


Scale for all Topologies on this page. Left is left, right is right, up is anterior and down is posterior.

Stim Week Baseline Average Moving Dipole

Figure 30

Shows location of the Stim Week Baseline Average Moving Dipole (of IEDs marked by Epileptologist 1) at different times during its rising flank until the peak. White matter for anatomic context.



E1 Stim Week Moving Dipole	Dipole 1	Dipole 2	Dipole 3	Dipole 4
Timepont in ms	-15	-10	-5	0
Signal to Noise Ratio	1	2.6	3.5	4.6
Explained Signal	71%	51%	90%	84%
Current Density in μ Amm	80.1	97.8	133	266
Maximum Amplitude at 0 ms in μ V			Max at: F3	-15.92

Table 13

Epileptologist 1 Stim Week Baseline Average Moving Dipole of IEDs. Summarizes information about dipoles of the rising flank of the average IED in the two hours before the first "Stim" marked by Epileptologist 1.

0s

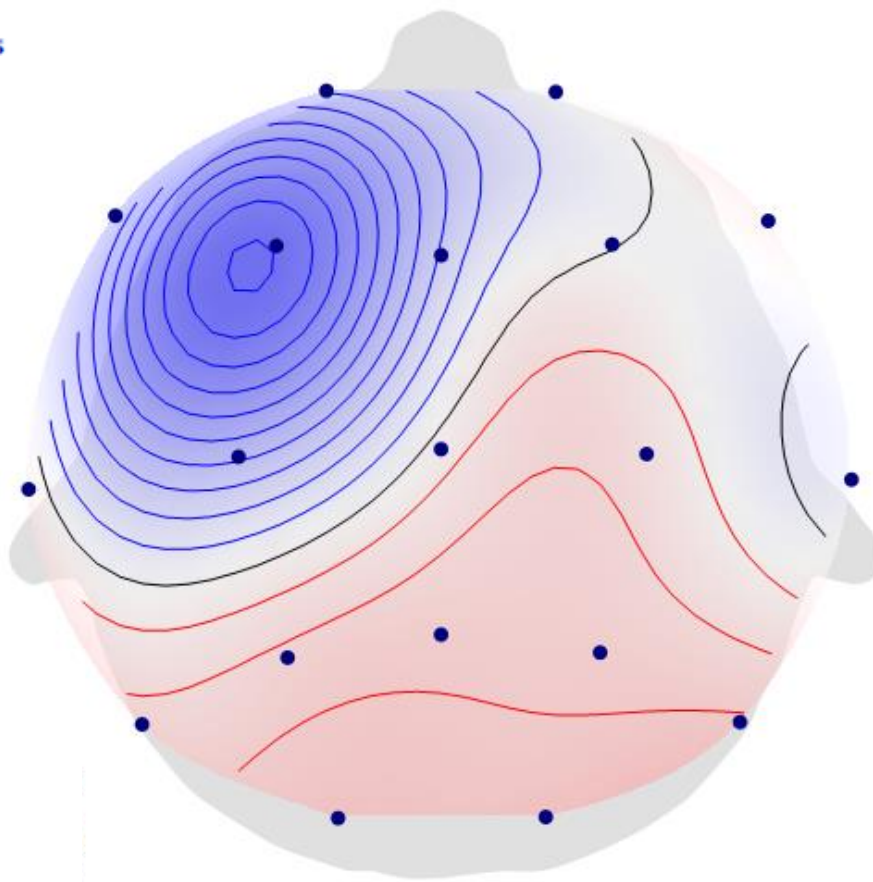


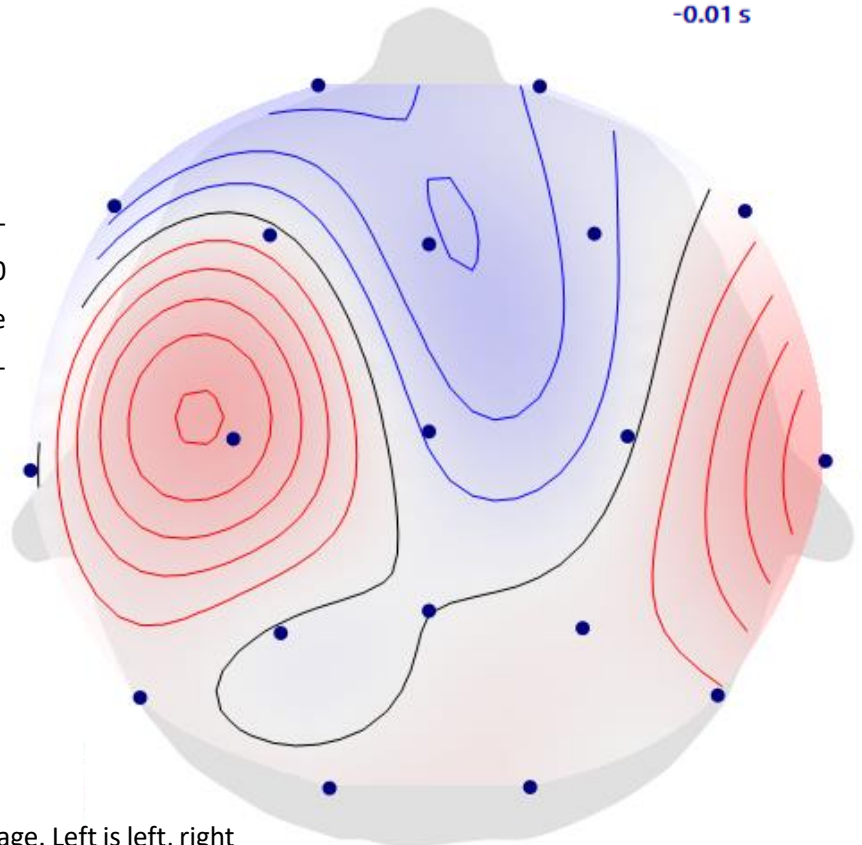
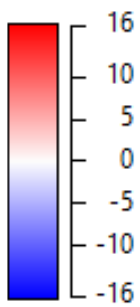
Figure 31
Shows topography of scalp potentials at the peak (0 ms) of the Stim Week Baseline average of IEDs marked by Epi-leptologist 1.

-0.01 s

Figure 32

Shows topography of scalp potentials at the rising flank (-10 ms) of the Stim Week Baseline average of IEDs marked by Epi-leptologist 1.

[μ V]

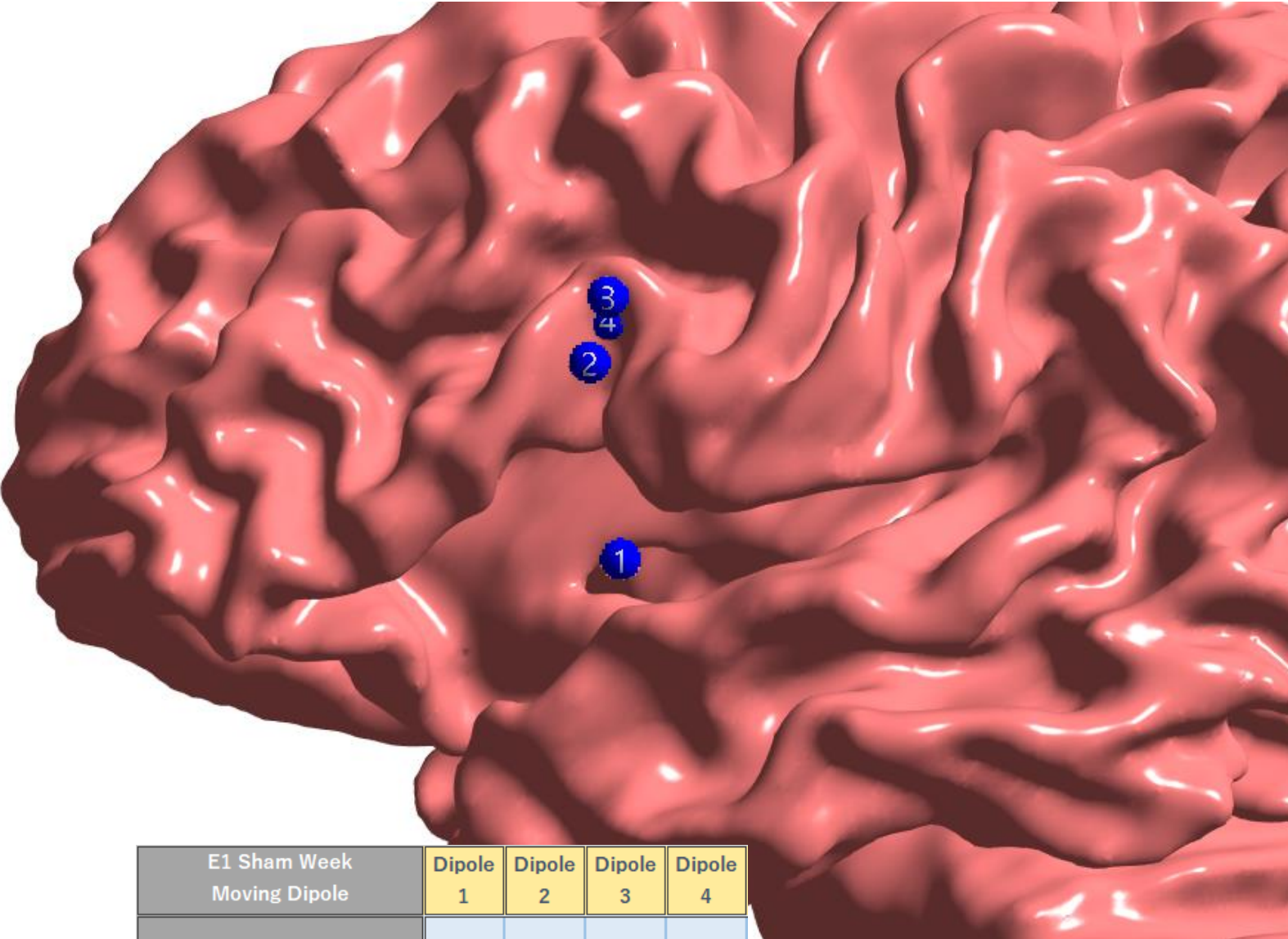


Scale for all Topologies on this page. Left is left, right is right, up is anterior and down is posterior.

Sham Week Baseline Average Moving Dipole

Figure 33

Shows location of the Sham Week Baseline Average Moving Dipole (of IEDs marked by Epileptologist 1) at different times during its rising flank until the peak. White matter for anatomic context.



E1 Sham Week Moving Dipole	Dipole 1	Dipole 2	Dipole 3	Dipole 4
Timepont in ms	-15	-10	-5	0
Signal to Noise Ratio	1.3	3.8	6.9	8.5
Explained Signal	84%	91%	95%	92%
Current Density in μ Amm	36.6	75.7	136	150
Maximum Amplitude at 0 ms in μ V			Max at: F3	-14.24

Table 14

Epileptologist 1 Sham Week Baseline Average Moving Dipole of IEDs. Summarizes information about dipoles of the rising flank of the average IED in the two hours before the first “Sham” marked by Epileptologist 1.

0s

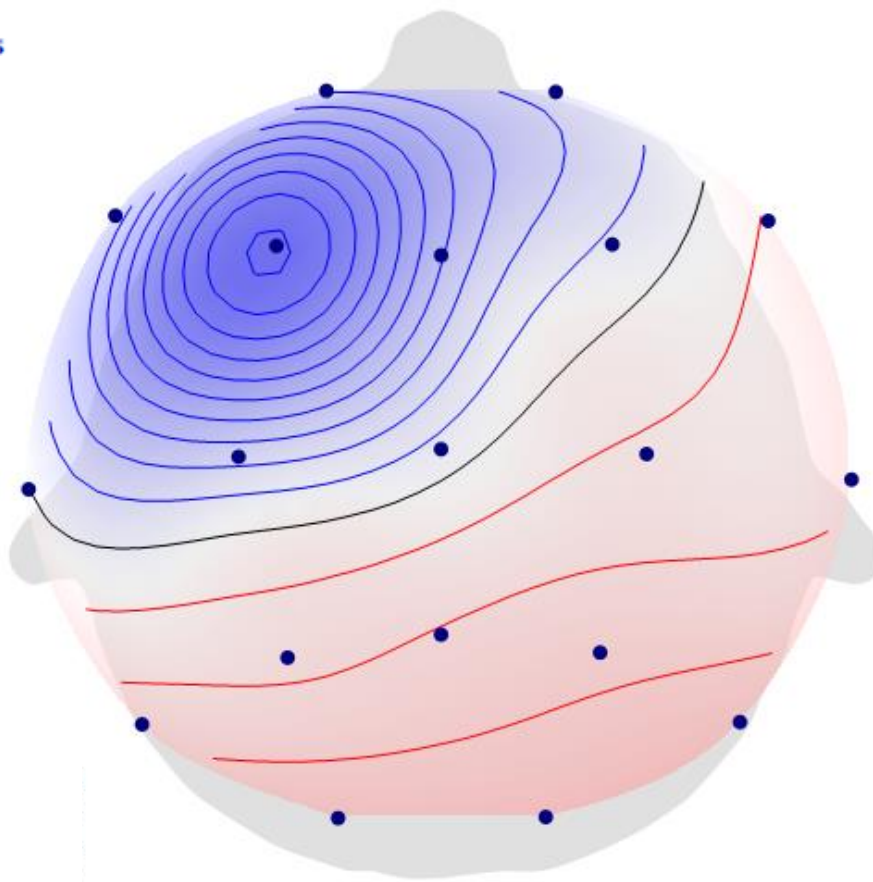


Figure 34

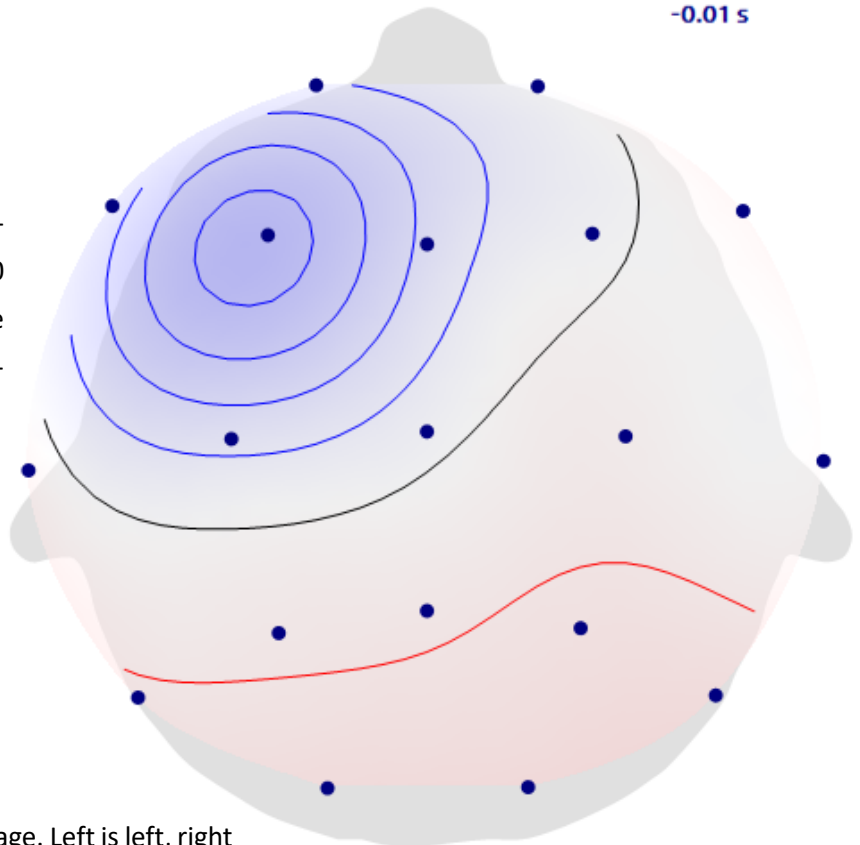
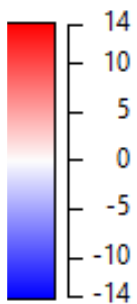
Shows topography of scalp potentials at the peak (0 ms) of the Sham Week Baseline average of IEDs marked by Epi-leptologist 1.

-0.01 s

Figure 35

Shows topography of scalp potentials at the rising flank (-10 ms) of the Sham Week Baseline average of IEDs marked by Epi-leptologist 1.

[μ V]



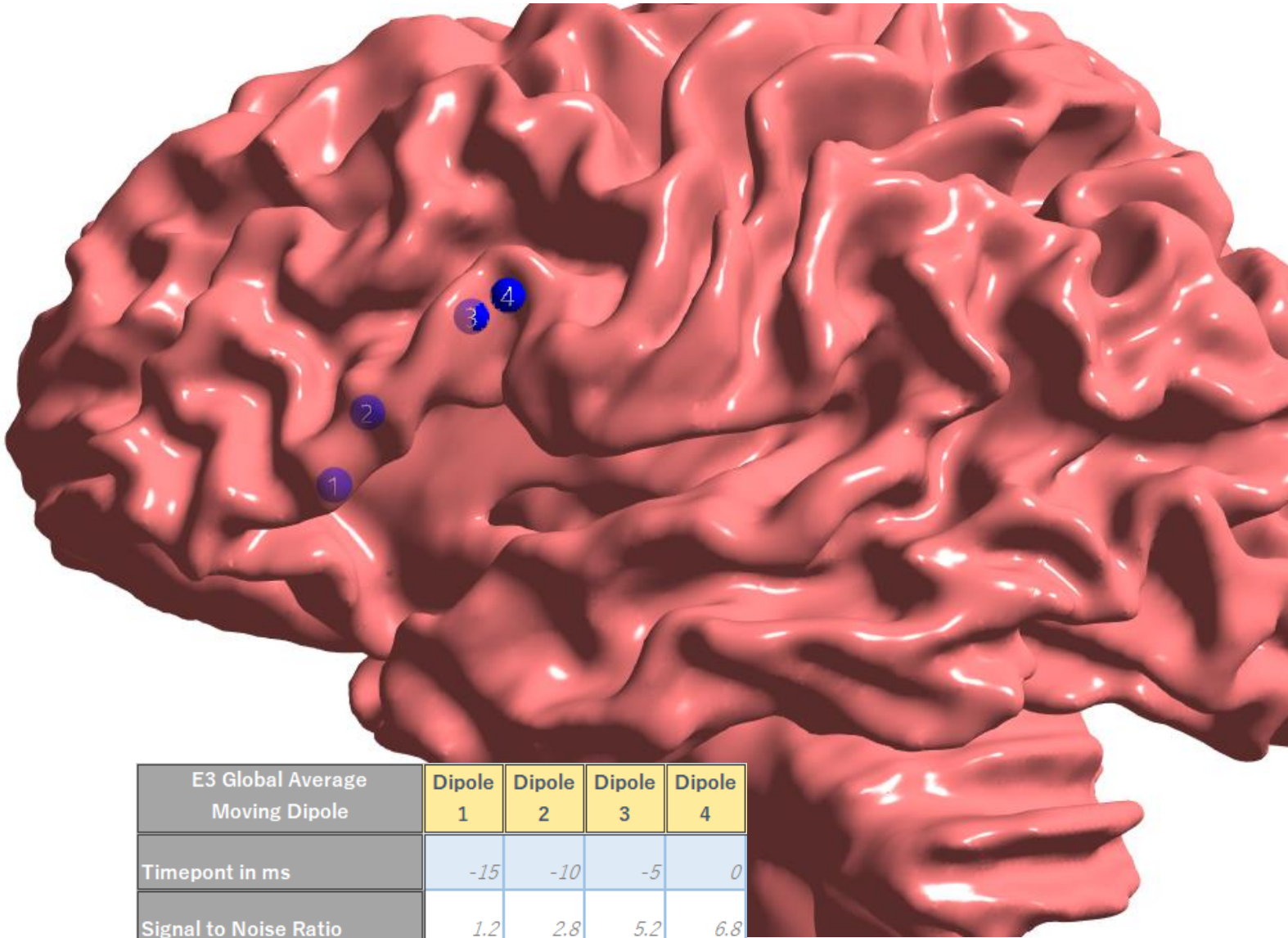
Scale for all Topologies on this page. Left is left, right is right, up is anterior and down is posterior.

Epileptologist 3

Global Average Moving Dipole

Figure 36

Shows location of the Global Average Moving Dipole (of IEDs marked by Epileptologist 3) at different times during its rising flank until the peak. White matter for anatomic context.



E3 Global Average Moving Dipole	Dipole 1	Dipole 2	Dipole 3	Dipole 4
Timepont in ms	-15	-10	-5	0
Signal to Noise Ratio	1.2	2.8	5.2	6.8
Explained Signal	89%	88%	96%	92%
Current Density in μ Amm	34.2	66	132	198
Maximum Amplitude at 0 ms in μ V			Max at: F3	-16.2

Table 15

Epileptologist 3 Global Average Moving Dipole of IEDs. Summarizes information about dipoles of the rising flank of the average IED marked by Epileptologist 3.

0s

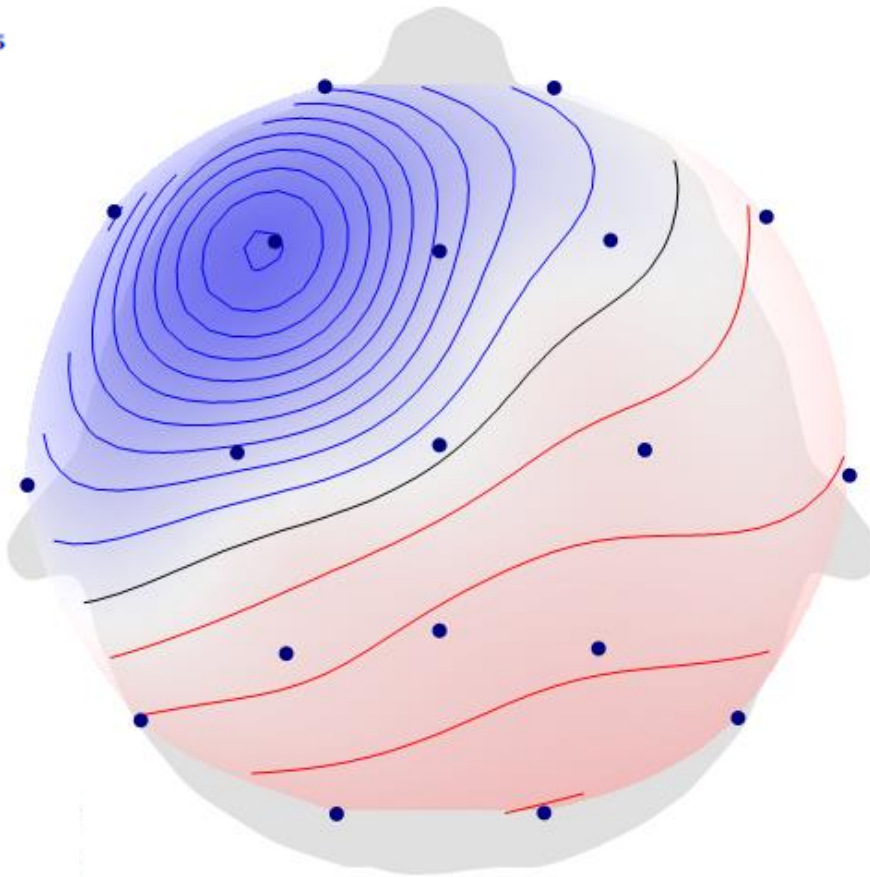
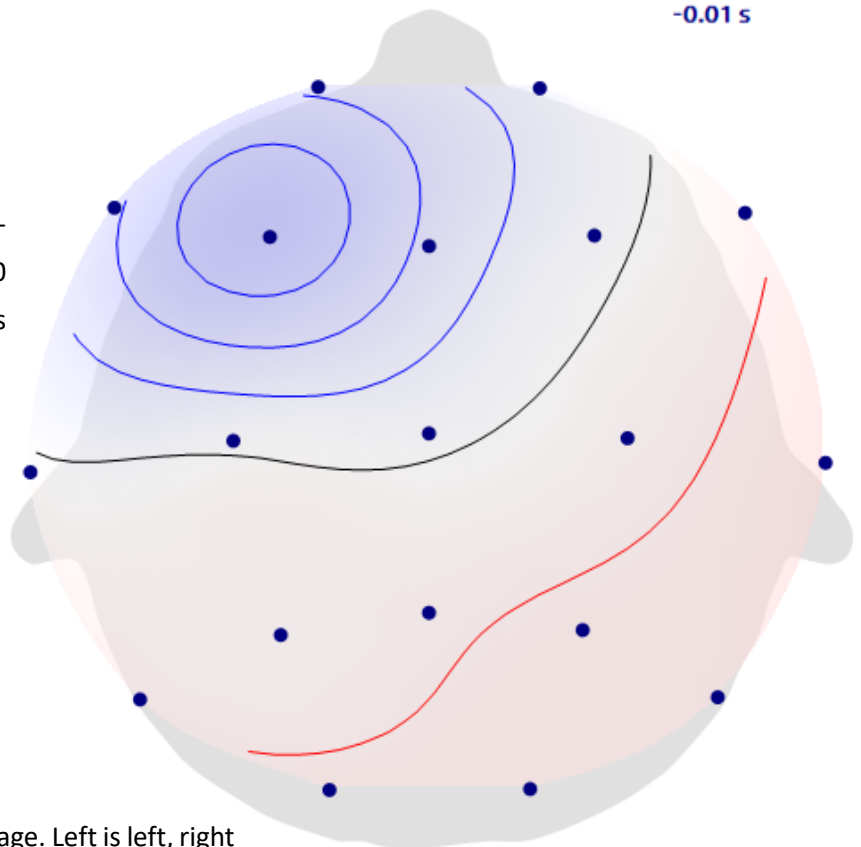
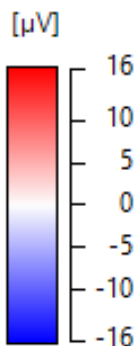


Figure 37
Shows topography of scalp potentials at the peak (0 ms) of the global average of IEDs marked by Epileptologist 3.

-0.01 s

Figure 38
Shows topography of scalp potentials at the rising flank (-10 ms) of the global average of IEDs marked by Epileptologist 3.

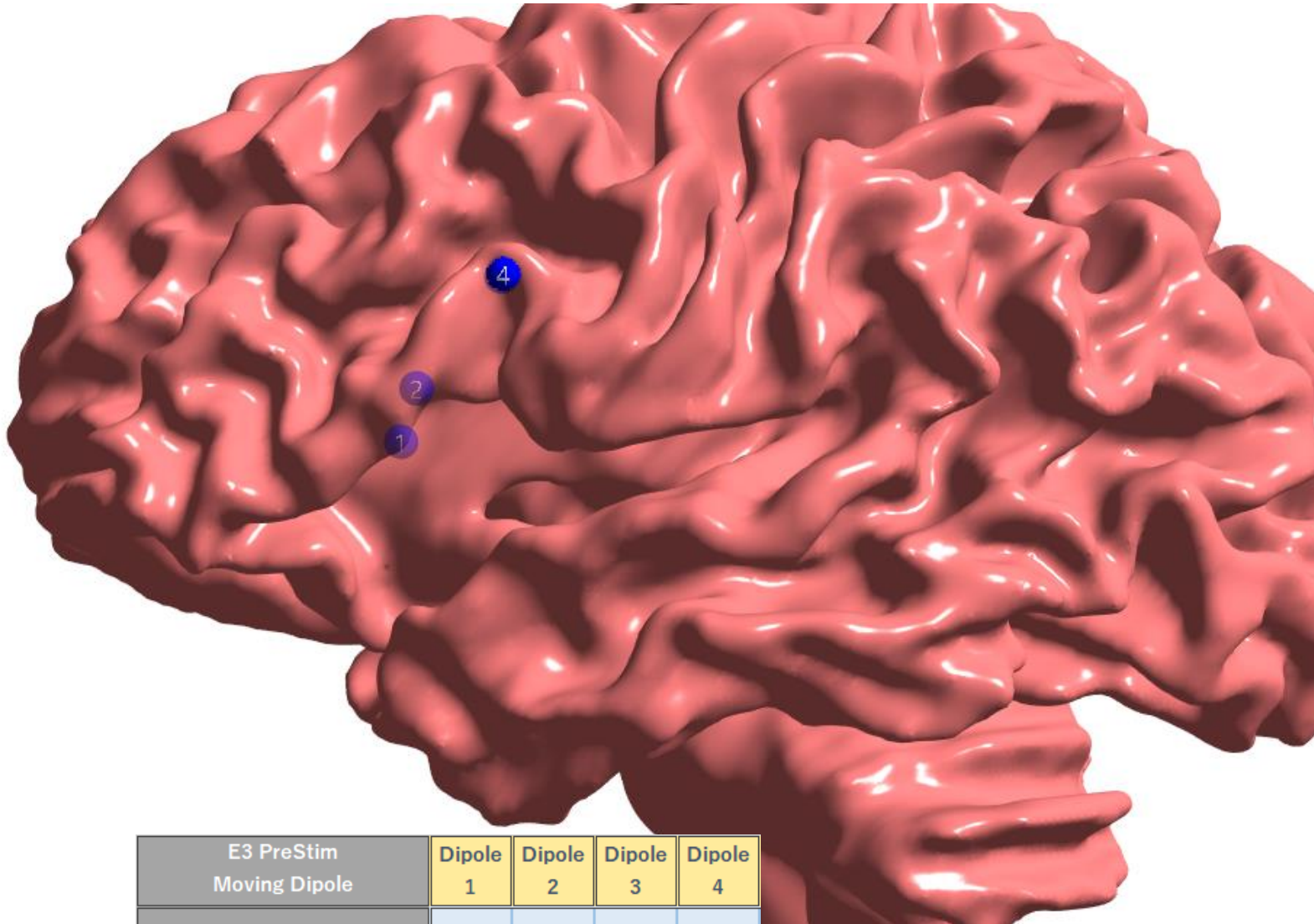


Scale for all Topologies on this page. Left is left, right is right, up is anterior and down is posterior.

PreStim Average Moving Dipole

Figure 39

Shows location of the PreStim Average Moving Dipole (of IEDs marked by Epileptologist 3) at different times during its rising flank until the peak. White matter for anatomic context.



E3 PreStim Moving Dipole	Dipole 1	Dipole 2	Dipole 3	Dipole 4
Timepont in ms	-15	-10	-5	0
Signal to Noise Ratio	1.4	3.4	6.1	7.6
Explained Signal	85%	89%	94%	92%
Current Density in μ Amm	45.8	84.6	161	267
Maximum Amplitude at 0 ms in μ V			Max at: F3	-17.81

Table 16

Epileptologist 3 PreStim Average Moving Dipole of IEDs. Summarizes information about dipoles of the rising flank of the average IED in the hour before “Stim” marked by Epileptologist 3.

0 s

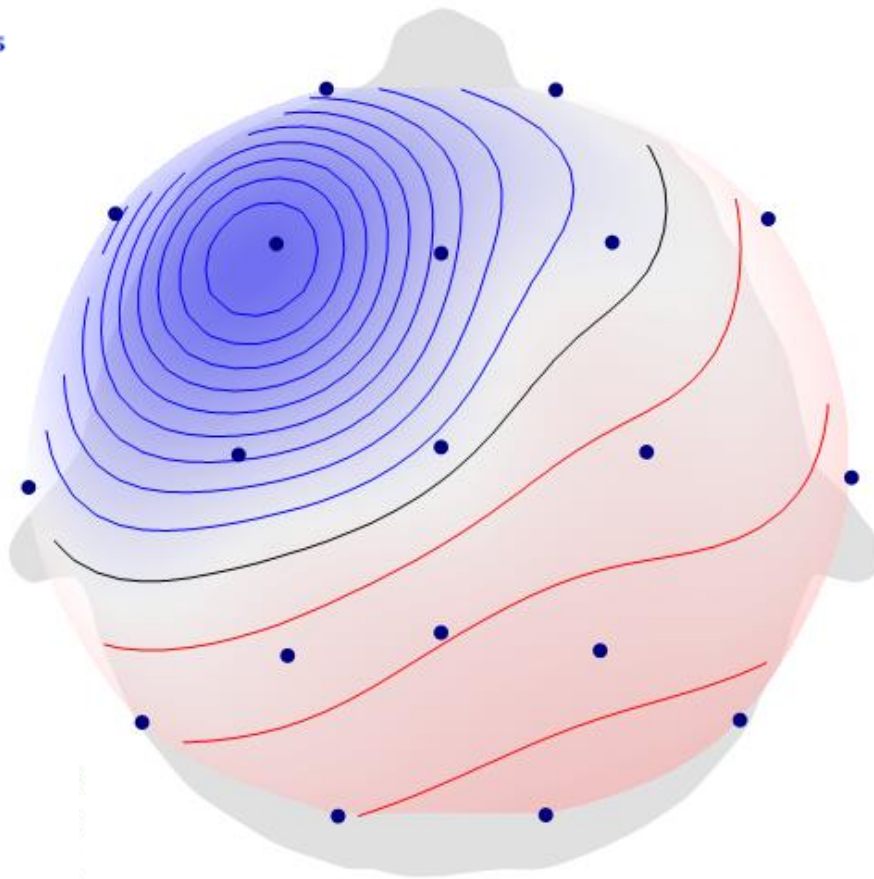
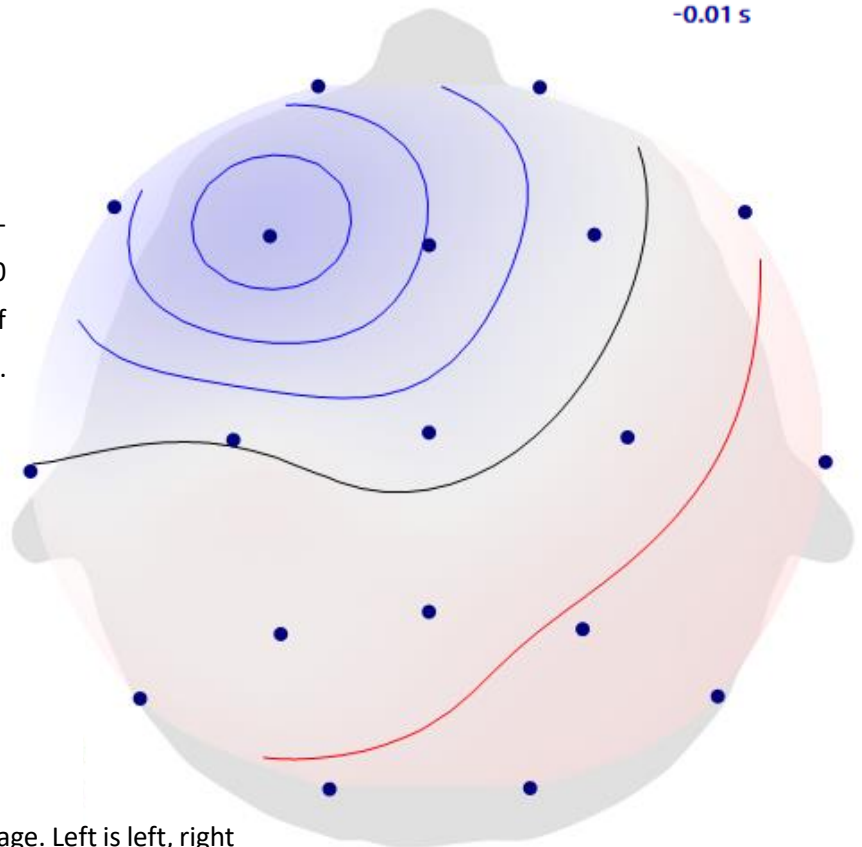
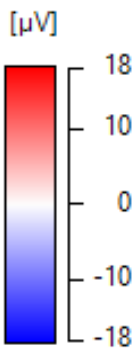


Figure 40
Shows topography of scalp potentials at the peak (0 ms) of the PreStim average of IEDs marked by Epileptologist 3.

-0.01 s

Figure 41
Shows topography of scalp potentials at the rising flank (-10 ms) of the PreStim average of IEDs marked by Epileptologist 3.

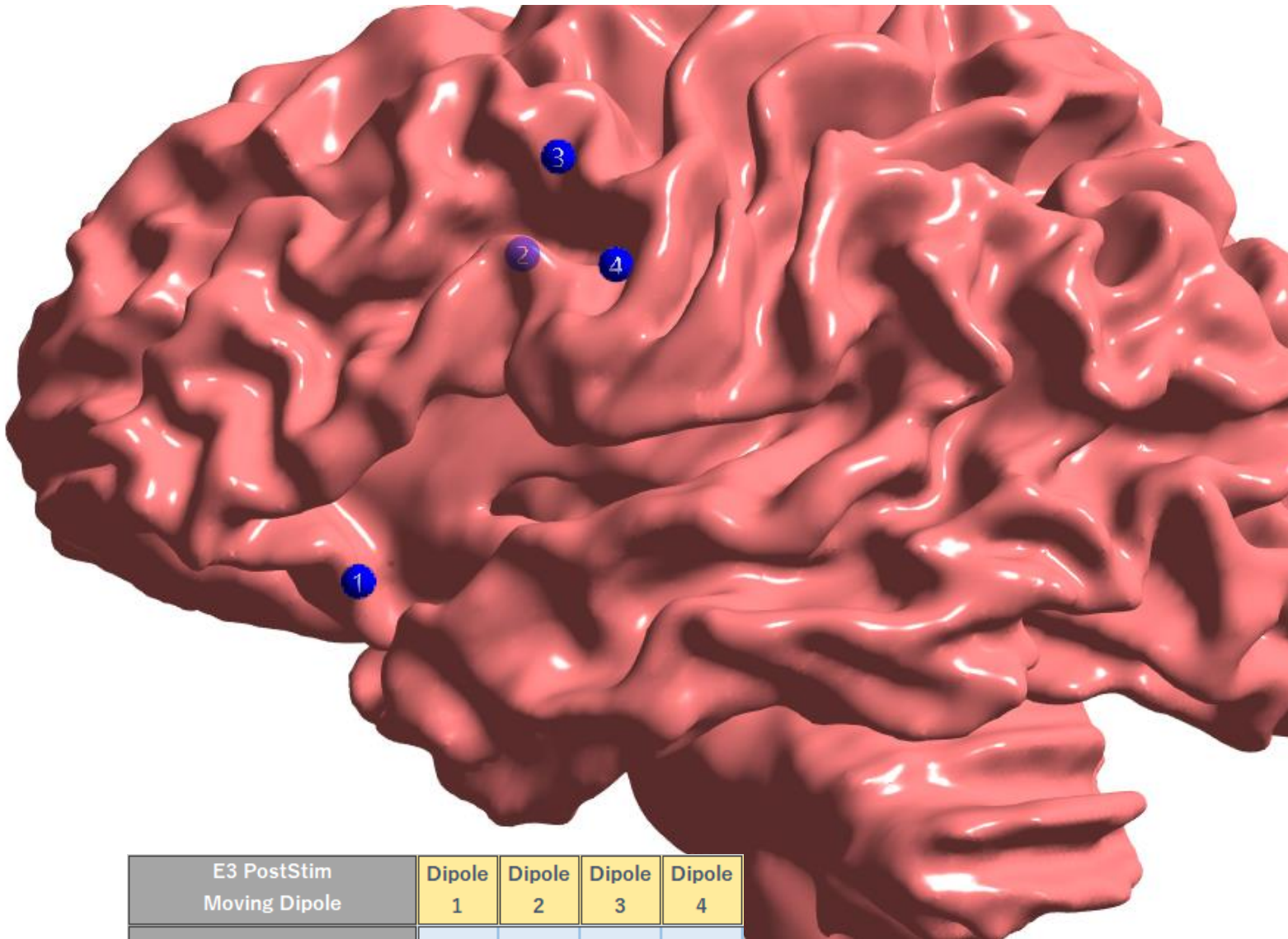


Scale for all Topologies on this page. Left is left, right is right, up is anterior and down is posterior.

PostStim Average Moving Dipole

Figure 42

Shows location of the PostStim Average Moving Dipole (of IEDs marked by Epileptologist 3) at different times during its rising flank until the peak. White matter for anatomic context.



E3 PostStim Moving Dipole	Dipole 1	Dipole 2	Dipole 3	Dipole 4
Timepont in ms	-15	-10	-5	0
Signal to Noise Ratio	0.9	1.3	2.2	3.1
Explained Signal	88%	83%	84%	80%
Current Density in μ Amm	24.9	26.8	66.4	67
Maximum Amplitude at 0 ms in μ V			Max at: F3	-6.71

Table 17

Epileptologist 3 PostStim Average Moving Dipole of IEDs. Summarizes information about dipoles of the rising flank of the average IED in the hour after “Stim” marked by Epileptologist 3.

0s

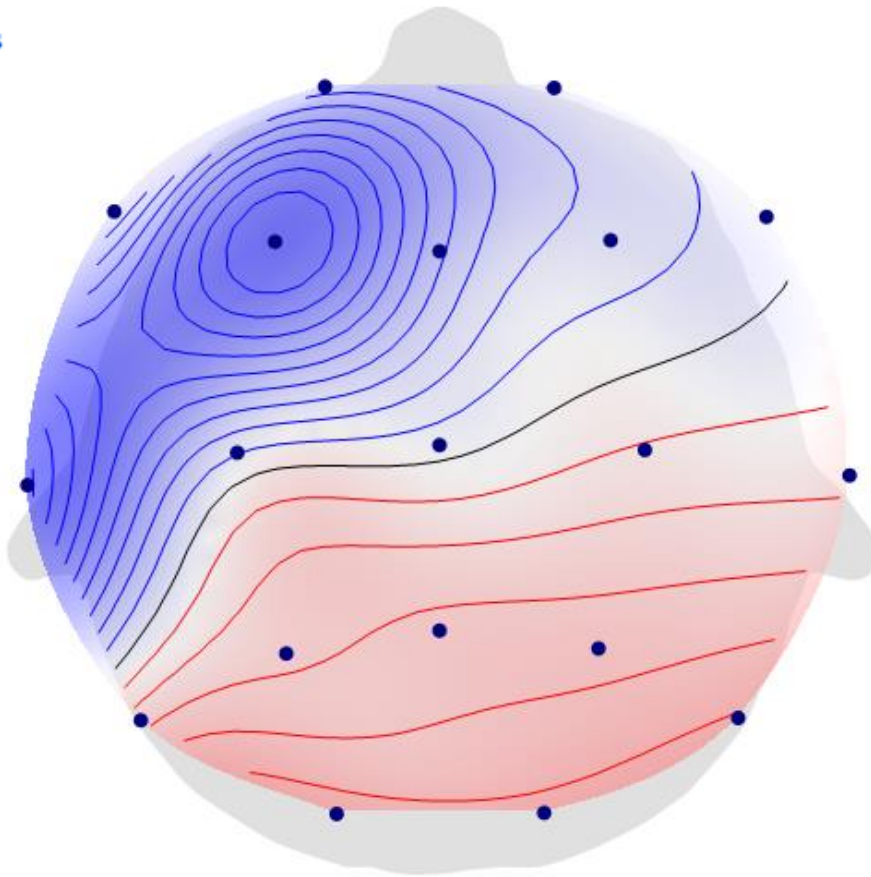
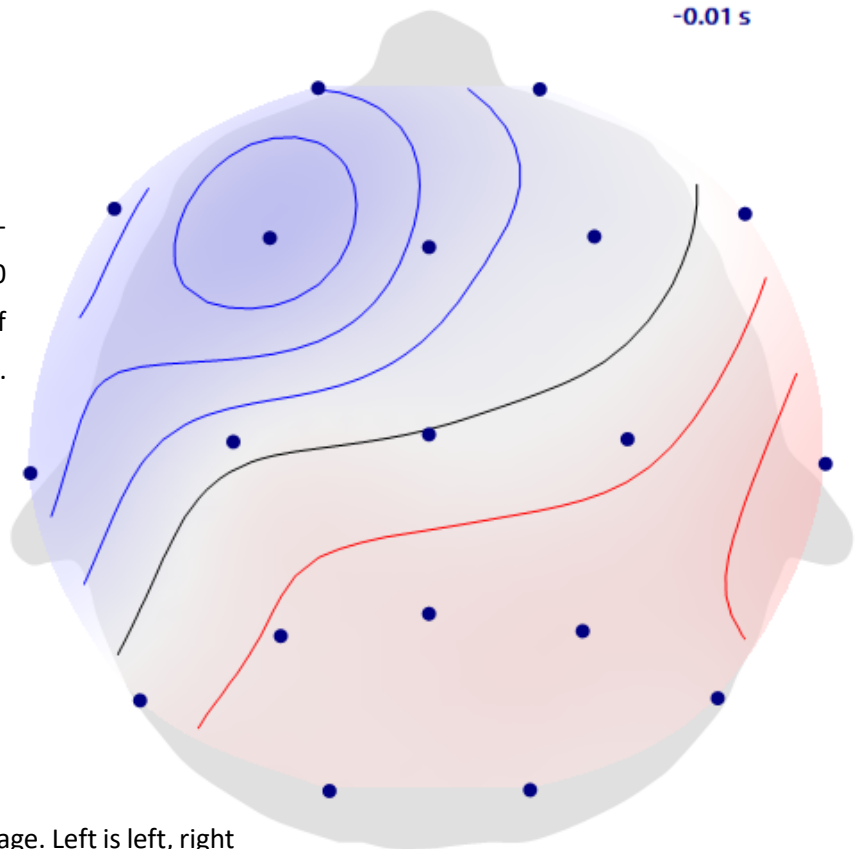
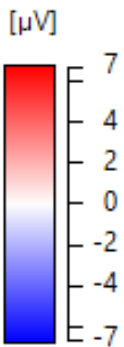


Figure 43
Shows topography of scalp potentials at the peak (0 ms) of the PostStim average of IEDs marked by Epileptologist 3.

Figure 44
Shows topography of scalp potentials at the rising flank (-10 ms) of the PostStim average of IEDs marked by Epileptologist 3.



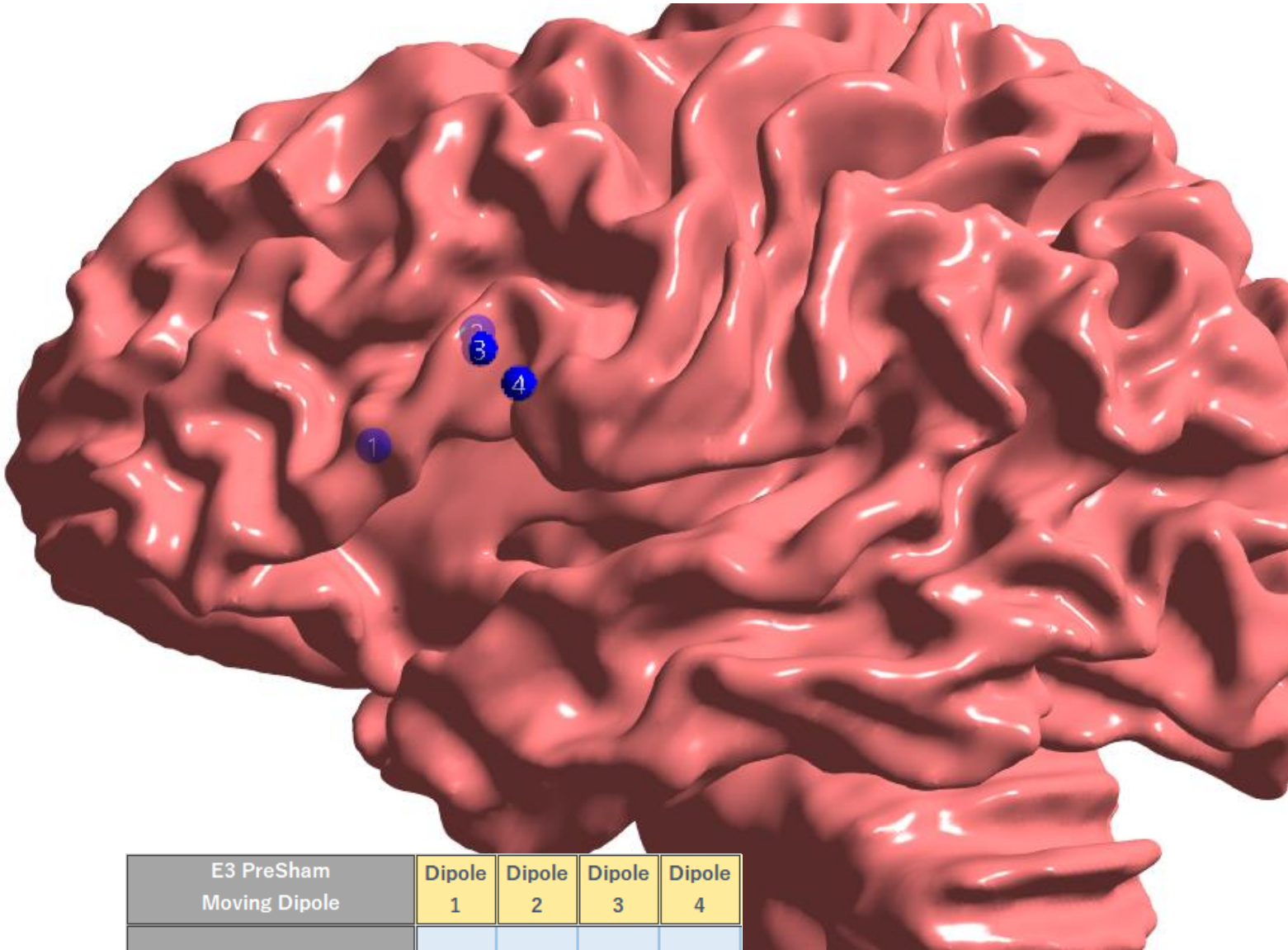
-0.01 s

Scale for all Topologies on this page. Left is left, right is right, up is anterior and down is posterior.

PreSham Average Moving Dipole

Figure 45

Shows location of the PreSham Average Moving Dipole (of IEDs marked by Epileptologist 3) at different times during its rising flank until the peak. White matter for anatomic context.



E3 PreSham Moving Dipole	Dipole 1	Dipole 2	Dipole 3	Dipole 4
Timepont in ms	-15	-10	-5	0
Signal to Noise Ratio	1.1	3.3	6.1	8.2
Explained Signal	78%	92%	96%	89%
Current Density in μ Amm	33.9	86.8	176	267
Maximum Amplitude at 0 ms in μ V			Max at: F3	-19.54

Table 18

Epileptologist 3 PreSham Average Moving Dipole of IEDs. Summarizes information about dipoles of the rising flank of the average IED in the hour before "Sham" marked by Epileptologist 3.

0 s

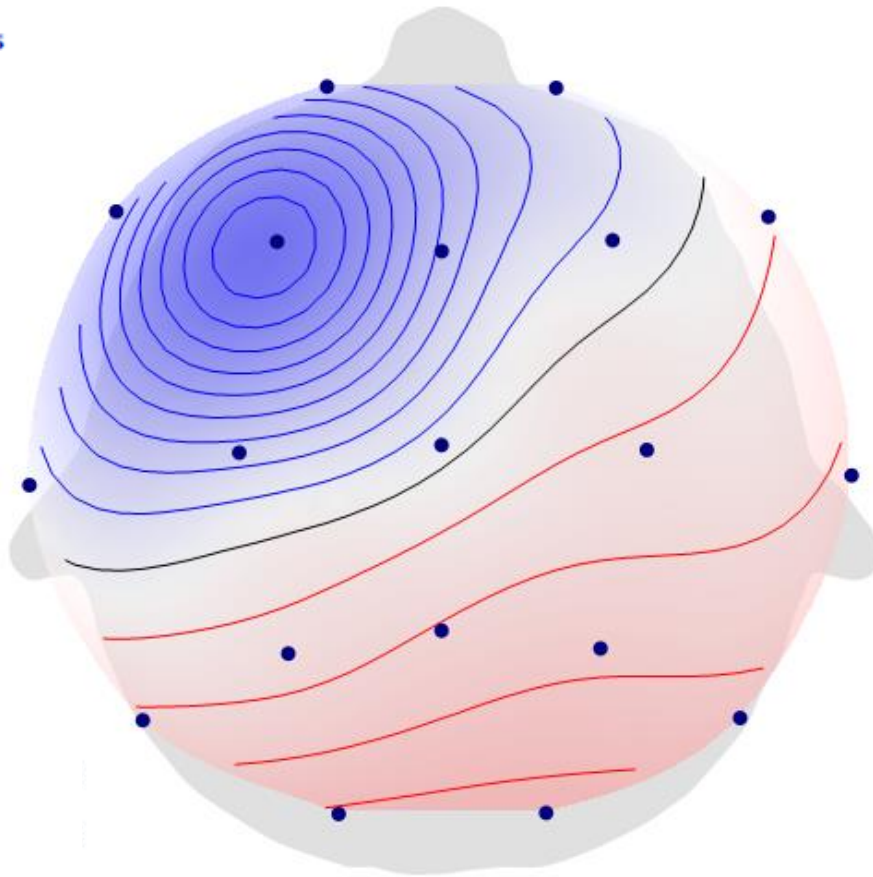
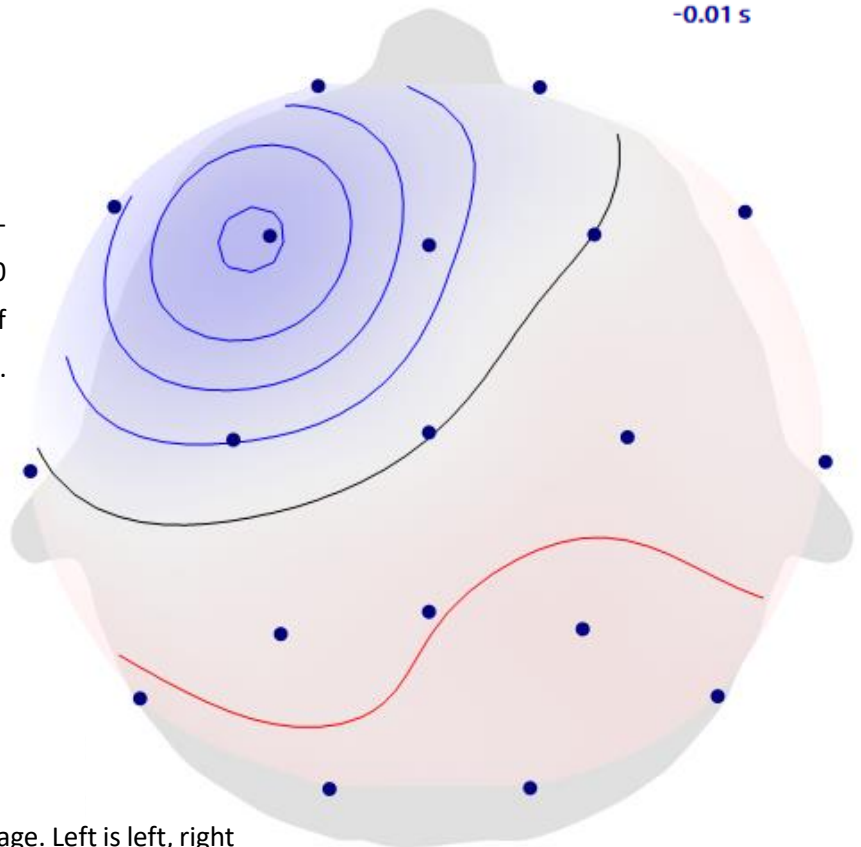
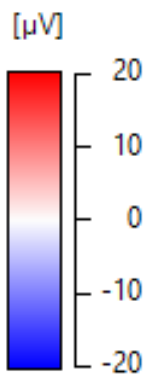


Figure 46
Shows topography of scalp potentials at the peak (0 ms) of the PreSham average of IEDs marked by Epileptologist 3.

-0.01 s

Figure 47
Shows topography of scalp potentials at the rising flank (-10 ms) of the PreSham average of IEDs marked by Epileptologist 3.

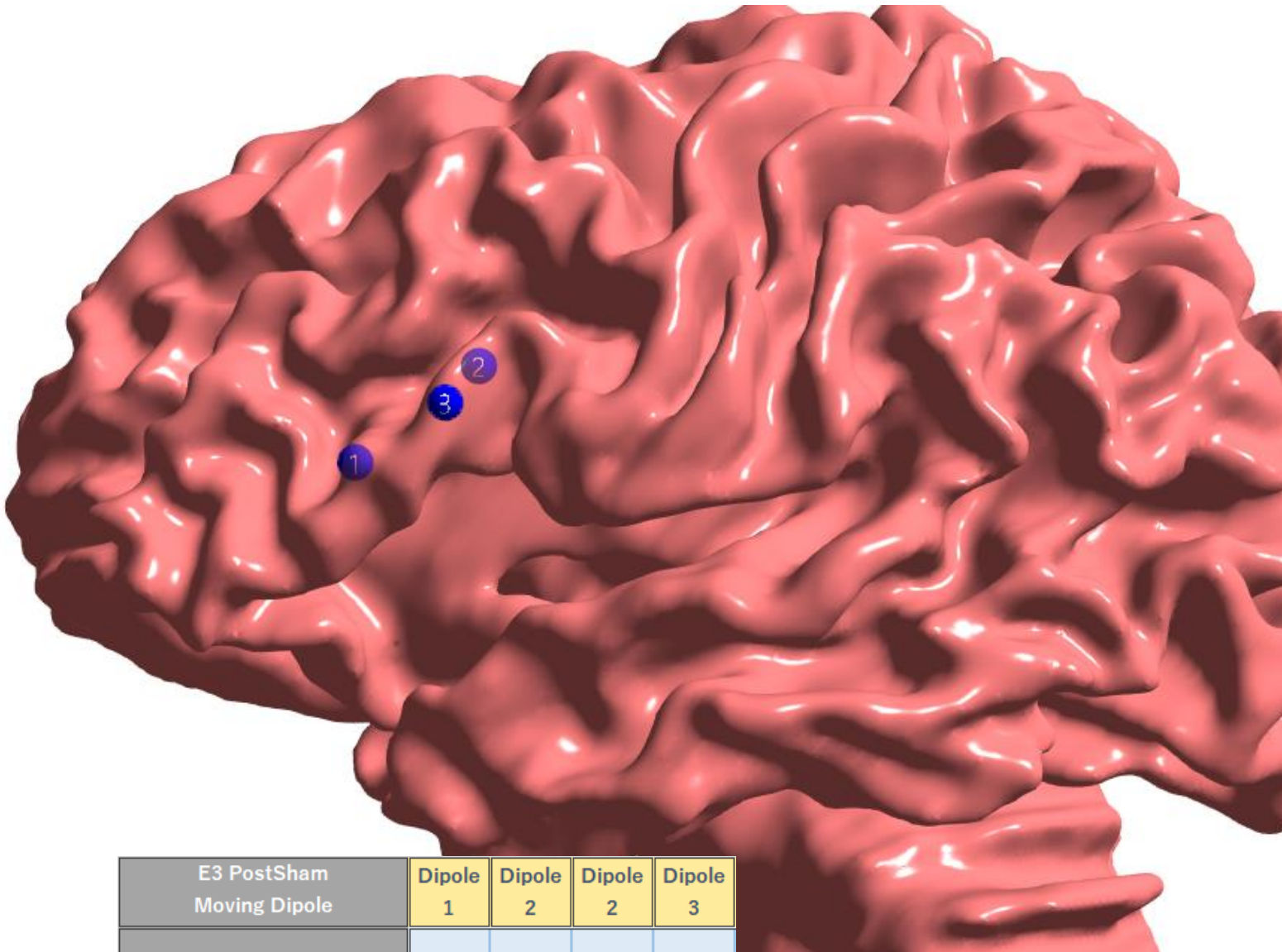


Scale for all Topologies on this page. Left is left, right is right, up is anterior and down is posterior.

PostSham Average Moving Dipole

Figure 48

Shows location of the PostSham Average Moving Dipole (of IEDs marked by Epileptologist 3) at different times during its rising flank until the peak. White matter for anatomic context.



E3 PostSham Moving Dipole	Dipole 1	Dipole 2	Dipole 2	Dipole 3
Timepont in ms	-15	-10	-5	0
Signal to Noise Ratio	1.2	2.7	4.7	6
Explained Signal	91%	90%	93%	92%
Current Density in μ A/mm	33.4	60.4	102	156
Maximum Amplitude at 0 ms in μ V			Max at: F3	-12.38

Table 19

Epileptologist 3 PostSham Average Moving Dipole of IEDs. Summarizes information about dipoles of the rising flank of the average IED in the hour after "Sham" marked by Epileptologist 3.

0s

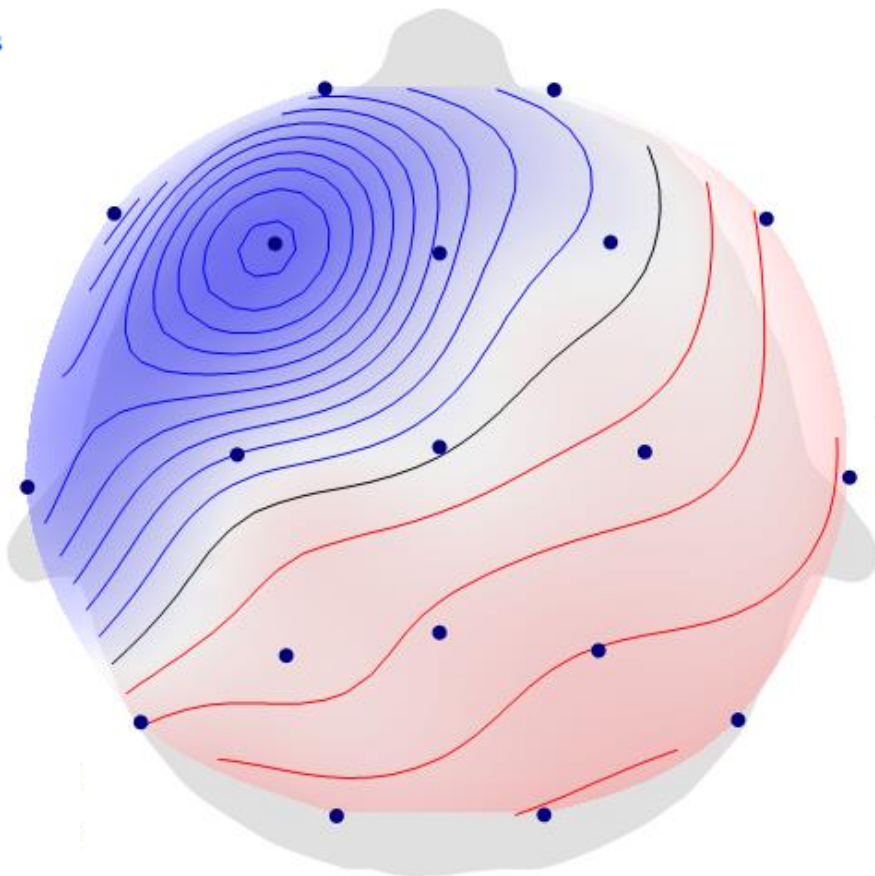
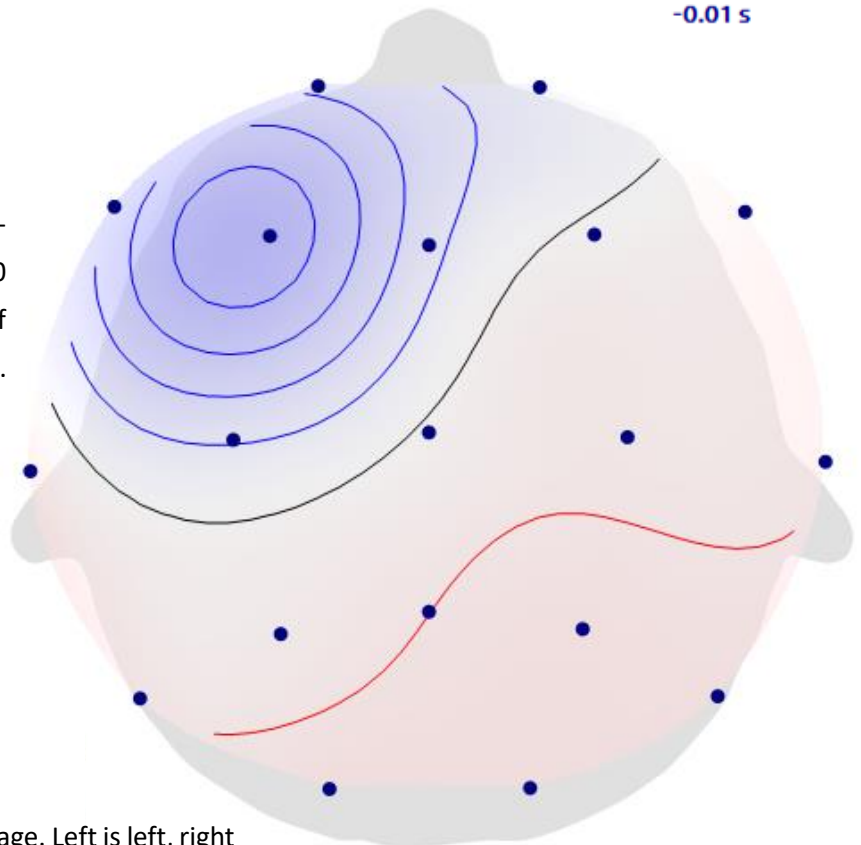
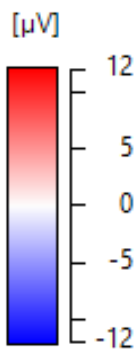


Figure 49
Shows topography of scalp potentials at the peak (0 ms) of the PostSham average of IEDs marked by Epileptologist 3.

-0.01 s

Figure 50
Shows topography of scalp potentials at the rising flank (-10 ms) of the PostSham average of IEDs marked by Epileptologist 3.

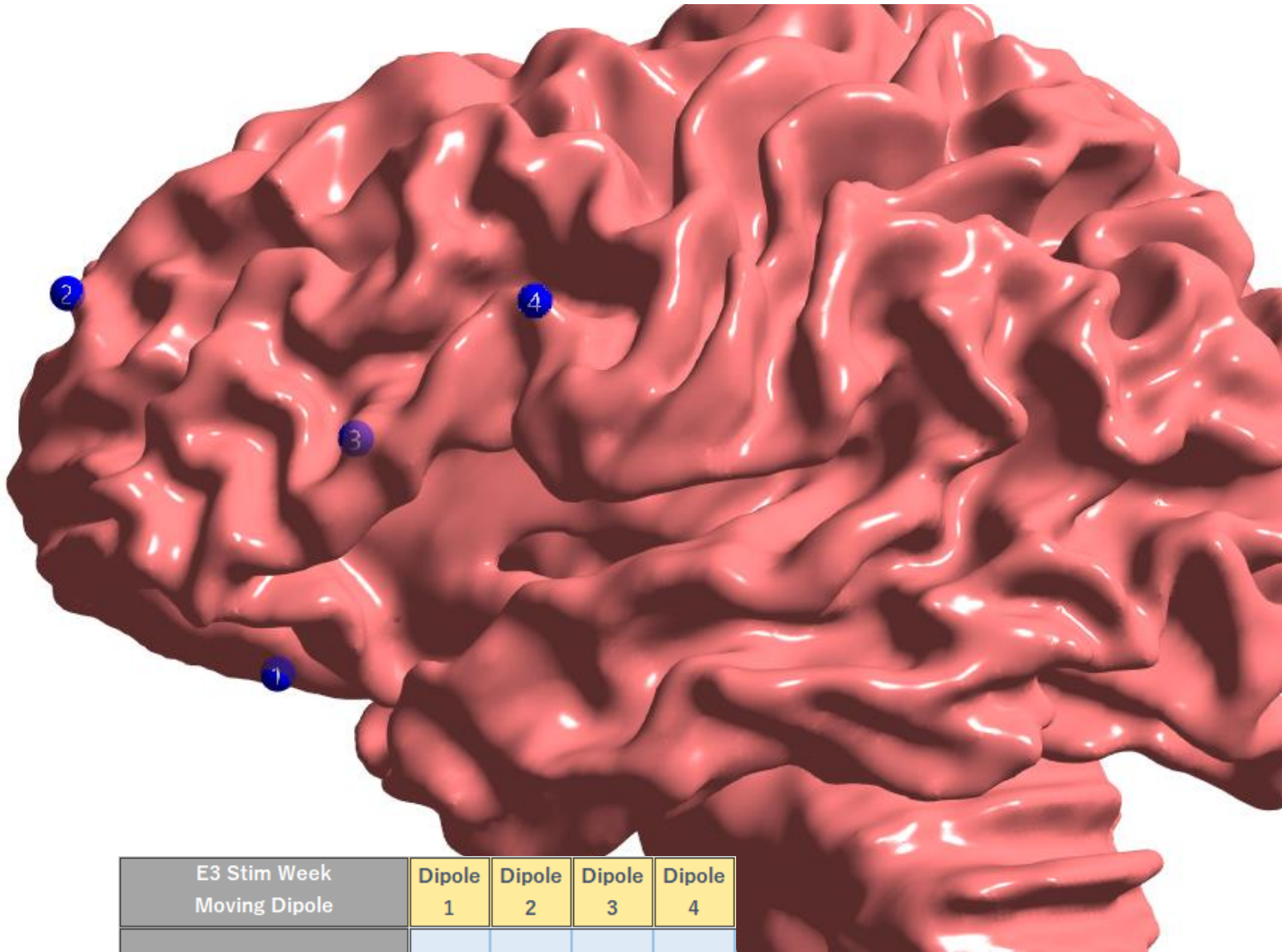


Scale for all Topologies on this page. Left is left, right is right, up is anterior and down is posterior.

Stim Week Baseline Average Moving Dipole

Figure 51

Shows location of the Stim Week Baseline Average Moving Dipole (of IEDs marked by Epileptologist 3) at different times during its rising flank until the peak. White matter for anatomic context.



E3 Stim Week Moving Dipole	Dipole 1	Dipole 2	Dipole 3	Dipole 4
Timepont in ms	-15	-10	-5	0
Signal to Noise Ratio	1.1	2.5	4.1	5.4
Explained Signal	74%	59%	92%	91%
Current Density in μ Amm	87.5	190	171	382
Maximum Amplitude at 0 ms in μ V			Max at: F3	-21.4

Table 20

Epileptologist 3 Stim Week Baseline Average Moving Dipole of IEDs. Summarizes information about dipoles of the rising flank of the average IED in the two hours before the first “Stim” marked by Epileptologist 3.

0s

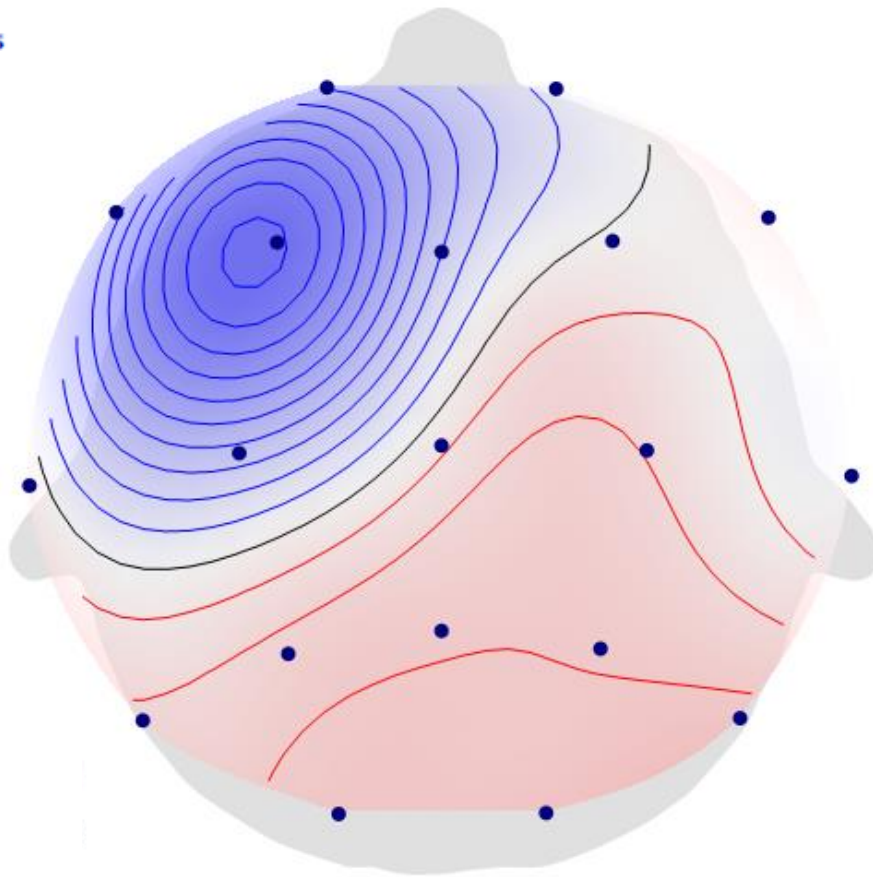
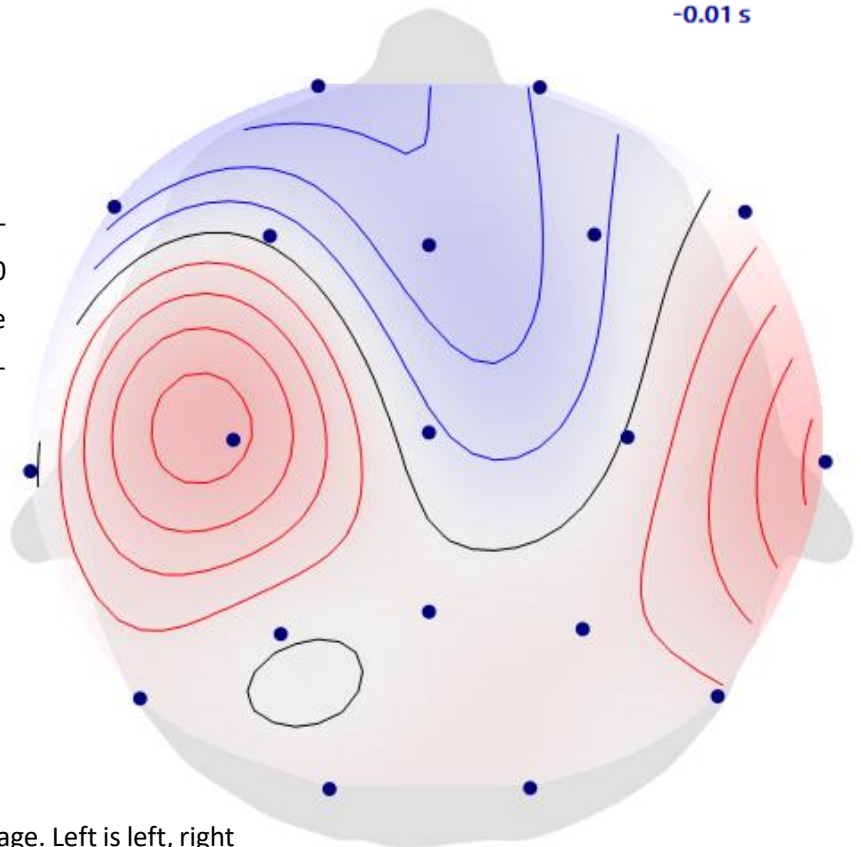
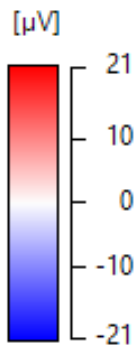


Figure 52
Shows topography of scalp potentials at the peak (0 ms) of the Stim Week Baseline average of IEDs marked by Epi-leptologist 3.

-0.01 s

Figure 53
Shows topography of scalp potentials at the rising flank (-10 ms) of the Stim Week Baseline average of IEDs marked by Epi-leptologist 3.

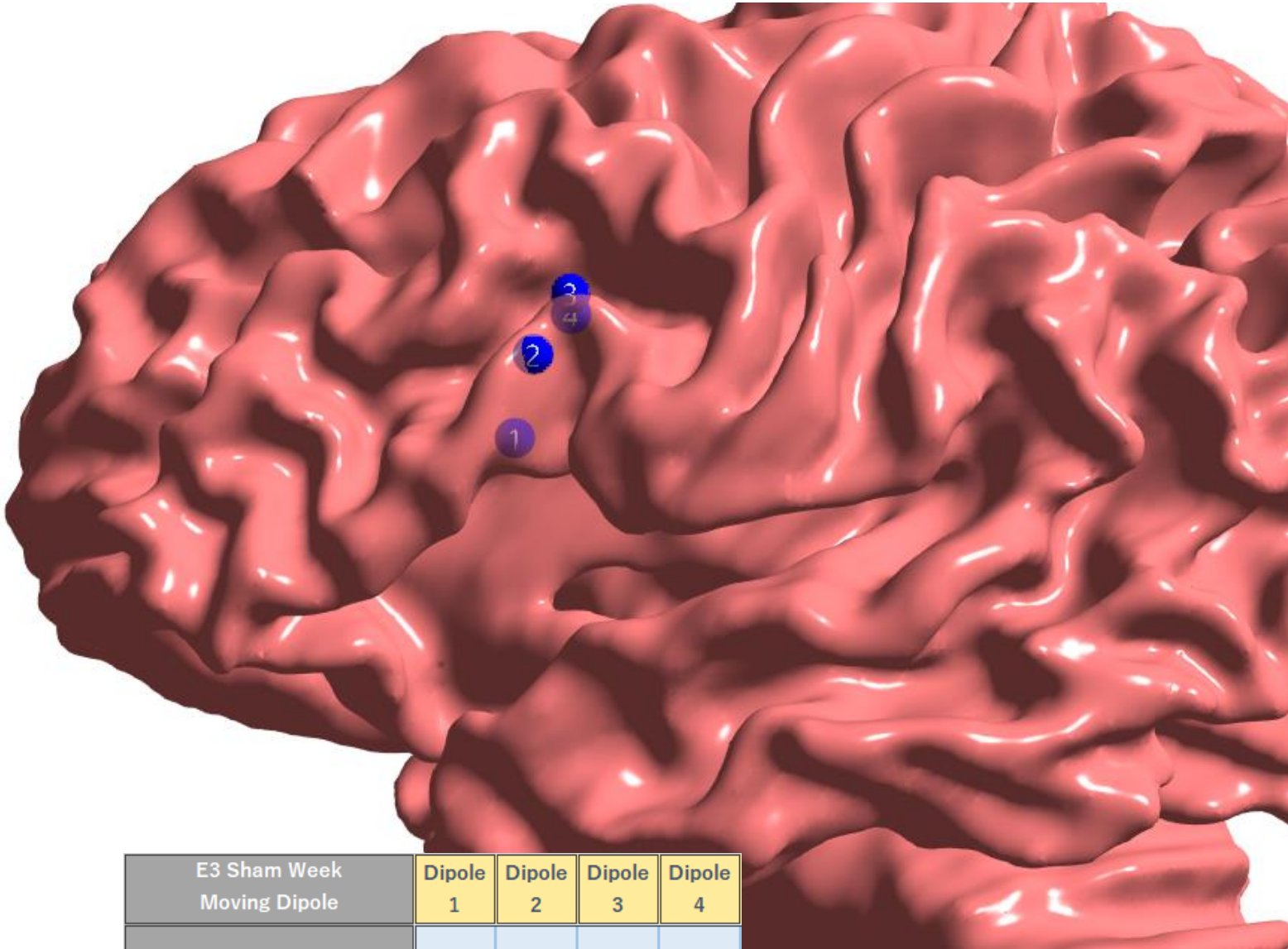


Scale for all Topologies on this page. Left is left, right is right, up is anterior and down is posterior.

Sham Week Baseline Average Moving Dipole

Figure 54

Shows location of the Sham Week Baseline Average Moving Dipole (of IEDs marked by Epileptologist 3) at different times during its rising flank until the peak. White matter for anatomic context.



E3 Sham Week Moving Dipole	Dipole 1	Dipole 2	Dipole 3	Dipole 4
Timepont in ms	-15	-10	-5	0
Signal to Noise Ratio	1.4	4.1	7.1	8.6
Explained Signal	82%	94%	96%	96%
Current Density in μ Amm	38.9	141	183	238
Maximum Amplitude at 0 ms in μ V			Max at: F3	-23.08

Table 21

Epileptologist 3 Sham Week Baseline Average Moving Dipole of IEDs. Summarizes information about dipoles of the rising flank of the average IED in the two hours before the first “Sham” marked by Epileptologist 3.

0s

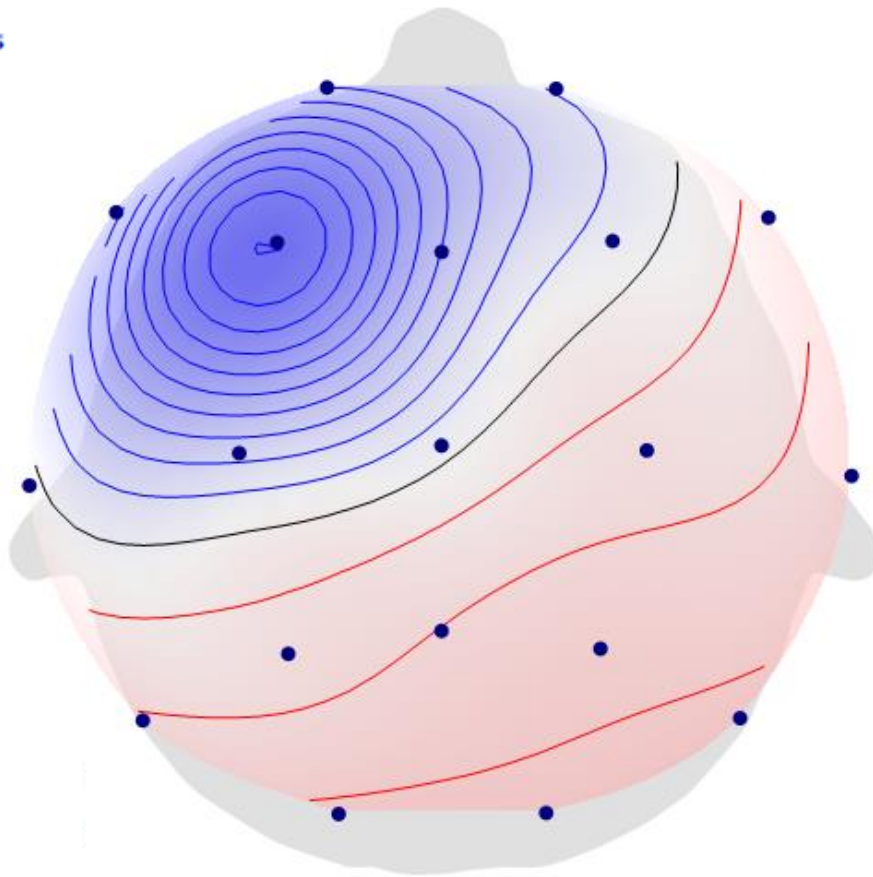
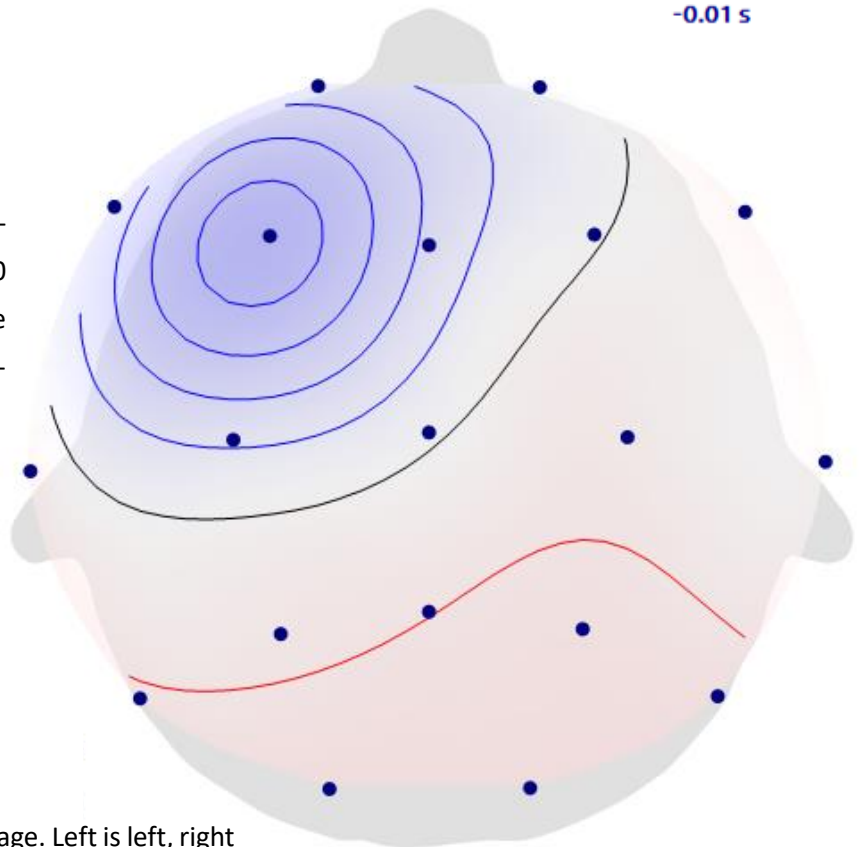
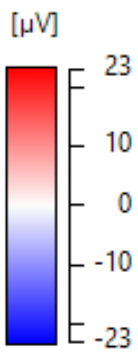


Figure 55
Shows topography of scalp potentials at the peak (0 ms) of the Sham Week Baseline average of IEDs marked by Epileptologist 3.

-0.01 s

Figure 56
Shows topography of scalp potentials at the rising flank (-10 ms) of the Sham Week Baseline average of IEDs marked by Epileptologist 3.



Scale for all Topologies on this page. Left is left, right is right, up is anterior and down is posterior.

Improved Segmentation

Skull leakages

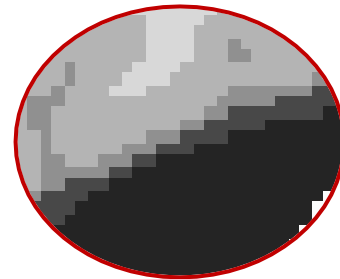
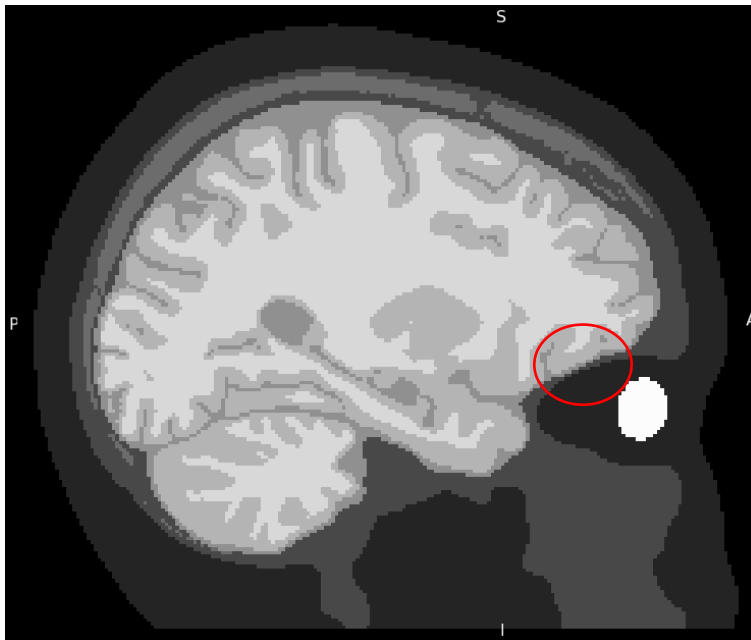


Figure 57

Shows skull leakages in otherwise improved segmentation. Sagittal plane: Right is anterior, left is posterior, up is superior and down is inferior. Red circle shows corners of scalp tissue and CSF / gray matter connected through skull.

Unfortunately, as can be seen in **Figure 57**, the new pipeline produced a segmentation with skull leakages, which is a known issue that introduces error in source estimation on the scale of centimeters and usually occurs when the spatial resolution of the MRI and segmentation is about the same or less than the thickness of the skull (Engwer et al., 2017; Sonntag et al., 2013).

Tolerability and Symptoms

No adverse effects occurred during or after personalized and dCMI optimized tDCS or ActiSham and none of the treatment blocks had to be cancelled. According to the questionnaire which uses a 5-point numerical rating scale (1 = no sensation, 5 = extreme sensation), the patient reported itching on the back of the head during “Stim” with a mean intensity of 3.4 ± 0.55 [3-4] and during “Sham” with a mean intensity of 2.8 ± 0.45 [2-3]. Further sensations were pain (under electrode F3; “Stim”: 4.2 ± 0.84 [3-5]; “Sham”: 3.4 ± 0.55 [3-4]), burning (“Stim”: 2 ± 1 [1-3]; “Sham”: 2 ± 1.41 [1-4]), warmth (“Stim”: 2.2 ± 0.84 [1-3]; “Sham”: 1.4 ± 0.89 [1-3]), tiredness or decreased attention (“Stim”: 1 ± 0 [1-1]; “Sham”: 1 ± 0 [1-1]) and dizziness (“Stim”: 3.2 ± 0.45 [3-4]; “Sham”: 1 ± 0 [1-1]). Only dizziness differed significantly in intensity between “Stim” and “Sham” ($p < 0.001$). The patient was unsure whether they experienced “Stim” or “Sham” on most days, only once during “Stim” and once during “Sham” they were sure it was “Sham” and once during “Sham” they were sure it was “Stim”. Statistical testing was done according to *Methods, Questionnaires*.

Discussion

Effect of personalized and dCMI optimized tDCS on IED frequency

As the results of the mixed ANOVA (**Table 5**) show, there is a highly significant ($p < 0.01$) interaction “TypeOfTreatment*PrePost” that produces a large F ratio ($F(2,26)=6.9$). The Tukey-HSD test results (**Table 6**) elucidates for us that this ratio is explained by the large difference between IED frequency before and after treatment with personalized and dCMI optimized tDCS (-313.7, $p < 0.00001$) and that treatment with ActiSham did not produce a significant difference (-64.47, $p > 0.05$).

While it is true that there is a significant main effect of “PrePost” on IED frequency with an even larger F ratio ($F(1,26)=18.18$), the fact that the interaction “TypeOfTreatment*PrePost” is disordinal (**Figure 8**), means that we can’t sensibly interpret that main effect. On the other hand, the interaction “Epileptologists*PrePost” has the smallest (but still large) F ratio, is significant ($F(2,26)=6.9$, $p < 0.01$) and ordinal (**Figure 9**). The reason for this is elucidated again by the Tukey-HSD test results (**Table 7**) which shows that it is all due to the difference in mean IEDs marked based on the personality of the epileptologist, especially for Epileptologist 1. But to be fair, this effect is not interesting or relevant to this study, being aware of it as context for the interesting effect is already sufficient.

Through the design of this study, specifically choosing “PrePost” as a within-subject factor, and the fact that we always measured and stimulated at the same times of day, multidien, circadian and ultradian (that go out of sync between days) rhythms in IED frequency should be controlled for (Baud et al., 2018; Langdon-Down & Russell Brain, 1929; Spencer et al., 2016).

Additionally, the effect of personalized and dCMI Optimized tDCS on IED frequency as compared to the effect of ActiSham on IED frequency can be clearly seen in **Figure 10**.

Coherent evidence with these results can be seen in **Figures 11,12** and **13**: Frequency of IEDs is always higher before “Stim” than after “Stim” for all Epileptologists except for Epileptologist 2 on day 1. This increase is explained by the outlier in **Figure 10** and the reason for the violation of normality for its data group (**Table 3**). Explanation of the origin of this outlier can be found under *Results, Absolute Frequency of IEDs in Detail*. Comparing the frequency of IEDs before and after “Sham” reveals that it can show an increase or decrease, as well as stay the same.

Effect of personalized and dCMI optimized tDCS on Seizure Severity

The effect of decreased seizure severity is postulated while only being supported by one self-reported seizure, so further investigation by future studies is needed: For the first time in the patient's life (as far as they can remember), they could resume a conversation that was interrupted by a seizure without forgetting the contents of it. This was during the week of daily treatment with personalized and dCMI optimized tDCS.

Effect of personalized and dCMI optimized tDCS on IED Source Location and Orientation

With the exception of "PostStim" the average moving dipole of the peak of IEDs seems to always inhabit a similar place, which we have seen in *Results, Source Estimation*. As a representative example for the localization of "Dipole 4" (peak), please consider **Figures 58 and 59**. In fact, we can see that it generally occurs in the pars opercularis and pars triangularis of the inferior frontal gyrus. These anatomical divisions are considered to be part of Broca's area but definitions of gross anatomy of Broca's area vary between researchers (Keller et al., 2009). In this patient, this finding is concordant with the estimation of the epileptogenic zone in presurgical evaluation.

For the average IED's rising flank (-10 ms) and the peak (0 ms) the dipole as seen from the scalp topography is generally the same with a minimum potential at F3 (**Figures 60, 61, 62 and 63**). This data is from the "PreStim" average moving dipole but is almost identical for "PreSham" and "PostSham" average moving dipoles across epileptologists (**Figures 25, 26, 28, 29, 46, 47, 49, 50**). The "PostStim" condition sees a new dipole (**Figures 64, 65, 66 and 67**). For Epileptologist 1, the "PostStim" average moving dipole sees its maximum and minimum amplitude at different electrodes (O1 and T3) than in all other conditions and since the T3 electrode couldn't be included in the source estimation, the relative explained signal is especially low at 71% (**Table 10, Figure 64**) compared to all other conditions across epileptologists. In the "PostStim" condition, the potential at T3 is more extreme than in all other conditions at the rising flank (-10 ms) and the peak (0 ms) across epileptologists (**Figures 64, 65, 66 and 67**).

In conclusion, shortly after "Stim" it seems the dipole's peak and rising flank can't occur in the same anatomical area anymore and are "kicked off course". The previous sentence has to be taken with a grain of salt, considering the scope of the study and my level of experience.

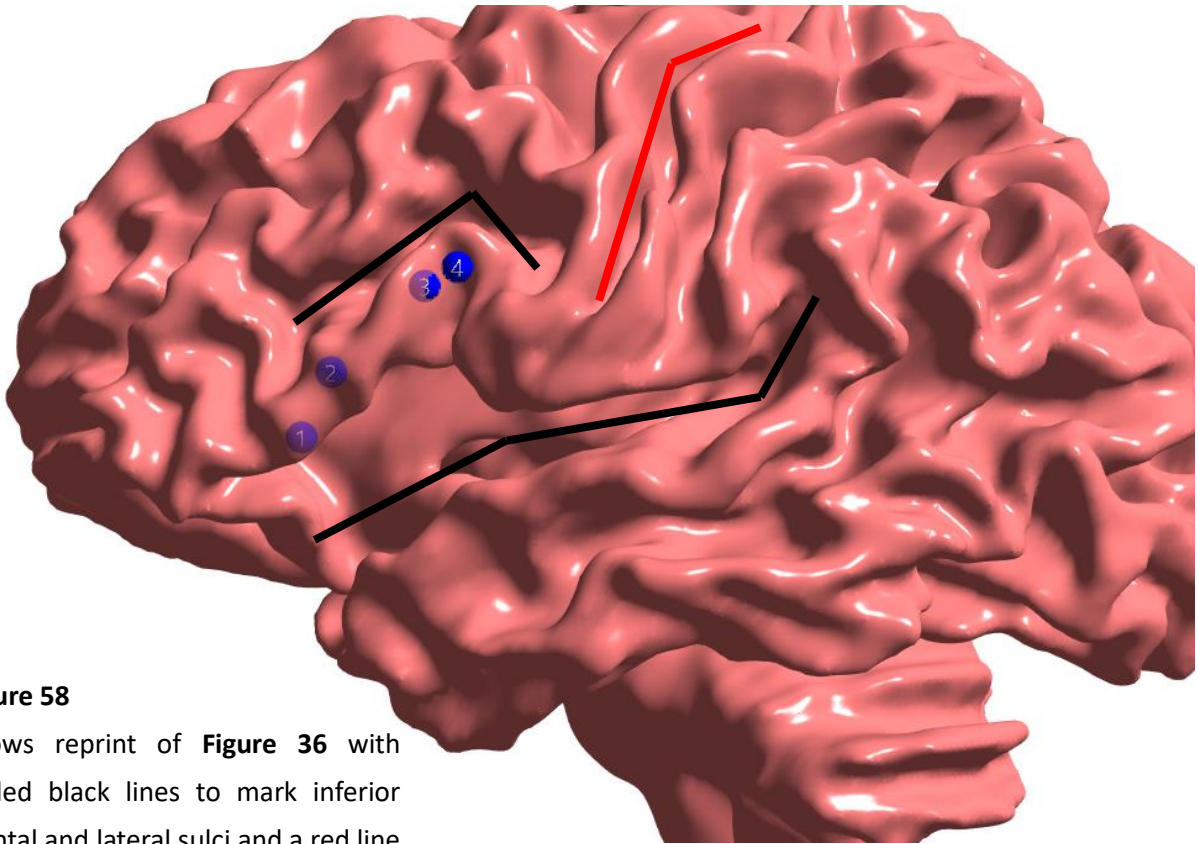


Figure 58
Shows reprint of **Figure 36** with added black lines to mark inferior frontal and lateral sulci and a red line to mark the central sulcus.

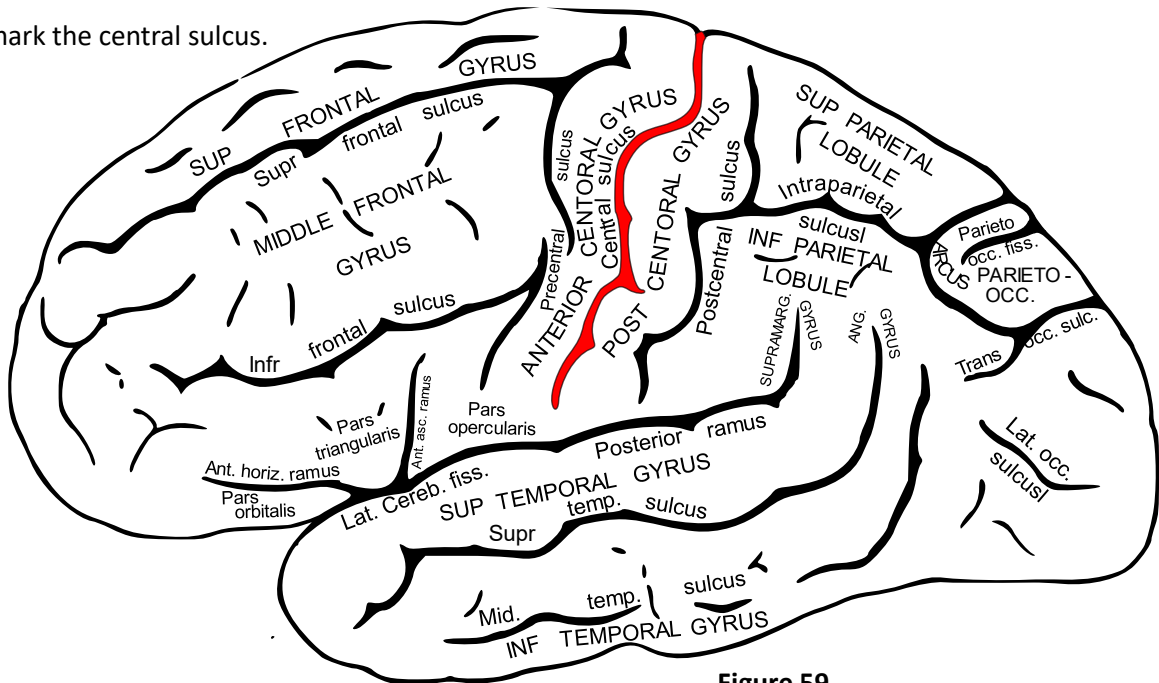
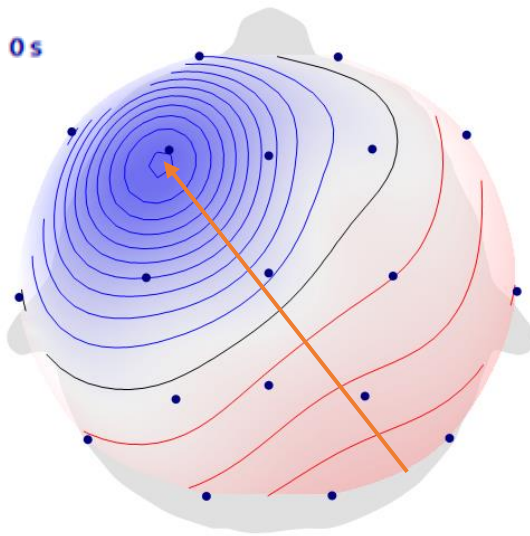
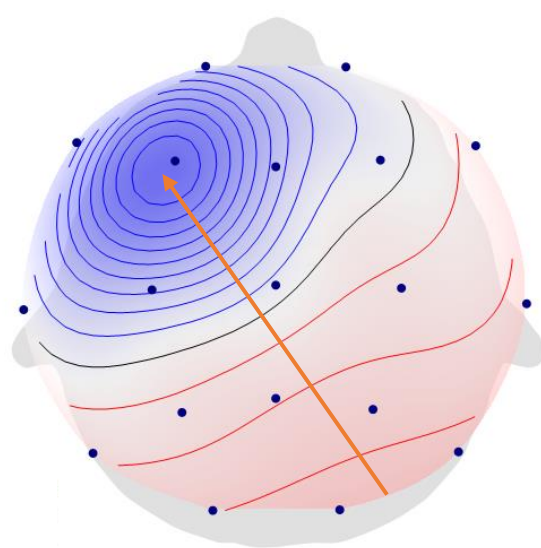


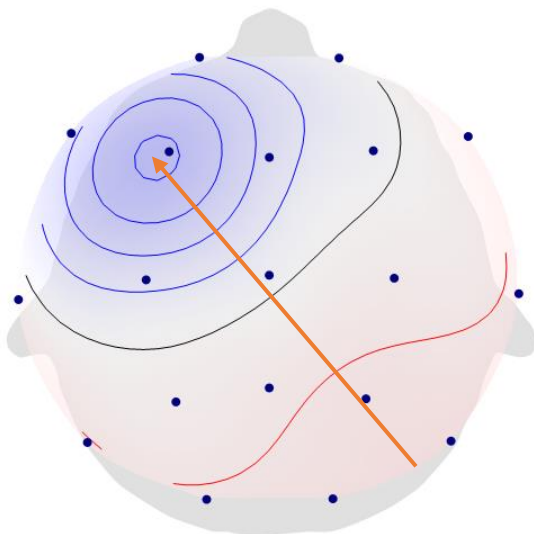
Figure 59
Shows a schematic map of anatomic zones of the brain on gray matter. Adapted from wikicommons.

**Figure 60**

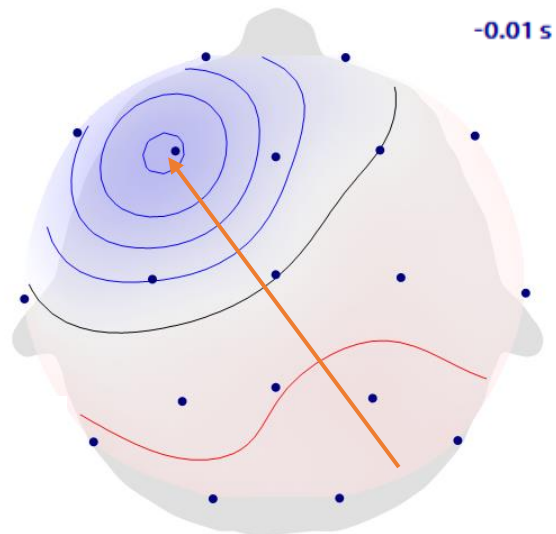
Shows topography of scalp potentials at the peak (0 ms) of the PreStim average of IEDs marked by Epileptologist 1. Orange arrow is a crude 2D representation of the dipole.

**Figure 61**

Shows topography of scalp potentials at the peak (0 ms) of the PreStim average of IEDs marked by Epileptologist 3. Orange arrow is a crude 2D representation of the dipole.

**Figure 62**

Shows topography of scalp potentials at the rising flank (-10 ms) of the PreStim average of IEDs marked by Epileptologist 1. Orange arrow is a crude 2D representation of the dipole.

**Figure 63**

Shows topography of scalp potentials at the rising flank (-10 ms) of the PreStim average of IEDs marked by Epileptologist 3. Orange arrow is a crude 2D representation of the dipole.

Left is left, right is right, up is anterior and down is posterior.

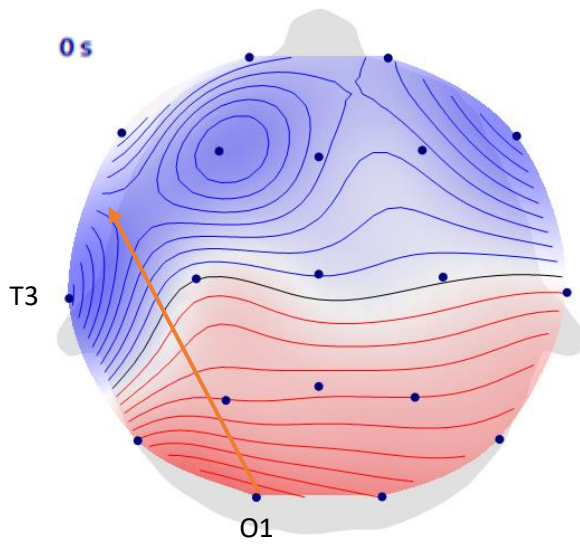


Figure 64
Shows topography of scalp potentials at the peak (0 ms) of the PostStim average of IEDs marked by Epileptologist 1. Orange arrow is a crude 2D representation of the dipole.

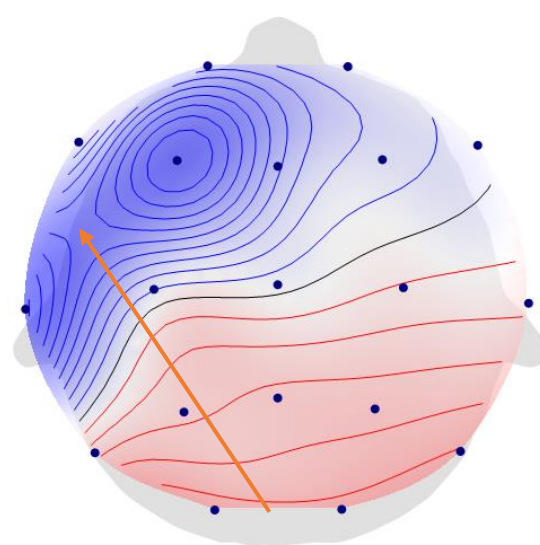


Figure 65
Shows topography of scalp potentials at the peak (0 ms) of the PostStim average of IEDs marked by Epileptologist 3. Orange arrow is a crude 2D representation of the dipole.

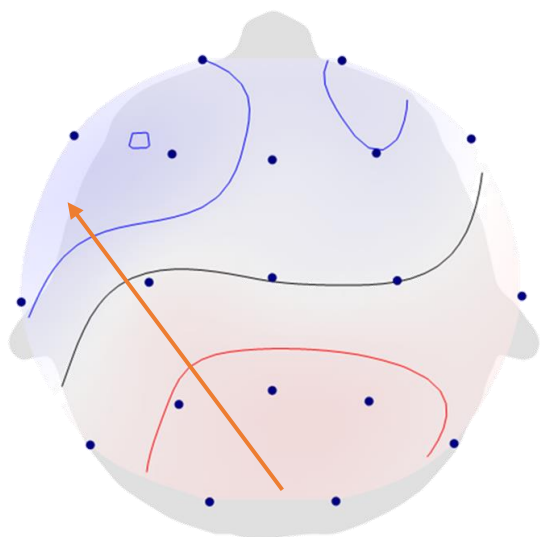


Figure 66
Shows topography of scalp potentials at the rising flank (-10 ms) of the PostStim average of IEDs marked by Epileptologist 1. Orange arrow is a crude 2D representation of the dipole.

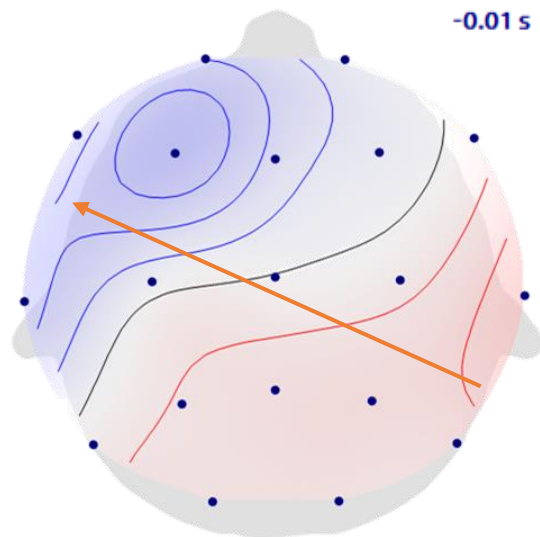


Figure 67
Shows topography of scalp potentials at the rising flank (-10 ms) of the PostStim average of IEDs marked by Epileptologist 3. Orange arrow is a crude 2D representation of the dipole.

Left is left, right is right, up is anterior and down is posterior.

Effect of personalized and dCMI optimized tDCS on IED Source Dipole Current Density

Current Density of Dipoles in μ A/mm	Baseline Stim Week	PreStim	PostStim	Baseline Sham Week	PreSham	PostSham
Epileptologist 1, Peak	266	136	155	150	182	86.4
Epileptologist 1, Flank	98	65.3	10.2	75.7	74.4	53.6
Epileptologist 3, Peak	382	267	67	238	267	156
Epileptologist 3, Flank	190	84.6	26.8	141	86.8	60.4

Table 22

Shows the current density of average dipoles in μ A/mm across conditions, gathered from **Tables 9-14** and **16-21**. Marked in red are values associated with especially low (~50-70%) relative explained signal.

Short-term

The following data is displayed in **Table 22**: The current density at the peak of the average IED's moving dipole sees a 14% increase from "PreStim" to "PostStim" (136 to 155 μ A/mm) but at "PostStim" it explains only a very low percentage of the signal. This likely means that the dipole is not representative of the data since the minimum amplitude is far less extreme after "Stim" than before ("PreStim" minimum amplitude: -9.55 μ V vs. "PostStim" minimum amplitude: -2.94 μ V) and the fact that T3, which shows the minimum amplitude in this condition, couldn't be included in source estimation. Generally, we see decreases in current density after treatment but the decrease after "Stim" is larger. This effect is best observed at the flank: E1Stim: 84% decrease vs. E1Sham: 28% decrease and E3Stim: 68% decrease vs. E3Sham: 30% decrease.

In conclusion, there seems to be a short-term effect of personalized and dCMI optimized tDCS on the current density of IED source dipoles since it sees a decrease at the flank or onset with treatment, that is much larger after "Stim" than after "Sham". This is concordant with reductions in peak amplitude.

Long-term

There could be made an argument for the decrease in current density of average dipoles between baselines of "Stim" and "Sham" weeks: E1Peak: 44% decrease, E1Flank: 23% decrease, E3Peak: 38% decrease and E3Flank: 26% decrease. But considering the stressful time the patient

was experiencing during the “Stim” week due to exams (stress is shown to be able to increase IED frequency (Van Campen et al., 2016)), which wasn’t the case for the “Sham” week, I don’t think this data necessarily gives a hint towards a potential long-term effect with only one week of personalized and dCMI optimized tDCS and over a month of downtime between “Stim” and “Sham” weeks. In fact, the study was set up with the control of a possible long-term effect in mind to keep conditions for “Sham” as close to “Stim” as possible (*Methods, Study Design*).

Effect of increased Quality in Segmentation on dCMI Montage

This thesis really cannot make a statement about the effect of increased quality in segmentation on the dCMI montage. In the end, there wasn’t enough time before this thesis’s deadline to fix the skull leakages and since they introduce error on the scale of centimeters, while differences in segmentation usually only result in differences in localization on the scale of millimeters, there wasn’t much sense in presenting anything more here. In my opinion, even though attempting to create a superior pipeline with improved segmentation bloated the scale of the thesis beyond a reasonable scope, it was worth a shot, though.

tDCS as an Epilepsy Therapy

No adverse effects occurred, and the reported sensations ranged from a minor inconvenience to “enough pain to be sure it’s not homeopathy”. Comparing this to other neurostimulation treatment modalities for refractory epilepsy, tDCS (and arguably TMS even though it’s not discussed in this thesis) has remarkably less serious side effects which are mild and transient sensations, is less expensive, shows short-term effects (as we have seen in this thesis) on IED frequency, while other neurostimulation approaches usually yield results in the time frame of years, and is reversible as opposed to invasive neurostimulation devices which surgeons often won’t dare to remove completely after some years have passed (Kaufmann et al., 2021).

Interestingly, dizziness only occurred in “Stim” and not in “Sham”. This could be due to ActiSham being designed to mostly channeling current through the scalp as opposed to through the brain. Lastly, the blinding of the patient was a success, as seen in *Results, Tolerability and Symptoms*.

Physiological Explanation

Physiologically, the tDCS's effects are best explained by a direct modulation of the neuronal threshold potential thus altering the presynaptic probability for release. If enough neurons are affected, even large cortical networks see a change in dynamics. One of these dynamics is the IED and one change would be a change in location and propagation like running water forming different rivers depending on the ground's surface and incline, while the other is a reduction in the current density of its moving dipole since it is a summation of the currents generated and propagated by the neurons in its area which would be decreased if the presynaptic probability for release was lowered. This is likely to be the explanation for the short-term effects.

Long-term effects (which we didn't see in this study) would be thusly explained by activity-dependent plasticity which allows neurons (and by extension large cortical networks) to change their excitability long term with use (use in this case is the change in dynamic of the cortical network) (Patten et al., 2016).

This explanation is supported by simulations with computational models (Denoyer et al., 2020).

Conclusion

The main work of the SIM-NEURO (Stimulation, Imaging and Modelling of NEURONal networks in the human brain) research group concerns the development of new methods and applications for multimodal brain imaging and stimulation. It is traditionally quite a bit removed from conducting clinical trials. But when a crude two-electrode implementation of tDCS, which it was indeed developing highly advanced methods for, showed promise as a potential effective treatment for focal refractory epilepsy while considering that the landscape of treatments for DRE patients who surgery isn't indicated for is otherwise especially disappointing, for the first time it seemed that the highly advanced but laborious methods used usually foremost in research could directly benefit patients immoderately, even in a clinical setting. Since presurgical examinations in epilepsy use a wide array of exhaustive diagnostics, the required preparations (source estimation, modalities etc.) for personalized and dCMI optimized tDCS are already given, minimizing the added effort as compared to a crude two-electrode approach that offers extremely limited directionality and focality. The theoretical upsides seemed obvious: precise and optimized directionality and focality of stimulation leading to a greater effect on the target while minimizing side effects of stimulating large unrelated parts of the patient's brain.

The double-blind sham-controlled pilot/feasibility clinical trial elucidated the following effects for personalized and dCMI optimized tDCS:

1. A large statistically significant short-term reduction of IED frequency.
2. Possibly, a reduction in seizure severity.
3. A large change in location and propagation of IED source dipoles.
4. A large short-term reduction in current density of IED source dipoles.

Since long-term effects of personalized and dCMI optimized tDCS had been controlled for in the study design, we can only say that no long-term effects were powerful enough to break through control.

Lastly, considering that our findings are concordant with the literature's assessment of very mild and transient sensations as side effects of tDCS, I can only conclude this thesis with:

“The future of tDCS as a treatment for DRE continues to be very exciting and promising. The next step is to increase the scope of clinical trials with the eventual goal for widespread approval for clinical use in treating DRE.”

Acknowledgements

As I write these words at 5:39 AM tired but absorbed in thought, I have to give thanks to the people along the way:

- My thesis supervisor Prof. Dr. rer. nat. Carsten Wolters who trusted me with this research even though I remember him talking about this being the highpoint of his career so far. I hope I could deliver even just partly on the grand expectations and that he will go on with Malte and the others to build on this and do even more amazing research in the future.
- My second thesis supervisor Prof. Dr. rer. nat. Ulrich Stöber who gave me a push out of the door, and into the door of IBB, yet again when I myself wasn't. I have him to thank for doing research, which was always my dream.
- Tim, Marios (Dr. Marios), Yvonne and Malte for surviving the onslaught of questions that came their way and for all their help they gave in response.
- The epileptologists for having to mark way more EEGs than usual for this kind of research next to taxing full time jobs (how do they do it?).
- Microsoft Word for proofreading this thesis at 6 AM in the morning.
- My parents for all the patience and support they gave me over the years, allowing me to study, go to Japan and follow my dreams without having to work jobs on the side. I would not be anywhere close to where I am today without their sacrifice.
- And finally, my girlfriend Norika who fought with me through this last year and who is the only one actually able to calm the chaos in my mind.

List of Figures

FIGURE 1

THE STRUCTURE OF A NEURON. ADAPTED FROM INTRODUCTION TO PSYCHOLOGY - 1ST CANADIAN EDITION BY JENNIFER WALINGA. 4

FIGURE 2

DIFFERENT PHASES OF A NEURONAL ACTION POTENTIAL. ① THRESHOLD POTENTIAL ② DEPOLARIZATION ③ RE- AND HYPERPOLARIZATION ADAPTED FROM (FINK, 2012). 4

FIGURE 3

SHOWS THAT THE MYELIN SHEATH INCREASES NERVE CONDUCTION VELOCITY OF AN AXON BY SALTATORY CONDUCTION. ADAPTED FROM AMBOSS. 4

FIGURE 4

GROSS ANATOMY OF THE BRAIN. CEREBRAL LOBES IN COLOR; CEREBELLUM AND SPINAL CORD IN GRAY. ADAPTED FROM JOHN HOPKINS UNIVERSITY. 6

FIGURE 5

SHOWS THE LOCATION OF THE LIMBIC LOBE IN RELATION TO CEREBRAL LOBES. ADAPTED FROM WIKICOMMONS. 6

FIGURE 6

FRAMEWORK FOR CLASSIFICATION OF THE EPILEPSIES. 10
ADAPTED FROM (SCHEFFER ET AL., 2017). 10

FIGURE 7

SHOWS THE DCMI OPTIMIZED MONTAGE WITH CURRENT IN A. 21

FIGURE 8

SHOWS INTERACTION EFFECT OF "PREPOST" AND "TYPEOFTREATMENT" ON IED FREQUENCY. 25

FIGURE 9

SHOWS INTERACTION EFFECT OF "PREPOST" AND "EPILEPTOLOGISTS" ON IED FREQUENCY. 25

FIGURE 10

SHOWS BOX PLOT FOR RELATIVE FREQUENCY OF IEDS AFTER TREATMENT TO BEFORE TREATMENT FOR EVERY "EPILEPTOLOGISTS" "TYPEOFTREATMENT" COMBINATION. THERE IS AN OUTLIER IN THE "STIM/EPILEPTOLOGIST2" DATA

GROUP.	28
FIGURE 11	
SHOWS FREQUENCY OF IEDS BEFORE AND AFTER TREATMENT (“PREPOST”) FOR EVERY DAY AND “TYPEOF TREATMENT” WITH DATA MARKED BY EPILEPTOLOGIST 1.	29
FIGURE 12	
SHOWS FREQUENCY OF IEDS BEFORE AND AFTER TREATMENT (“PREPOST”) FOR EVERY DAY AND “TYPEOF TREATMENT” WITH DATA MARKED BY EPILEPTOLOGIST 2.	30
FIGURE 13	
SHOWS FREQUENCY OF IEDS BEFORE AND AFTER TREATMENT (“PREPOST”) FOR EVERY DAY AND “TYPEOF TREATMENT” WITH DATA MARKED BY EPILEPTOLOGIST 3.	30
FIGURE 14	
SHOWS AVERAGED DAILY FREQUENCY OF IEDS OVER THE “STIM” AND “SHAM” WEEKS. THE IEDS CONSIDERED FOR THIS FIGURE ARE THE ONES THAT EVERY EPILEPTOLOGIST COULD AGREE ON, HENCE THE COMPARABLY LOW VALUES. THE AVERAGE FREQUENCY OF IEDS IS 31.27 IEDS PER HOUR FOR THE “STIM” WEEK AND 34.07 IEDS PER HOUR FOR THE “SHAM” WEEK.	31
FIGURE 15	
SHOWS LOCATION OF THE GLOBAL AVERAGE MOVING DIPOLE (OF IEDS MARKED BY EPILEPTOLOGIST 1) AT DIFFERENT TIMES DURING ITS RISING FLANK UNTIL THE PEAK.	33
WHITE MATTER FOR ANATOMIC CONTEXT.	33
	33
	33
	33
FIGURE 16	
SHOWS TOPOGRAPHY OF SCALP POTENTIALS AT THE PEAK (0 MS) OF THE GLOBAL AVERAGE OF IEDS MARKED BY EPILEPTOLOGIST 1.	34
SCALE FOR ALL TOPOLOGIES ON THIS PAGE. LEFT IS LEFT, RIGHT IS RIGHT, UP IS ANTERIOR AND DOWN IS POSTERIOR.	34
FIGURE 17	
SHOWS TOPOGRAPHY OF SCALP POTENTIALS AT THE RISING FLANK (-10 MS) OF THE GLOBAL AVERAGE OF IEDS MARKED BY EPILEPTOLOGIST 1.	34
FIGURE 18	

SHOWS LOCATION OF THE PRESTIM AVERAGE MOVING DIPOLE (OF IEDS MARKED BY EPILEPTOLOGIST 1) AT DIFFERENT TIMES DURING ITS RISING FLANK UNTIL THE PEAK. WHITE MATTER FOR ANATOMIC CONTEXT.	35
FIGURE 19	
SHOWS TOPOGRAPHY OF SCALP POTENTIALS AT THE PEAK (0 MS) OF THE PRESTIM AVERAGE OF IEDS MARKED BY EPILEPTOLOGIST 1.	36
SCALE FOR ALL TOPOLOGIES ON THIS PAGE. LEFT IS LEFT, RIGHT IS RIGHT, UP IS ANTERIOR AND DOWN IS POSTERIOR.	36
FIGURE 20	
SHOWS TOPOGRAPHY OF SCALP POTENTIALS AT THE RISING FLANK (-10 MS) OF THE PRESTIM AVERAGE OF IEDS MARKED BY EPILEPTOLOGIST 1.	36
FIGURE 21	
SHOWS LOCATION OF THE POSTSTIM AVERAGE MOVING DIPOLE (OF IEDS MARKED BY EPILEPTOLOGIST 1) AT DIFFERENT TIMES DURING ITS RISING FLANK UNTIL THE PEAK. WHITE MATTER FOR ANATOMIC CONTEXT.	37
FIGURE 22	
SHOWS TOPOGRAPHY OF SCALP POTENTIALS AT THE PEAK (0 MS) OF THE POSTSTIM AVERAGE OF IEDS MARKED BY EPILEPTOLOGIST 1.	38
SCALE FOR ALL TOPOLOGIES ON THIS PAGE. LEFT IS LEFT, RIGHT IS RIGHT, UP IS ANTERIOR AND DOWN IS POSTERIOR.	38
FIGURE 23	
SHOWS TOPOGRAPHY OF SCALP POTENTIALS AT THE RISING FLANK (-10 MS) OF THE POSTSTIM AVERAGE OF IEDS MARKED BY EPILEPTOLOGIST 1.	38
FIGURE 24	
SHOWS LOCATION OF THE PRESHAM AVERAGE MOVING DIPOLE (OF IEDS MARKED BY EPILEPTOLOGIST 1) AT DIFFERENT TIMES DURING ITS RISING FLANK UNTIL THE PEAK. WHITE MATTER FOR ANATOMIC CONTEXT.	39
FIGURE 25	
SHOWS TOPOGRAPHY OF SCALP POTENTIALS AT THE PEAK (0 MS) OF THE PRESHAM AVERAGE OF IEDS MARKED BY EPILEPTOLOGIST 1.	40
SCALE FOR ALL TOPOLOGIES ON THIS PAGE. LEFT IS LEFT, RIGHT IS RIGHT, UP IS ANTERIOR AND DOWN IS POSTERIOR.	40
FIGURE 26	
SHOWS TOPOGRAPHY OF SCALP POTENTIALS AT THE RISING FLANK (-10 MS) OF THE PRESHAM AVERAGE OF IEDS MARKED BY EPILEPTOLOGIST 1.	40
FIGURE 27	

SHOWS LOCATION OF THE POSTSHAM AVERAGE MOVING DIPOLE (OF IEDS MARKED BY EPILEPTOLOGIST 1) AT DIFFERENT TIMES DURING ITS RISING FLANK UNTIL THE PEAK. WHITE MATTER FOR ANATOMIC CONTEXT.	41
FIGURE 28	
SHOWS TOPOGRAPHY OF SCALP POTENTIALS AT THE PEAK (0 MS) OF THE POSTSHAM AVERAGE OF IEDS MARKED BY EPILEPTOLOGIST 1.	42
SCALE FOR ALL TOPOLOGIES ON THIS PAGE. LEFT IS LEFT, RIGHT IS RIGHT, UP IS ANTERIOR AND DOWN IS POSTERIOR.	42
FIGURE 29	
SHOWS TOPOGRAPHY OF SCALP POTENTIALS AT THE RISING FLANK (-10 MS) OF THE POSTSHAM AVERAGE OF IEDS MARKED BY EPILEPTOLOGIST 1.	42
FIGURE 30	
SHOWS LOCATION OF THE STIM WEEK BASELINE AVERAGE MOVING DIPOLE (OF IEDS MARKED BY EPILEPTOLOGIST 1) AT DIFFERENT TIMES DURING ITS RISING FLANK UNTIL THE PEAK. WHITE MATTER FOR ANATOMIC CONTEXT.	43
FIGURE 31	
SHOWS TOPOGRAPHY OF SCALP POTENTIALS AT THE PEAK (0 MS) OF THE STIM WEEK BASELINE AVERAGE OF IEDS MARKED BY EPILEPTOLOGIST 1.	44
SCALE FOR ALL TOPOLOGIES ON THIS PAGE. LEFT IS LEFT, RIGHT IS RIGHT, UP IS ANTERIOR AND DOWN IS POSTERIOR.	44
FIGURE 32	
SHOWS TOPOGRAPHY OF SCALP POTENTIALS AT THE RISING FLANK (-10 MS) OF THE STIM WEEK BASELINE AVERAGE OF IEDS MARKED BY EPILEPTOLOGIST 1.	44
FIGURE 33	
SHOWS LOCATION OF THE SHAM WEEK BASELINE AVERAGE MOVING DIPOLE (OF IEDS MARKED BY EPILEPTOLOGIST 1) AT DIFFERENT TIMES DURING ITS RISING FLANK UNTIL THE PEAK. WHITE MATTER FOR ANATOMIC CONTEXT.	45
FIGURE 34	
SHOWS TOPOGRAPHY OF SCALP POTENTIALS AT THE PEAK (0 MS) OF THE SHAM WEEK BASELINE AVERAGE OF IEDS MARKED BY EPILEPTOLOGIST 1.	46
SCALE FOR ALL TOPOLOGIES ON THIS PAGE. LEFT IS LEFT, RIGHT IS RIGHT, UP IS ANTERIOR AND DOWN IS POSTERIOR.	46
FIGURE 35	
SHOWS TOPOGRAPHY OF SCALP POTENTIALS AT THE RISING FLANK (-10 MS) OF THE SHAM WEEK BASELINE AVERAGE OF IEDS MARKED BY EPILEPTOLOGIST 1.	46
FIGURE 36	

SHOWS LOCATION OF THE GLOBAL AVERAGE MOVING DIPOLE (OF IEDS MARKED BY EPILEPTOLOGIST 3) AT DIFFERENT TIMES DURING ITS RISING FLANK UNTIL THE PEAK. WHITE MATTER FOR ANATOMIC CONTEXT.	47
FIGURE 37	
SHOWS TOPOGRAPHY OF SCALP POTENTIALS AT THE PEAK (0 MS) OF THE GLOBAL AVERAGE OF IEDS MARKED BY EPILEPTOLOGIST 3.	48
SCALE FOR ALL TOPOLOGIES ON THIS PAGE. LEFT IS LEFT, RIGHT IS RIGHT, UP IS ANTERIOR AND DOWN IS POSTERIOR.	48
FIGURE 38	
SHOWS TOPOGRAPHY OF SCALP POTENTIALS AT THE RISING FLANK (-10 MS) OF THE GLOBAL AVERAGE OF IEDS MARKED BY EPILEPTOLOGIST 3.	48
FIGURE 39	
SHOWS LOCATION OF THE PRESTIM AVERAGE MOVING DIPOLE (OF IEDS MARKED BY EPILEPTOLOGIST 3) AT DIFFERENT TIMES DURING ITS RISING FLANK UNTIL THE PEAK. WHITE MATTER FOR ANATOMIC CONTEXT.	49
FIGURE 40	
SHOWS TOPOGRAPHY OF SCALP POTENTIALS AT THE PEAK (0 MS) OF THE PRESTIM AVERAGE OF IEDS MARKED BY EPILEPTOLOGIST 3.	50
SCALE FOR ALL TOPOLOGIES ON THIS PAGE. LEFT IS LEFT, RIGHT IS RIGHT, UP IS ANTERIOR AND DOWN IS POSTERIOR.	50
FIGURE 41	
SHOWS TOPOGRAPHY OF SCALP POTENTIALS AT THE RISING FLANK (-10 MS) OF THE PRESTIM AVERAGE OF IEDS MARKED BY EPILEPTOLOGIST 3.	50
FIGURE 42	
SHOWS LOCATION OF THE POSTSTIM AVERAGE MOVING DIPOLE (OF IEDS MARKED BY EPILEPTOLOGIST 3) AT DIFFERENT TIMES DURING ITS RISING FLANK UNTIL THE PEAK. WHITE MATTER FOR ANATOMIC CONTEXT.	51
FIGURE 43	
SHOWS TOPOGRAPHY OF SCALP POTENTIALS AT THE PEAK (0 MS) OF THE POSTSTIM AVERAGE OF IEDS MARKED BY EPILEPTOLOGIST 3.	52
SCALE FOR ALL TOPOLOGIES ON THIS PAGE. LEFT IS LEFT, RIGHT IS RIGHT, UP IS ANTERIOR AND DOWN IS POSTERIOR.	52
FIGURE 44	
SHOWS TOPOGRAPHY OF SCALP POTENTIALS AT THE RISING FLANK (-10 MS) OF THE POSTSTIM AVERAGE OF IEDS MARKED BY EPILEPTOLOGIST 3.	52
FIGURE 45	

SHOWS LOCATION OF THE PRESHAM AVERAGE MOVING DIPOLE (OF IEDS MARKED BY EPILEPTOLOGIST 3) AT DIFFERENT TIMES DURING ITS RISING FLANK UNTIL THE PEAK. WHITE MATTER FOR ANATOMIC CONTEXT.	53
FIGURE 46	
SHOWS TOPOGRAPHY OF SCALP POTENTIALS AT THE PEAK (0 MS) OF THE PRESHAM AVERAGE OF IEDS MARKED BY EPILEPTOLOGIST 3.	54
SCALE FOR ALL TOPOLOGIES ON THIS PAGE. LEFT IS LEFT, RIGHT IS RIGHT, UP IS ANTERIOR AND DOWN IS POSTERIOR.	54
FIGURE 47	
SHOWS TOPOGRAPHY OF SCALP POTENTIALS AT THE RISING FLANK (-10 MS) OF THE PRESHAM AVERAGE OF IEDS MARKED BY EPILEPTOLOGIST 3.	54
FIGURE 48	
SHOWS LOCATION OF THE POSTSHAM AVERAGE MOVING DIPOLE (OF IEDS MARKED BY EPILEPTOLOGIST 3) AT DIFFERENT TIMES DURING ITS RISING FLANK UNTIL THE PEAK. WHITE MATTER FOR ANATOMIC CONTEXT.	55
FIGURE 49	
SHOWS TOPOGRAPHY OF SCALP POTENTIALS AT THE PEAK (0 MS) OF THE POSTSHAM AVERAGE OF IEDS MARKED BY EPILEPTOLOGIST 3.	56
SCALE FOR ALL TOPOLOGIES ON THIS PAGE. LEFT IS LEFT, RIGHT IS RIGHT, UP IS ANTERIOR AND DOWN IS POSTERIOR.	56
FIGURE 50	
SHOWS TOPOGRAPHY OF SCALP POTENTIALS AT THE RISING FLANK (-10 MS) OF THE POSTSHAM AVERAGE OF IEDS MARKED BY EPILEPTOLOGIST 3.	56
FIGURE 51	
SHOWS LOCATION OF THE STIM WEEK BASELINE AVERAGE MOVING DIPOLE (OF IEDS MARKED BY EPILEPTOLOGIST 3) AT DIFFERENT TIMES DURING ITS RISING FLANK UNTIL THE PEAK. WHITE MATTER FOR ANATOMIC CONTEXT.	57
FIGURE 52	
SHOWS TOPOGRAPHY OF SCALP POTENTIALS AT THE PEAK (0 MS) OF THE STIM WEEK BASELINE AVERAGE OF IEDS MARKED BY EPILEPTOLOGIST 3.	58
SCALE FOR ALL TOPOLOGIES ON THIS PAGE. LEFT IS LEFT, RIGHT IS RIGHT, UP IS ANTERIOR AND DOWN IS POSTERIOR.	58
FIGURE 53	
SHOWS TOPOGRAPHY OF SCALP POTENTIALS AT THE RISING FLANK (-10 MS) OF THE STIM WEEK BASELINE AVERAGE OF IEDS MARKED BY EPILEPTOLOGIST 3.	58
FIGURE 54	

- SHOWS LOCATION OF THE SHAM WEEK BASELINE AVERAGE MOVING DIPOLE (OF IEDS MARKED BY EPILEPTOLOGIST 3) AT DIFFERENT TIMES DURING ITS RISING FLANK UNTIL THE PEAK. WHITE MATTER FOR ANATOMIC CONTEXT. 59
- FIGURE 55**
- SHOWS TOPOGRAPHY OF SCALP POTENTIALS AT THE PEAK (0 MS) OF THE SHAM WEEK BASELINE AVERAGE OF IEDS MARKED BY EPILEPTOLOGIST 3. 60
- SCALE FOR ALL TOPOLOGIES ON THIS PAGE. LEFT IS LEFT, RIGHT IS RIGHT, UP IS ANTERIOR AND DOWN IS POSTERIOR. 60
- FIGURE 56**
- SHOWS TOPOGRAPHY OF SCALP POTENTIALS AT THE RISING FLANK (-10 MS) OF THE SHAM WEEK BASELINE AVERAGE OF IEDS MARKED BY EPILEPTOLOGIST 3. 60
- FIGURE 57**
- SHOWS SKULL LEAKAGES IN OTHERWISE IMPROVED SEGMENTATION. SAGITTAL PLANE: RIGHT IS ANTERIOR, LEFT IS POSTERIOR, UP IS SUPERIOR AND DOWN IS INFERIOR. RED CIRCLE SHOWS CORNERS OF SCALP TISSUE AND CSF / GRAY MATTER CONNECTED THROUGH SKULL. 61
- FIGURE 58**
- SHOWS REPRINT OF **FIGURE 36** WITH ADDED BLACK LINES TO MARK INFERIOR FRONTAL AND LATERAL SULCI AND A RED LINE TO MARK THE CENTRAL SULCUS. 64
- FIGURE 59**
- SHOWS A SCHEMATIC MAP OF ANATOMIC ZONES OF THE BRAIN ON GRAY MATTER. ADAPTED FROM WIKICOMMONS. 64
- FIGURE 60**
- SHOWS TOPOGRAPHY OF SCALP POTENTIALS AT THE PEAK (0 MS) OF THE PRESTIM AVERAGE OF IEDS MARKED BY EPILEPTOLOGIST 1. ORANGE ARROW IS A CRUDE 2D REPRESENTATION OF THE DIPOLE. 65
- LEFT IS LEFT, RIGHT IS RIGHT, UP IS ANTERIOR AND DOWN IS POSTERIOR. 65
- FIGURE 61**
- SHOWS TOPOGRAPHY OF SCALP POTENTIALS AT THE PEAK (0 MS) OF THE PRESTIM AVERAGE OF IEDS MARKED BY EPILEPTOLOGIST 3. ORANGE ARROW IS A CRUDE 2D REPRESENTATION OF THE DIPOLE. 65
- FIGURE 62**
- SHOWS TOPOGRAPHY OF SCALP POTENTIALS AT THE RISING FLANK (-10 MS) OF THE PRESTIM AVERAGE OF IEDS MARKED BY EPILEPTOLOGIST 1. ORANGE ARROW IS A CRUDE 2D REPRESENTATION OF THE DIPOLE. 65
- FIGURE 63**
- SHOWS TOPOGRAPHY OF SCALP POTENTIALS AT THE RISING FLANK (-10 MS) OF THE PRESTIM AVERAGE OF IEDS MARKED

BY EPILEPTOLOGIST 3. ORANGE ARROW IS A CRUDE 2D REPRESENTATION OF THE DIPOLE. 65

FIGURE 64

SHOWS TOPOGRAPHY OF SCALP POTENTIALS AT THE PEAK (0 MS) OF THE POSTSTIM AVERAGE OF IEDS MARKED BY EPILEPTOLOGIST 1. ORANGE ARROW IS A CRUDE 2D REPRESENTATION OF THE DIPOLE. 66

LEFT IS LEFT, RIGHT IS RIGHT, UP IS ANTERIOR AND DOWN IS POSTERIOR. 66

FIGURE 65

SHOWS TOPOGRAPHY OF SCALP POTENTIALS AT THE PEAK (0 MS) OF THE POSTSTIM AVERAGE OF IEDS MARKED BY EPILEPTOLOGIST 3. ORANGE ARROW IS A CRUDE 2D REPRESENTATION OF THE DIPOLE. 66

FIGURE 66

SHOWS TOPOGRAPHY OF SCALP POTENTIALS AT THE RISING FLANK (-10 MS) OF THE POSTSTIM AVERAGE OF IEDS MARKED BY EPILEPTOLOGIST 1. ORANGE ARROW IS A CRUDE 2D REPRESENTATION OF THE DIPOLE. 66

FIGURE 67

SHOWS TOPOGRAPHY OF SCALP POTENTIALS AT THE RISING FLANK (-10 MS) OF THE POSTSTIM AVERAGE OF IEDS MARKED BY EPILEPTOLOGIST 3. ORANGE ARROW IS A CRUDE 2D REPRESENTATION OF THE DIPOLE. 66

List of Tables

TABLE 1		
	BASIC ILAE 2017 OPERATIONAL CLASSIFICATION OF SEIZURE TYPES.	9
TABLE 2		
	SHOWS CURRENT DENSITY IN A/m^2 FOR THE DCMI MONTAGE WITH A λ OF 80 AND THE ACTISHAM MONTAGE. THE VALUES FOR ACTISHAM ARE VERY SMALL WHICH IMPLIES NEAR ZERO EFFICACY.	20
TABLE 3		
	TESTS FOR NORMALITY WITH SHAPIRO-WILK. NORMALITY IS ONLY REJECTED FOR THE "STIM/EPILEPTOLOGIST 2" DATA GROUP.	24
TABLE 4		
	HOMOSCEDASTICITY BETWEEN GROUPS ESTABLISHED USING LEVENE'S TEST ($P > 0.05$).	24
TABLE 5		
	SHOWS THE MIXED ANOVA RESULTS OF EFFECTS OF WITHIN-SUBJECT FACTOR "PREPOST" AND ITS INTERACTIONS WITH BETWEEN-SUBJECT FACTORS "EPILEPTOLOGISTS" AND "TYPEOFTREATMENT" ON THE DEPENDENT VARIABLE "IED FREQUENCY".	25
TABLE 6		
	SHOWS THE TUKEY-HSD RESULTS OF EFFECTS OF STAGES OF BETWEEN-SUBJECT FACTOR "TYPEOFTREATMENT" ON THE DIFFERENCE IN IED FREQUENCY BETWEEN LEVELS OF WITHIN-SUBJECT FACTOR "PREPOST".	26
TABLE 7		
	SHOWS THE TUKEY-HSD RESULTS OF EFFECTS OF STAGES OF BETWEEN-SUBJECT FACTOR "EPILEPTOLOGISTS" ON THE DIFFERENCE IN IED FREQUENCY BETWEEN LEVELS OF WITHIN-SUBJECT FACTOR "PREPOST".	26
TABLE 8		
	EPILEPTOLOGIST 1 GLOBAL AVERAGE MOVING DIPOLE OF IEDS. SUMMARIZES INFORMATION ABOUT DIPOLES OF THE RISING FLANK OF THE AVERAGE IED MARKED BY EPILEPTOLOGIST 1.	33
TABLE 9		
	EPILEPTOLOGIST 1 PRESTIM AVERAGE MOVING DIPOLE OF IEDS. SUMMARIZES INFORMATION ABOUT DIPOLES OF THE RISING FLANK OF THE AVERAGE IED IN THE HOUR BEFORE "STIM" MARKED BY EPILEPTOLOGIST 1.	35

TABLE 10

EPILEPTOLOGIST 1 POSTSTIM AVERAGE MOVING DIPOLE OF IEDS. SUMMARIZES INFORMATION ABOUT DIPOLES OF THE RISING FLANK OF THE AVERAGE IED IN THE HOUR AFTER "STIM" MARKED BY EPILEPTOLOGIST 1. 37

TABLE 11

EPILEPTOLOGIST 1 PRESHAM AVERAGE MOVING DIPOLE OF IEDS. SUMMARIZES INFORMATION ABOUT DIPOLES OF THE RISING FLANK OF THE AVERAGE IED IN THE HOUR BEFORE "SHAM" MARKED BY EPILEPTOLOGIST 1. 39

TABLE 12

EPILEPTOLOGIST 1 POSTSHAM AVERAGE MOVING DIPOLE OF IEDS. SUMMARIZES INFORMATION ABOUT DIPOLES OF THE RISING FLANK OF THE AVERAGE IED IN THE HOUR AFTER "SHAM" MARKED BY EPILEPTOLOGIST 1. 41

TABLE 13

EPILEPTOLOGIST 1 STIM WEEK BASELINE AVERAGE MOVING DIPOLE OF IEDS. SUMMARIZES INFORMATION ABOUT DIPOLES OF THE RISING FLANK OF THE AVERAGE IED IN THE TWO HOURS BEFORE THE FIRST "STIM" MARKED BY EPILEPTOLOGIST 1. 43

TABLE 14

EPILEPTOLOGIST 1 SHAM WEEK BASELINE AVERAGE MOVING DIPOLE OF IEDS. SUMMARIZES INFORMATION ABOUT DIPOLES OF THE RISING FLANK OF THE AVERAGE IED IN THE TWO HOURS BEFORE THE FIRST "SHAM" MARKED BY EPILEPTOLOGIST 1. 45

TABLE 15

EPILEPTOLOGIST 3 GLOBAL AVERAGE MOVING DIPOLE OF IEDS. SUMMARIZES INFORMATION ABOUT DIPOLES OF THE RISING FLANK OF THE AVERAGE IED MARKED BY EPILEPTOLOGIST 3. 47

TABLE 16

EPILEPTOLOGIST 3 PRESTIM AVERAGE MOVING DIPOLE OF IEDS. SUMMARIZES INFORMATION ABOUT DIPOLES OF THE RISING FLANK OF THE AVERAGE IED IN THE HOUR BEFORE "STIM" MARKED BY EPILEPTOLOGIST 3. 49

TABLE 17

EPILEPTOLOGIST 3 POSTSTIM AVERAGE MOVING DIPOLE OF IEDS. SUMMARIZES INFORMATION ABOUT DIPOLES OF THE RISING FLANK OF THE AVERAGE IED IN THE HOUR AFTER "STIM" MARKED BY EPILEPTOLOGIST 3. 51

TABLE 18

EPILEPTOLOGIST 3 PRESHAM AVERAGE MOVING DIPOLE OF IEDS. SUMMARIZES INFORMATION ABOUT DIPOLES OF THE RISING FLANK OF THE AVERAGE IED IN THE HOUR BEFORE "SHAM" MARKED BY EPILEPTOLOGIST 3. 53

TABLE 19

EPILEPTOLOGIST 3 POSTSHAM AVERAGE MOVING DIPOLE OF IEDs. SUMMARIZES INFORMATION ABOUT DIPOLES OF THE RISING FLANK OF THE AVERAGE IED IN THE HOUR AFTER "SHAM" MARKED BY EPILEPTOLOGIST 3. 55

TABLE 20

EPILEPTOLOGIST 3 STIM WEEK BASELINE AVERAGE MOVING DIPOLE OF IEDs. SUMMARIZES INFORMATION ABOUT DIPOLES OF THE RISING FLANK OF THE AVERAGE IED IN THE TWO HOURS BEFORE THE FIRST "STIM" MARKED BY EPILEPTOLOGIST 3. 57

TABLE 21

EPILEPTOLOGIST 3 SHAM WEEK BASELINE AVERAGE MOVING DIPOLE OF IEDs. SUMMARIZES INFORMATION ABOUT DIPOLES OF THE RISING FLANK OF THE AVERAGE IED IN THE TWO HOURS BEFORE THE FIRST "SHAM" MARKED BY EPILEPTOLOGIST 3. 59

TABLE 22

SHOWS THE CURRENT DENSITY OF AVERAGE DIPOLES IN μAMM ACROSS CONDITIONS, GATHERED FROM **TABLES 9-14** AND **16-21**. MARKED IN RED ARE VALUES ASSOCIATED WITH ESPECIALLY LOW (~50-70%) RELATIVE EXPLAINED SIGNAL. 67

References

- Agur, A. M. R., & Dalley, A. F. (2018). Moore's essential clinical anatomy. In *Moore's Essential Clinical Anatomy*. <https://shop.lww.com/Moore-s-Essential-Clinical-Anatomy/p/9781496369659>
- Almubarak, S., Alexopoulos, A., Von-Podewils, F., Wang, Z. I., Kakisaka, Y., Mosher, J. C., Bulacio, J., González-Martínez, J., Bingaman, W., & Burgess, R. C. (2014). The correlation of magnetoencephalography to intracranial EEG in localizing the epileptogenic zone: A study of the surgical resection outcome. *Epilepsy Research, 108*(9), 1581–1590. <https://doi.org/10.1016/j.eplepsyres.2014.08.016>
- Antal, A., Alekseichuk, I., Bikson, M., Brockmüller, J., Brunoni, A. R., Chen, R., Cohen, L. G., Douthwaite, G., Ellrich, J., Flöel, A., Fregni, F., George, M. S., Hamilton, R., Haueisen, J., Herrmann, C. S., Hummel, F. C., Lefaucheur, J. P., Liebetanz, D., Loo, C. K., ... Paulus, W. (2017). Low intensity transcranial electric stimulation: Safety, ethical, legal regulatory and application guidelines. *Clinical Neurophysiology : Official Journal of the International Federation of Clinical Neurophysiology, 128*(9), 1774–1809. <https://doi.org/10.1016/J.CLINPH.2017.06.001>
- Asadi-Pooya, A. A., Sharan, A., Nei, M., & Sperling, M. R. (2008). Corpus callosotomy. *Epilepsy and Behavior, 13*(2), 271–278. <https://doi.org/10.1016/j.yebeh.2008.04.020>
- Auvichayapat, N., Rotenberg, A., Gersner, R., Ngodklang, S., Tiamkao, S., Tassaneeyakul, W., & Auvichayapat, P. (2013). Transcranial direct current stimulation for treatment of refractory childhood focal epilepsy. *Brain Stimulation, 6*(4), 696–700. <https://doi.org/10.1016/j.brs.2013.01.009>
- Aydin, Ü., Vorwerk, J., Küpper, P., Heers, M., Kugel, H., Galka, A., Hamid, L., Wellmer, J., Kellinghaus, C., Rampp, S., & Wolters, C. H. (2014). Combining EEG and MEG for the reconstruction of epileptic activity using a calibrated realistic volume conductor model. *PLoS ONE, 9*(3), e93154. <https://doi.org/10.1371/journal.pone.0093154>
- Barnett, M. W., & Larkman, P. M. (2007). The action potential. *Practical Neurology, 7*(3), 192–197. <https://doi.org/10.1016/b978-0-12-800883-6.00024-0>
- Baud, M. O., Kleen, J. K., Mirro, E. A., Andrechak, J. C., King-Stephens, D., Chang, E. F., & Rao, V. R. (2018). Multi-day rhythms modulate seizure risk in epilepsy. *Nature Communications, 9*(1), 1–10. <https://doi.org/10.1038/s41467-017-02577-y>
- Beghi, E., Carpio, A., Forsgren, L., Hesdorffer, D. C., Malmgren, K., Sander, J. W., Tomson, T., & Hauser, W. A. (2010). Recommendation for a definition of acute symptomatic seizure.

- Epilepsia*, 51(4), 671–675. <https://doi.org/10.1111/j.1528-1167.2009.02285.x>
- Beghi, E., De Maria, G., Gobbi, G., & Veneselli, E. (2006). Diagnosis and treatment of the first epileptic seizure: Guidelines of the Italian League against Epilepsy. *Epilepsia*, 47(SUPPL. 5), 2–8. <https://doi.org/10.1111/j.1528-1167.2006.00869.x>
- Ben-Menachem, E., Hamberger, A., Hedner, T., Hammond, E. J., Uthman, B. M., Slater, J., Treig, T., Stefan, H., Ramsay, R. E., Wernicke, J. F., & Wilder, B. J. (1995). Effects of vagus nerve stimulation on amino acids and other metabolites in the CSF of patients with partial seizures. *Epilepsy Research*, 20(3), 221–227. [https://doi.org/10.1016/0920-1211\(94\)00083-9](https://doi.org/10.1016/0920-1211(94)00083-9)
- Berg, A. T., Berkovic, S. F., Brodie, M. J., Buchhalter, J., Cross, J. H., Van Emde Boas, W., Engel, J., French, J., Glauser, T. A., Mathern, G. W., Moshé, S. L., Nordli, D., Plouin, P., & Scheffer, I. E. (2010). Revised terminology and concepts for organization of seizures and epilepsies: Report of the ILAE Commission on Classification and Terminology, 2005-2009. *Epilepsia*, 51(4), 676–685. <https://doi.org/10.1111/j.1528-1167.2010.02522.x>
- Bergey, G. K., Morrell, M. J., Mizrahi, E. M., Goldman, A., King-Stephens, D., Nair, D., Srinivasan, S., Jobst, B., Gross, R. E., Shields, D. C., Barkley, G., Salanova, V., Olejniczak, P., Cole, A., Cash, S. S., Noe, K., Wharen, R., Worrell, G., Murro, A. M., ... Seale, C. G. (2015). Long-term treatment with responsive brain stimulation in adults with refractory partial seizures. *Neurology*, 84(8), 810–817. <https://doi.org/10.1212/WNL.0000000000001280>
- Bernasconi, A., Cendes, F., Theodore, W. H., Gill, R. S., Koepp, M. J., Hogan, R. E., Jackson, G. D., Federico, P., Labate, A., Vaudano, A. E., Blümcke, I., Ryvlin, P., & Bernasconi, N. (2019). Recommendations for the use of structural magnetic resonance imaging in the care of patients with epilepsy: A consensus report from the International League Against Epilepsy Neuroimaging Task Force. *Epilepsia*, 60(6), 1054–1068. <https://doi.org/10.1111/epi.15612>
- Bondy, M. L., Scheurer, M. E., Malmer, B., Barnholtz-Sloan, J. S., Davis, F. G., Il'yasova, D., Kruchko, C., McCarthy, B. J., Rajaraman, P., Schwartzbaum, J. A., Sadetzki, S., Schlehofer, B., Tihan, T., Wiemels, J. L., Wrensch, M., & Buffler, P. A. (2008). Brain tumor epidemiology: Consensus from the Brain Tumor Epidemiology Consortium. *Cancer*, 113(7), 1953–1968. <https://doi.org/10.1002/cncr.23741>
- Boon, P., De Cock, E., Mertens, A., & Trinka, E. (2018). Neurostimulation for drug-resistant epilepsy: A systematic review of clinical evidence for efficacy, safety, contraindications and predictors for response. *Current Opinion in Neurology*, 31(2), 198–210. <https://doi.org/10.1097/WCO.0000000000000534>
- Brodbeck, V., Spinelli, L., Lascano, A. M., Pollo, C., Schaller, K., Vargas, M. I., Wissmeyer, M., Michel, C. M., & Seeck, M. (2010). Electrical source imaging for presurgical focus

- localization in epilepsy patients with normal MRI. *Epilepsia*, 51(4), 583–591.
<https://doi.org/10.1111/j.1528-1167.2010.02521.x>
- Brodie, M. J. (2005). Medical therapy of epilepsy: When to initiate treatment and when to combine? *Journal of Neurology*, 252(2), 125–130. <https://doi.org/10.1007/s00415-005-0735-x>
- Carreño, M., & Lüders, H. (2013). General principles of pre-surgical evaluation. In *Textbook of Epilepsy Surgery* (pp. 449–464). CRC Press. <https://doi.org/10.3109/9780203091708-54>
- Chadwick, D., & Smith, D. (2002, March 2). The misdiagnosis of epilepsy. *British Medical Journal*, 324(7336), 495–496. <https://doi.org/10.1136/bmj.324.7336.495>
- Chambers, A., & Bowen, J. M. (2013). Electrical stimulation for drug-resistant epilepsy: An evidence-based analysis. *Ontario Health Technology Assessment Series*, 13(18), 1. [/pmc/articles/PMC3817921/](https://doi.org/10.1007/s11464-013-0181-1)
- Chassoux, F., Rodrigo, S., Semah, F., Beuvon, F., Landre, E., Devaux, B., Turak, B., Mellerio, C., Meder, J. F., Roux, F. X., Daumas-Duport, C., Merlet, P., Dulac, O., & Chiron, C. (2010). FDG-PET improves surgical outcome in negative MRI Taylor-type focal cortical dysplasias. *Neurology*, 75(24), 2168–2175. <https://doi.org/10.1212/WNL.0b013e31820203a9>
- Chiken, S., & Nambu, A. (2016). Mechanism of Deep Brain Stimulation: Inhibition, Excitation, or Disruption? *Neuroscientist*, 22(3), 313–322. <https://doi.org/10.1177/1073858415581986>
- Choi, S. A., & Kim, K. J. (2019). The Surgical and Cognitive Outcomes of Focal Cortical Dysplasia. *Journal of Korean Neurosurgical Society*, 62(3), 321–327. <https://doi.org/10.3340/jkns.2019.0005>
- Compumedics Neuroscan. (2022). *CURRY 8*. <https://compumedicsneuroscan.com/>
- Dalic, L., & Cook, M. J. (2016). Managing drug-resistant epilepsy: Challenges and solutions. *Neuropsychiatric Disease and Treatment*, 12, 2605–2616. <https://doi.org/10.2147/NDT.S84852>
- de Ribaupierre, S., & Delalande, O. (2008). Hemispherotomy and other disconnective techniques. *Neurosurgical Focus*, 25(3). <https://doi.org/10.3171/FOC/2008/25/9/E14>
- Deckers, C. L. P., Hekster, Y. A., Keyser, A., Van Lier, H. J. J., Meinardi, H., & Renier, W. O. (2001). Monotherapy versus polytherapy for epilepsy: A multicenter double-blind randomized study. *Epilepsia*, 42(11), 1387–1394. <https://doi.org/10.1046/j.1528-1157.2001.30800.x>
- Denoyer, Y., Merlet, I., Wendling, F., & Benquet, P. (2020). Modelling acute and lasting effects of tDCS on epileptic activity. *Journal of Computational Neuroscience*, 48(2), 161–176. <https://doi.org/10.1007/s10827-020-00745-6>
- Devinsky, O., Gazzola, D., & LaFrance, W. C. (2011). Differentiating between nonepileptic and

- epileptic seizures. *Nature Reviews Neurology*, 7(4), 210–220.
<https://doi.org/10.1038/nrneurol.2011.24>
- Dewan, M. C., Rattani, A., Gupta, S., Baticulon, R. E., Hung, Y. C., Punchak, M., Agrawal, A., Adeleye, A. O., Shrimel, M. G., Rubiano, A. M., Rosenfeld, J. V., & Park, K. B. (2019). Estimating the global incidence of traumatic brain injury. *Journal of Neurosurgery*, 130(4), 1080–1097. <https://doi.org/10.3171/2017.10.JNS17352>
- Duez, L., Tankisi, H., Hansen, P. O., Sidenius, P., Sabers, A., Pinborg, L. H., Fabricius, M., Rásonyi, G., Rubboli, G., Pedersen, B., Leffers, A. M., Uldall, P., Jespersen, B., Brennum, J., Henriksen, O. M., Fuglsang-Frederiksen, A., & Beniczky, S. (2019). Electromagnetic source imaging in presurgical workup of patients with epilepsy: A prospective study. *Neurology*, 92(6), e576–e586. <https://doi.org/10.1212/WNL.0000000000006877>
- Engwer, C., Vorwerk, J., Ludewig, J., & Wolters, C. H. (2017). A discontinuous Galerkin method to solve the EEG forward problem using the subtraction approach. *SIAM Journal on Scientific Computing*, 39(1), B138–B164. <https://doi.org/10.1137/15M1048392>
- ERA PerMed. (n.d.). Retrieved January 2, 2022, from <https://erapermed.isciii.es/>
- Erkinen, M. G., Kim, M. O., & Geschwind, M. D. (2018). Clinical neurology and epidemiology of the major neurodegenerative diseases. *Cold Spring Harbor Perspectives in Biology*, 10(4). <https://doi.org/10.1101/cshperspect.a033118>
- Eyndhoven, S. Van, Hunyadi, B., Dupont, P., Paesschen, W. Van, & Huffel, S. Van. (2019). Semi-automated EEG enhancement improves localization of ictal onset zone with EEG-correlated fmri. *Frontiers in Neurology*, 10(JUL), 805.
<https://doi.org/10.3389/fneur.2019.00805>
- Falco-Walter, J. (2020). Epilepsy-Definition, Classification, Pathophysiology, and Epidemiology. *Seminars in Neurology*, 40(6), 617–623. <https://doi.org/10.1055/s-0040-1718719>
- Falco-Walter, J. J., Scheffer, I. E., & Fisher, R. S. (2018). The new definition and classification of seizures and epilepsy. In *Epilepsy Research* (Vol. 139, pp. 73–79). Elsevier.
<https://doi.org/10.1016/j.eplepsyres.2017.11.015>
- Fattorusso, A., Matricardi, S., Mencaroni, E., Dell'Isola, G. B., Di Cara, G., Striano, P., & Verrotti, A. (2021). The Pharmacoresistant Epilepsy: An Overview on Existant and New Emerging Therapies. *Frontiers in Neurology*, 12, 1030.
<https://doi.org/10.3389/FNEUR.2021.674483/BIBTEX>
- Fernandes Filho, J. A., & Shapiro, B. E. (2004). Tay-sachs disease. In *Archives of Neurology* (Vol. 61, Issue 9, pp. 1466–1468). American Medical Association.
<https://doi.org/10.1001/archneur.61.9.1466>
- Fink, C. (2012). *Using Phase Response Curves to Understand Neuronal Synchronization and Sleep*.

- Fisher, R. S., Acevedo, C., Arzimanoglou, A., Bogacz, A., Cross, J. H., Elger, C. E., Engel, J., Forsgren, L., French, J. A., Glynn, M., Hesdorffer, D. C., Lee, B. I., Mathern, G. W., Moshé, S. L., Perucca, E., Scheffer, I. E., Tomson, T., Watanabe, M., & Wiebe, S. (2014). ILAE Official Report: A practical clinical definition of epilepsy. *Epilepsia*, *55*(4), 475–482. <https://doi.org/10.1111/epi.12550>
- Fisher, R. S., Cross, J. H., French, J. A., Higurashi, N., Hirsch, E., Jansen, F. E., Lagae, L., Moshé, S. L., Peltola, J., Roulet Perez, E., Scheffer, I. E., & Zuberi, S. M. (2017). Operational classification of seizure types by the International League Against Epilepsy: Position Paper of the ILAE Commission for Classification and Terminology. *Epilepsia*, *58*(4), 522–530. <https://doi.org/10.1111/epi.13670>
- Fisher, R. S., Van Emde Boas, W., Blume, W., Elger, C., Genton, P., Lee, P., & Engel, J. (2005). Epileptic seizures and epilepsy: Definitions proposed by the International League Against Epilepsy (ILAE) and the International Bureau for Epilepsy (IBE). In *Epilepsia* (Vol. 46, Issue 4, pp. 470–472). John Wiley & Sons, Ltd. <https://doi.org/10.1111/j.0013-9580.2005.66104.x>
- Fisher, R., Salanova, V., Witt, T., Worth, R., Henry, T., Gross, R., Oommen, K., Osorio, I., Nazzaro, J., Labar, D., Kaplitt, M., Sperling, M., Sandok, E., Neal, J., Handforth, A., Stern, J., DeSalles, A., Chung, S., Shetter, A., ... Young, C. (2010). Electrical stimulation of the anterior nucleus of thalamus for treatment of refractory epilepsy. *Epilepsia*, *51*(5), 899–908. <https://doi.org/10.1111/j.1528-1167.2010.02536.x>
- Fregni, F., Thome-Souza, S., Nitsche, M. A., Freedman, S. D., Valente, K. D., & Pascual-Leone, A. (2006). A controlled clinical trial of cathodal DC polarization in patients with refractory epilepsy. *Epilepsia*, *47*(2), 335–342. <https://doi.org/10.1111/j.1528-1167.2006.00426.x>
- Fry, A. E., Cushion, T. D., & Pilz, D. T. (2014). The genetics of lissencephaly. *American Journal of Medical Genetics, Part C: Seminars in Medical Genetics*, *166*(2), 198–210. <https://doi.org/10.1002/ajmg.c.31402>
- Ginsborg, B. L. (1964). THE PHYSIOLOGY OF SYNAPSES. *Quarterly Journal of Experimental Physiology and Cognate Medical Sciences*, *49*(4), 488–489. <https://doi.org/10.1113/expphysiol.1964.sp001756>
- Glass, G. V., Peckham, P. D., & Sanders, J. R. (1972). Consequences of Failure to Meet Assumptions Underlying the Fixed Effects Analyses of Variance and Covariance. *Review of Educational Research*, *42*(3), 237–288. <https://doi.org/10.3102/00346543042003237>
- Gouveia, F. V., Germann, J., Oliveira, C. C., Castro, M. C., Antunes, G. F., Gomes, G. C. V., Pinto, T. R. C., Martinez, R. C. R., & Valle, A. C. (2021). Transcranial Direct Current Stimulation Reduces Anxiety, Depression and Plasmatic Corticosterone in a Rat Model of Atypical

- Generalized Epilepsy. *Neuroscience*. <https://doi.org/10.1016/j.neuroscience.2021.11.003>
- Harwell, M. R., Rubinstein, E. N., Hayes, W. S., & Olds, C. C. (1992). Summarizing Monte Carlo Results in Methodological Research: The One- and Two-Factor Fixed Effects ANOVA Cases. *Journal of Educational Statistics*, *17*(4), 315–339.
<https://doi.org/10.3102/10769986017004315>
- Itabashi, H., Jin, K., Iwasaki, M., Okumura, E., Kanno, A., Kato, K., Tominaga, T., Kawashima, R., & Nakasato, N. (2014). Electro- and magneto-encephalographic spike source localization of small focal cortical dysplasia in the dorsal peri-rolandic region. *Clinical Neurophysiology*, *125*(12), 2358–2363. <https://doi.org/10.1016/j.clinph.2014.02.028>
- Jawabri, K. H., & Sharma, S. (2019). Physiology, Cerebral Cortex Functions. In *StatPearls*. StatPearls Publishing. <https://www.ncbi.nlm.nih.gov/books/NBK538496/>
- Jimshelishvili, S., & Dididze, M. (2019). Neuroanatomy, Cerebellum. In *StatPearls*. StatPearls Publishing. <https://www.ncbi.nlm.nih.gov/books/NBK538167/>
- Johnson, R. T. (2005). Prion diseases. In *Lancet Neurology* (Vol. 4, Issue 10, pp. 635–642). Elsevier. [https://doi.org/10.1016/S1474-4422\(05\)70192-7](https://doi.org/10.1016/S1474-4422(05)70192-7)
- Johnson, R. T., & Gibbs, C. J. (1998). Creutzfeldt–Jakob Disease and Related Transmissible Spongiform Encephalopathies. *New England Journal of Medicine*, *339*(27), 1994–2004. <https://doi.org/10.1056/nejm199812313392707>
- Johnston, D., Magee, J. C., Colbert, C. M., & Christie, B. R. (1996). Active properties of neuronal dendrites. In *Annual Review of Neuroscience* (Vol. 19, pp. 165–186). Annu Rev Neurosci. <https://doi.org/10.1146/annurev.ne.19.030196.001121>
- Jones, K. (Karen J. (2011). *Neurological Assessment: A Clinician's Guide*. Elsevier.
- Kakisaka, Y., Jin, K., Fujikawa, M., Kitazawa, Y., & Nakasato, N. (2018). Teleconference-based education of epileptic seizure semiology. *Epilepsy Research*, *145*, 73–76. <https://doi.org/10.1016/j.eplepsyres.2018.06.007>
- Kalilani, L., Sun, X., Pelgrims, B., Noack-Rink, M., & Villanueva, V. (2018). The epidemiology of drug-resistant epilepsy: A systematic review and meta-analysis. *Epilepsia*, *59*(12), 2179–2193. <https://doi.org/10.1111/epi.14596>
- Kaufmann, E., Hordt, M., Lauseker, M., Palm, U., & Noachtar, S. (2021). Acute effects of spaced cathodal transcranial direct current stimulation in drug resistant focal epilepsies. *Clinical Neurophysiology*, *132*(7), 1444–1451. <https://doi.org/10.1016/j.clinph.2021.03.048>
- Keller, S. S., Crow, T., Foundas, A., Amunts, K., & Roberts, N. (2009). Broca's area: Nomenclature, anatomy, typology and asymmetry. *Brain and Language*, *109*(1), 29–48. <https://doi.org/10.1016/j.bandl.2008.11.005>
- Khan, A., Antonakakis, M., Vogenauer, N., Haueisen, J., & Wolters, C. H. (2022). Individually optimized multi-channel tDCS for targeting somatosensory cortex. *Clinical*

- Neurophysiology*, 134, 9–26. <https://doi.org/10.1016/j.clinph.2021.10.016>
- Khan, A., Antonakakis, M., Vogenauer, N., Wollbrink, A., Suntrup-Krueger, S., Schneider, T. R., Herrmann, C. S., Nitsche, M., Paulus, W., Haueisen, J., & Wolters, C. H. (2019). Constrained maximum intensity optimized multi-electrode tDCS targeting of human somatosensory network. *Proceedings of the Annual International Conference of the IEEE Engineering in Medicine and Biology Society, EMBS, 2019*, 5894–5897. <https://doi.org/10.1109/EMBC.2019.8857253>
- Krishnamurthi, R. V., Ikeda, T., & Feigin, V. L. (2020). Global, Regional and Country-Specific Burden of Ischaemic Stroke, Intracerebral Haemorrhage and Subarachnoid Haemorrhage: A Systematic Analysis of the Global Burden of Disease Study 2017. *Neuroepidemiology*, 54(2), 171–179. <https://doi.org/10.1159/000506396>
- Kwan, P., Arzimanoglou, A., Berg, A. T., Brodie, M. J., Hauser, W. A., Mathern, G., Moshé, S. L., Perucca, E., Wiebe, S., & French, J. (2010). Definition of drug resistant epilepsy: Consensus proposal by the ad hoc Task Force of the ILAE Commission on Therapeutic Strategies. *Epilepsia*, 51(6), 1069–1077. <https://doi.org/10.1111/j.1528-1167.2009.02397.x>
- Kwan, P., & Brodie, M. J. (2000). Epilepsy after the first drug fails: Substitution or add-on? *Seizure*, 9(7), 464–468. <https://doi.org/10.1053/seiz.2000.0442>
- Langdon-Down, M., & Russell Brain, W. (1929). TIME OF DAY IN RELATION TO CONVULSIONS IN EPILEPSY. *The Lancet*, 213(5516), 1029–1032. [https://doi.org/10.1016/S0140-6736\(00\)79288-9](https://doi.org/10.1016/S0140-6736(00)79288-9)
- Lattanzi, S., Cagnetti, C., Matricardi, S., & Silvestrini, M. (2018). Palliative non-resective surgery for drug-resistant epilepsy. *Brain and Development*, 40(6), 512–513. <https://doi.org/10.1016/j.braindev.2017.12.012>
- Leach, J. P., Lauder, R., Nicolson, A., & Smith, D. F. (2005). Epilepsy in the UK: Misdiagnosis, mistreatment, and undertreatment? *Seizure*, 14(7), 514–520. <https://doi.org/10.1016/j.seizure.2005.08.008>
- Lee, B. I., Park, K. M., Kim, S. E., & Heo, K. (2019). Clinical opinion: Earlier employment of polytherapy in sequential pharmacotherapy of epilepsy. In *Epilepsy Research* (Vol. 156). Epilepsy Res. <https://doi.org/10.1016/j.eplepsyres.2019.106165>
- Lettori, D., Battaglia, D., Sacco, A., Veredice, C., Chieffo, D., Massimi, L., Tartaglione, T., Chiricozzi, F., Staccioli, S., Mittica, A., Di Rocco, C., & Guzzetta, F. (2008). Early hemispherectomy in catastrophic epilepsy. A neuro-cognitive and epileptic long-term follow-up. *Seizure*, 17(1), 49–63. <https://doi.org/10.1016/j.seizure.2007.06.006>
- López González, F. J., Rodríguez Osorio, X., Gil-Nagel Rein, A., Carreño Martínez, M., Serratos

- Fernández, J., Villanueva Haba, V., Donaire Pedraza, A. J., & Mercadé Cerdá, J. M. (2015). Epilepsia resistente a fármacos. Concepto y alternativas terapéuticas. *Neurología, 30*(7), 439–446. <https://doi.org/10.1016/j.nrl.2014.04.012>
- Lüders, H., Acharya, J., Baumgartner, C., Benbadis, S., Bleasel, A., Burgess, R., Dinner, D. S., Ebner, A., Foldvary, N., Geller, E., Hamer, H., Holthausen, H., Kotagal, P., Morris, H., Meencke, H. J., Noachtar, S., Rosenow, F., Sakamoto, A., Steinhoff, B. J., ... Wyllie, E. (1998). Semiological seizure classification. *Epilepsia, 39*(9), 1006–1013. <https://doi.org/10.1111/j.1528-1157.1998.tb01452.x>
- Marios Antonakakis, D. (2021). *The Effect of Experimental and Modeling Parameters on Combined EEG/MEG Source Analysis and Transcranial Electric Stimulation Optimization of Somatosensory and Epilepsy Activity*.
- Martin-McGill, K. J., Bresnahan, R., Levy, R. G., & Cooper, P. N. (2020). Ketogenic diets for drug-resistant epilepsy. *Cochrane Database of Systematic Reviews, 2020*(6). <https://doi.org/10.1002/14651858.CD001903.pub5>
- Maschio, M. (2012). Brain Tumor-Related Epilepsy. *Current Neuropharmacology, 10*(2), 124–133. <https://doi.org/10.2174/157015912800604470>
- MathWorks. (2021a). *MATLAB*. <https://www.mathworks.com/company/newsroom/mathworks-introduces-release-2021a-of-matlab-and-simulink.html>
- MathWorks. (2021b). *Statistics and Machine Learning Toolbox*. <https://www.mathworks.com/products/statistics.html>
- Matias, C. M., Sharan, A., & Wu, C. (2019). Responsive Neurostimulation for the Treatment of Epilepsy. *Neurosurgery Clinics of North America, 30*(2), 231–242. <https://doi.org/10.1016/j.nec.2018.12.006>
- McCarthy, P. (2021). *FSLeyes*. <https://doi.org/10.5281/ZENODO.5576035>
- Meisenhelter, S., & Jobst, B. C. (2018). Neurostimulation for Memory Enhancement in Epilepsy. In *Current Neurology and Neuroscience Reports* (Vol. 18, Issue 6). Curr Neurol Neurosci Rep. <https://doi.org/10.1007/s11910-018-0837-3>
- Microsoft Corporation. (2022). *Microsoft 365*. <https://www.microsoft.com/en-us/microsoft-365>
- Monte-Silva, K., Kuo, M. F., Liebetanz, D., Paulus, W., & Nitsche, M. A. (2010). Shaping the optimal repetition interval for cathodal transcranial direct current stimulation (tDCS). *Journal of Neurophysiology, 103*(4), 1735–1740. <https://doi.org/10.1152/jn.00924.2009>
- Moore, J. L., Cascino, G. D., Trenerry, M. R., Kelly, P. J., & Marsh, W. R. (1993). A comparative study of lesionectomy versus corticectomy in patients with temporal lobe lesional epilepsy. *Journal of Epilepsy, 6*(4), 239–242. <https://doi.org/10.1016/0896->

6974(93)90008-X

- Morris, G. L., Gloss, D., Buchhalter, J., Mack, K. J., Nickels, K., & Harden, C. (2013). Evidence-based guideline update: vagus nerve stimulation for the treatment of epilepsy: report of the guideline development subcommittee of the american academy of neurology. *Epilepsy Currents*, *13*(6), 297–303. <https://doi.org/10.5698/1535-7597-13.6.297>
- Nair, D. R., Laxer, K. D., Weber, P. B., Murro, A. M., Park, Y. D., Barkley, G. L., Smith, B. J., Gwinn, R. P., Doherty, M. J., Noe, K. H., Zimmerman, R. S., Bergey, G. K., Anderson, W. S., Heck, C., Liu, C. Y., Lee, R. W., Sadler, T., Duckrow, R. B., Hirsch, L. J., ... Morrell, M. J. (2020). Nine-year prospective efficacy and safety of brain-responsive neurostimulation for focal epilepsy. *Neurology*, *95*(9), e1244–e1256. <https://doi.org/10.1212/WNL.0000000000010154>
- Neligan, A., Hauser, W. A., & Sander, J. W. (2012). The epidemiology of the epilepsies. In *Handbook of Clinical Neurology* (Vol. 107, pp. 113–133). Handb Clin Neurol. <https://doi.org/10.1016/B978-0-444-52898-8.00006-9>
- Neuroelectrics. (2015). *Starstim® tES systems*. <https://www.neuroelectrics.com/solutions/starstim>
- Nitsche, M. A., & Paulus, W. (2000). Excitability changes induced in the human motor cortex by weak transcranial direct current stimulation. *Journal of Physiology*, *527*(3), 633–639. <https://doi.org/10.1111/j.1469-7793.2000.t01-1-00633.x>
- Noachtar, S., Rosenow, F., Arnold, S., Baumgartner, C., Ebner, A., Hamer, H., Holthausen, H., Meencke, H. J., Müller, A., Sakamoto, A. C., Steinhoff, B. J., Tuxhorn, I., Werhahn, K. J., Winkler, P. A., & Lüders, H. O. (1998). Die semiologische klassifikation epileptischer anfälle. *Nervenarzt*, *69*(2), 117–126. <https://doi.org/10.1007/s001150050247>
- Noachtar, Soheyl, & Rémi, J. (2009). The role of EEG in epilepsy: A critical review. *Epilepsy and Behavior*, *15*(1), 22–33. <https://doi.org/10.1016/j.yebeh.2009.02.035>
- Nowacki, T. A., & Jirsch, J. D. (2017). Evaluation of the first seizure patient: Key points in the history and physical examination. *Seizure*, *49*, 54–63. <https://doi.org/10.1016/j.seizure.2016.12.002>
- Operto, F. F., Matricardi, S., Pastorino, G. M. G., Verrotti, A., & Coppola, G. (2020). The Ketogenic Diet for the Treatment of Mood Disorders in Comorbidity With Epilepsy in Children and Adolescents. *Frontiers in Pharmacology*, *11*. <https://doi.org/10.3389/fphar.2020.578396>
- Panebianco, M., Rigby, A., Weston, J., & Marson, A. G. (2015). Vagus nerve stimulation for partial seizures. *Cochrane Database of Systematic Reviews*, *2015*(4). https://doi.org/10.1002/14651858.CD002896.PUB2/MEDIA/CDSR/CD002896/IMAGE_N/

- NCD002896-CMP-001-11.PNG
- Parikh, S., Koch, M., & Narayan, R. K. (2007). Traumatic brain injury. In *International Anesthesiology Clinics* (Vol. 45, Issue 3, pp. 119–135).
<https://doi.org/10.1097/AIA.0b013e318078cfe7>
- Park, K. M., Kim, S. E., & Lee, B. I. (2019). Antiepileptic Drug Therapy in Patients with Drug-Resistant Epilepsy. *Journal of Epilepsy Research*, 9(1), 14–26.
<https://doi.org/10.14581/jer.19002>
- Patten, A. R., Yau, S. Y., Fontaine, C. J., Meconi, A., Wortman, R. C., & Christie, B. R. (2016). The Benefits of Exercise on Structural and Functional Plasticity in the Rodent Hippocampus of Different Disease Models. *Brain Plasticity*, 1(1), 97–127. <https://doi.org/10.3233/bpl-150016>
- Pedhazur, E. J., & Schmelkin, L. P. (1991). Measurement, Design, and Analysis. In *Measurement, design, and analysis: An integrated approach (Student ed.)*. Lawrence Erlbaum Associates, Inc.
- Pérez-Carbonell, L., Faulkner, H., Higgins, S., Koutroumanidis, M., & Leschziner, G. (2020). Vagus nerve stimulation for drug-resistant epilepsy. *Practical Neurology*, 20(3), 189–198.
<https://doi.org/10.1136/practneurol-2019-002210>
- Picot, M. C., Baldy-Moulinier, M., Daurès, J. P., Dujols, P., & Crespel, A. (2008). The prevalence of epilepsy and pharmaco-resistant epilepsy in adults: A population-based study in a Western European country. *Epilepsia*, 49(7), 1230–1238. <https://doi.org/10.1111/j.1528-1167.2008.01579.x>
- Pressler, R. M., Cilio, M. R., Mizrahi, E. M., Moshé, S. L., Nunes, M. L., Plouin, P., Vanhatalo, S., Yozowitz, E., de Vries, L. S., Puthenveetil Vinayan, K., Triki, C. C., Wilmschurst, J. M., Yamamoto, H., & Zuberi, S. M. (2021). The ILAE classification of seizures and the epilepsies: Modification for seizures in the neonate. Position paper by the ILAE Task Force on Neonatal Seizures. *Epilepsia*, 62(3), 615–628. <https://doi.org/10.1111/epi.16815>
- Rasband, M. N. (2016). Glial contributions to neural function and disease. *Molecular and Cellular Proteomics*, 15(2), 355–361. <https://doi.org/10.1074/mcp.R115.053744>
- Ritter, D. M., & Holland, K. (2020). Genetic Testing in Epilepsy. *Seminars in Neurology*, 40(6), 730–738. <https://doi.org/10.1055/s-0040-1719070>
- Sacco, R. L., Kasner, S. E., Broderick, J. P., Caplan, L. R., Connors, J. J., Culebras, A., Elkind, M. S. V., George, M. G., Hamdan, A. D., Higashida, R. T., Hoh, B. L., Janis, L. S., Kase, C. S., Kleindorfer, D. O., Lee, J. M., Moseley, M. E., Peterson, E. D., Turan, T. N., Valderrama, A. L., & Vinters, H. V. (2013). An updated definition of stroke for the 21st century: A statement for healthcare professionals from the American heart association/American stroke association. *Stroke*, 44(7), 2064–2089.

- <https://doi.org/10.1161/STR.0b013e318296aeca>
- Salanova, V., Witt, T., Worth, R., Henry, T. R., Gross, R. E., Nazzaro, J. M., Labar, D., Sperling, M. R., Sharan, A., Sandok, E., Handforth, A., Stern, J. M., Chung, S., Henderson, J. M., French, J., Baltuch, G., Rosenfeld, W. E., Garcia, P., Barbaro, N. M., ... Fisher, R. (2015). Long-term efficacy and safety of thalamic stimulation for drug-resistant partial epilepsy. *Neurology*, *84*(10), 1017–1025. <https://doi.org/10.1212/WNL.0000000000001334>
- San-Juan, D., Espinoza López, D. A., Vázquez Gregorio, R., Trenado, C., Fernández-González Aragón, M., Morales-Quezada, L., Hernandez Ruiz, A., Hernandez-González, F., Alcaraz-Guzmán, A., Ansel, D. J., & Fregni, F. (2017). Transcranial Direct Current Stimulation in Mesial Temporal Lobe Epilepsy and Hippocampal Sclerosis. *Brain Stimulation*, *10*(1), 28–35. <https://doi.org/10.1016/j.brs.2016.08.013>
- Sarrazin, J. L., Bonneville, F., & Martin-Blondel, G. (2012). Brain infections. *Diagnostic and Interventional Imaging*, *93*(6), 473–490. <https://doi.org/10.1016/j.diii.2012.04.020>
- Scheepers, B., Clough, P., & Pickles, C. (1998). The misdiagnosis of epilepsy: Findings of a population study. *Seizure*, *7*(5), 403–406. [https://doi.org/10.1016/S1059-1311\(05\)80010-X](https://doi.org/10.1016/S1059-1311(05)80010-X)
- Scheffer, I. E., Berkovic, S., Capovilla, G., Connolly, M. B., French, J., Guilhoto, L., Hirsch, E., Jain, S., Mathern, G. W., Moshé, S. L., Nordli, D. R., Perucca, E., Tomson, T., Wiebe, S., Zhang, Y. H., & Zuberi, S. M. (2017). ILAE classification of the epilepsies: Position paper of the ILAE Commission for Classification and Terminology. *Epilepsia*, *58*(4), 512–521. <https://doi.org/10.1111/epi.13709>
- Scherg, M., Berg, P., & BESA. (2018). *BESA® | Brain Electrical Source Analysis*. BESA® | Brain Electrical Source Analysis - <https://www.besa.de>. <https://www.besa.de>
- SCHMITT, F. O., & BEAR, R. S. (1939). THE ULTRASTRUCTURE OF THE NERVE AXON SHEATH. *Biological Reviews*, *14*(1), 27–50. <https://doi.org/10.1111/j.1469-185X.1939.tb00922.x>
- Shekhawat, G. S., Sundram, F., Bikson, M., Truong, D., De Ridder, D., Stinear, C. M., Welch, D., & Searchfield, G. D. (2016). Intensity, duration, and location of high-definition transcranial direct current stimulation for tinnitus relief. *Neurorehabilitation and Neural Repair*, *30*(4), 349–359. <https://doi.org/10.1177/1545968315595286>
- Shih, J. J., Whitlock, J. B., Chimato, N., Vargas, E., Karceski, S. C., & Frank, R. D. (2017). Epilepsy treatment in adults and adolescents: Expert opinion, 2016. *Epilepsy and Behavior*, *69*, 186–222. <https://doi.org/10.1016/j.yebeh.2016.11.018>
- Shorvon, S. D. (2009). A history of neuroimaging in epilepsy 1909–2009. *Epilepsia*, *50*(SUPPL. 3), 39–49. <https://doi.org/10.1111/j.1528-1167.2009.02038.x>
- Snell, R. S. (2016). Clinical Neuroanatomy, 7th Edition. In *Neurology Secrets: Sixth Edition* (7th

- Editio). <https://doi.org/10.1016/B978-0-323-35948-1.00002-4>
- Sonntag, H., Vorwerk, J., Wolters, C. H., Grasedyck, L., Hauelsen, J., & Maeß, B. (2013). Leakage effect in hexagonal FEM meshes of the EEG forward problem. *Clinical EEG and Neuroscience: Official Journal of the EEG and Clinical Neuroscience Society (ECNS)*, *44*, 2013(4), E60–E61. <https://doi.org/10.1177/1550059413507209>
- Spencer, D. C., Sun, F. T., Brown, S. N., Jobst, B. C., Fountain, N. B., Wong, V. S. S., Mirro, E. A., & Quigg, M. (2016). Circadian and ultradian patterns of epileptiform discharges differ by seizure-onset location during long-term ambulatory intracranial monitoring. *Epilepsia*, *57*(9), 1495–1502. <https://doi.org/10.1111/epi.13455>
- Sprengers, M., Vonck, K., Carrette, E., Marson, A. G., & Boon, P. (2017). Deep brain and cortical stimulation for epilepsy. *Cochrane Database of Systematic Reviews*, 2017(7). https://doi.org/10.1002/14651858.CD008497.PUB3/MEDIA/CDSR/CD008497/IMAGE_N/NCD008497-CMP-002-06.PNG
- St. Louis, E. (2009). Truly “Rational” Polytherapy: Maximizing Efficacy and Minimizing Drug Interactions, Drug Load, and Adverse Effects. *Current Neuropharmacology*, *7*(2), 96–105. <https://doi.org/10.2174/157015909788848929>
- Starnes, K., Miller, K., Wong-Kisiel, L., & Lundstrom, B. N. (2019). A Review of Neurostimulation for Epilepsy in Pediatrics. *Brain Sciences 2019, Vol. 9, Page 283*, *9*(10), 283. <https://doi.org/10.3390/BRAINSCI9100283>
- Stroink, H., Van Donselaar, C. A., Geerts, A. T., Peters, A. C. B., Brouwer, O. F., & Arts, W. F. M. (2003). The accuracy of the diagnosis of paroxysmal events in children. *Neurology*, *60*(6), 979–982. <https://doi.org/10.1212/01.WNL.0000049914.25434.72>
- Sudbrack-Oliveira, P., Barbosa, M. Z., Thome-Souza, S., Razza, L. B., Gallucci-Neto, J., da Costa Lane Valiengo, L., & Brunoni, A. R. (2021). Transcranial direct current stimulation (tDCS) in the management of epilepsy: A systematic review. In *Seizure* (Vol. 86, pp. 85–95). *Seizure*. <https://doi.org/10.1016/j.seizure.2021.01.020>
- Telles-Correia, D., Saraiva, S., & Gonçalves, J. (2018). Mental disorder-The need for an accurate definition. *Frontiers in Psychiatry*, *9*(MAR), 64. <https://doi.org/10.3389/fpsy.2018.00064>
- Thurman, D. J., Beghi, E., Begley, C. E., Berg, A. T., Buchhalter, J. R., Ding, D., Hesdorffer, D. C., Hauser, W. A., Kazis, L., Kobau, R., Kroner, B., Labiner, D., Liow, K., Logroscino, G., Medina, M. T., Newton, C. R., Parko, K., Paschal, A., Preux, P. M., ... Wiebe, S. (2011). Standards for epidemiologic studies and surveillance of epilepsy. *Epilepsia*, *52*(SUPPL. 7), 2–26. <https://doi.org/10.1111/j.1528-1167.2011.03121.x>
- Van Campen, J. S., Hompe, E. L., Jansen, F. E., Velis, D. N., Otte, W. M., Van De Berg, F., Braun, K. P. J., Visser, G. H., Sander, J. W., Joels, M., & Zijlmans, M. (2016). Cortisol fluctuations relate to interictal epileptiform discharges in stress sensitive epilepsy. *Brain*, *139*(6),

- 1673–1679. <https://doi.org/10.1093/brain/aww071>
- Vanhaerents, S., Chang, B. S., Rotenberg, A., Pascual-Leone, A., & Shafi, M. M. (2020). Noninvasive Brain Stimulation in Epilepsy. In *Journal of Clinical Neurophysiology* (Vol. 37, Issue 2, pp. 118–130). J Clin Neurophysiol. <https://doi.org/10.1097/WNP.0000000000000573>
- Verrotti, A., Iapadre, G., Di Francesco, L., Zagaroli, L., & Farello, G. (2020). Diet in the Treatment of Epilepsy: What We Know So Far. *Nutrients*, 12(9), 1–19. <https://doi.org/10.3390/NU12092645>
- Vogl, R., Rudolph, D., Angenent, H., Thoring, A., Schild, C., Stieglitz, S., & Meske, C. (2015). sciebo – the Campuscloud: a Sync and Share Cloud Storage Service for the Academic and Research Community in North Rhine-Westphalia. *PIK - Praxis Der Informationsverarbeitung Und Kommunikation*, 38(3–4). <https://doi.org/10.1515/pik-2015-0007>
- Wiebe, S., & Jetté, N. (2012). Epilepsy surgery utilization: Who, when, where, and why? In *Current Opinion in Neurology* (Vol. 25, Issue 2, pp. 187–193). <https://doi.org/10.1097/WCO.0b013e328350baa6>
- Wolf, P., Benbadis, S., Dimova, P. S., Vinayan, K. P., Michaelis, R., Reuber, M., & Yacubian, E. M. (2020). The importance of semiological information based on epileptic seizure history. *Epileptic Disorders*, 22(1), 15–31. <https://doi.org/10.1684/epd.2020.1137>
- Wong, S. H., Adams, P., & Jackson, M. (2008). The electrocardiograph (ECG) in a first seizure clinic. *Seizure*, 17(8), 707–710. <https://doi.org/10.1016/j.seizure.2008.05.002>
- Yang, D., Wang, Q., Xu, C., Fang, F., Fan, J., Li, L., Du, Q., Zhang, R., Wang, Y., Lin, Y., Huang, Z., Wang, H., Chen, C., Xu, Q., Wang, Y., Zhang, Y., Zhang, Z., Zhao, X., Zhao, X., ... Wang, Y. (2020). Transcranial direct current stimulation reduces seizure frequency in patients with refractory focal epilepsy: A randomized, double-blind, sham-controlled, and three-arm parallel multicenter study. *Brain Stimulation*, 13(1), 109–116. <https://doi.org/10.1016/j.brs.2019.09.006>
- Zaidi, A., Clough, P., Cooper, P., Scheepers, B., & Fitzpatrick, A. P. (2000). Misdiagnosis of epilepsy: Many seizure-like attacks have a cardiovascular cause. *Journal of the American College of Cardiology*, 36(1), 181–184. [https://doi.org/10.1016/S0735-1097\(00\)00700-2](https://doi.org/10.1016/S0735-1097(00)00700-2)

Eidesstattliche Erklärung

„Ich erkläre hiermit ehrenwörtlich, dass ich die vorliegende Arbeit selbständig angefertigt habe. Die aus fremden Quellen direkt und indirekt übernommenen Gedanken sind als solche kenntlich gemacht.

Mir ist bewusst, dass die Arbeit in digitaler Form daraufhin überprüft werden kann, ob unerlaubte Hilfsmittel verwendet wurden und ob es sich - insgesamt oder in Teilen – um ein Plagiat handelt. Zum Vergleich meiner Arbeit mit existierenden Quellen darf sie in eine Datenbank eingestellt werden und nach der Überprüfung zum Vergleich mit künftig eingehenden Arbeiten dort verbleiben. Weitere Vervielfältigungs- und Verwertungsrechte werden dadurch nicht eingeräumt. Die Arbeit wurde keiner anderen Prüfungsbehörde vorgelegt.“

X F. Kaiser

Steinfurt, den 03.01.2022
Fabian Kaiser